REPUBLIC OF TURKEY
HACETTEPE UNIVERSITY
INSTITUTE OF HEALTH SCIENCES

THE EFFECT OF INDUCIBLE COSTIMULATORY LIGAND (ICOS-LG) EXPRESSING MYELOID LEUKEMIA CELLS ON HELPER T LYMPHOCYTE ACTIVATION AND EXHAUSTION

B.Sc. Didem ÖZKAZANÇ

Tumor Biology and Immunology Program
M.Sc.THESIS

ANKARA
2015

REPUBLIC OF TURKEY
HACETTEPE UNIVERSITY
INSTITUTE OF HEALTH SCIENCES

THE EFFECT OF INDUCIBLE COSTIMULATORY LIGAND (ICOS-LG) EXPRESSING MYELOID LEUKEMIA CELLS ON HELPER T LYMPHOCYTE ACTIVATION AND EXHAUSTION

B.Sc. Didem ÖZKAZANÇ

Tumor Biology and Immunology Program
M.Sc.THESIS

Supervisor of Thesis
ASSOC. PROF. DR. GÜNEŞ ESENDAĞLI

ANKARA
2015

Department	**:Basic Oncology**
Program	**:Tumor Biology and Immunology**
Dissertation Title	**:The effect of inducible costimulatory ligand (ICOS-LG) expressing myeloid leukemia cells on helper T lymphocyte activation and exhaustion.**
Name of the Student	**:Didem Özkazanç**
Date of Dissertation Defence	**:03.07.2015**

This study has been accepted and approved as a Master / PhD dissertation by the examining committee, whose members are listed below.

Chair of the Committee:	**Prof.Dr.A.Lale Doğan** **Hacettepe University**	(Signature)
Advisor of the Dissertation:	**Assoc.Prof.Dr.Güneş Esendağlı** **Hacettepe University**	(Signature)
Member:	**Prof.Dr.Dicle Güç** **Hacettepe University**	(Signature)
Member:	**Assoc.Prof.Dr.Mayda Gürsel** **Middle East Techical University**	(Signature)
Member:	**Assist.Prof.Dr.Emre Dayanç** **Inonu University**	(Signature)

APPROVAL

This dissertation has been approved by the committee above in conformity to the regulations and bylaws of Hacettepe University Graduate Programs and has been accepted by the Board of Directors of the Institute of Health Sciences.

(Signature)

Prof. Ersin FADILLIOĞLU, MD

Institute Director

ACKNOWLEDGEMENTS

I would like to express my deep gratitude to my supervisor Assoc. Prof. Dr. Güneş Esendağlı for his valued and constructive suggestions, and his patient guidance all through my studies and this research. His willingness to give his time so generously has been very much appreciated.

I would like to record my gratitude to the faculty members, Prof. Dr. A. Lale Doğan, Prof. Dr. Dicle Güç, Assist. Prof. Dr. Füsun Özmen, Dr.Hande Canpınar for their continous encouragement, sincere advice and support in every aspect. I would like to express my special thanks to Prof. Dr. Emin Kansu for his kindness and passion in science, which promoted my enthusiasm as a researcher.

I would like to thank Diğdem Yöyen Ermiş and Pınar Karaşar for valuable moral and scientific support we shared. I also would like to express my appreciation to Burcu Şirin, Emre Gedik, Parisa Sarmadi, Burcu Beksaç, Alper Kurşunel, Çiğdem Aras, Mohammed Azim Ebrahimi and Gürcan Tunalı for creating such a pleasant and nurturing environment.

My special thanks are extended to Semra Solmaz, Burçin Taşbasan, Banu Avşar, Necla Çelik, Canip Ulubey, Halime Mesci and Gülay Çelik for their kindness and positive energy.

I owe a special debt of heart-felt gratitude to İlker Ünsal and Dilara Özdemir for their understanding, faith in me, unceasing presence and unconditional fostering to follow my dreams in all of my pursuits.

I dedicate this thesis to my parents, Ercan and Canan Özkazanç, and my sister Sinem, for their financial and moral support, and inspiring me to do the very best I can. None of this would have been possible without the unconditional love and patience of my family.

ÖZET

Özkazanç D. Uyarılabilen kostimülatör ligand (ICOS-LG) eksprese eden akut miyeloid lösemi hücrelerinin yardımcı T lenfosit aktivasyonu ve yorulmasına etkisi. Hacettepe Üniversitesi Sağlık Bilimleri Enstitüsü, Tümör Biyolojisi ve İmmünolojisi Yüksek Lisans Programı, Ankara, 2015. T hücre yorulması sürekli antijen uyarımı etkisinde kademeli olarak gelişen sitokin üretiminin kaybı, çoğalma kapasitesinde azalma ve tekrar aktivasyona direnç ile tanımlanmıştır. Yardımcı T lenfosit (Th) yanıtlarının, AML hücreleri tarafından uyarabilmesine rağmen, anti-lösemik etkisi sınırlıdır. Bu çalışmada, AML kaynaklı kostimülasyon sinyallerinin Th yorulmasına olan etkilerini incelemek amacıyla ilk kez bir *in vitro* model geliştirilmiştir. Öncelikle AML hücrelerinin (HL-60, THP-1, U937, Kasumi-1, KG-1) ve $CD14^+$ monositlerin normal fizyolojik ve proinflamatuar koşullardaki ICOS-LG ifade düzeyleri ve zamana bağlı değişimleri belirlendi. Daha sonra, $CD4^+$ T lenfositlerin AML hücre hatları veya monositler ile farklı hücre oranları ve farklı konsantrasyonlarda anti-CD3 (aCD3) uyarımı ile ko-kültürleri gerçekleştirildi. aCD3 ve kültür ortamı düzenli olarak tazelendi. Th hücrelerinin CD25, CD127, FoxP3, CD69, PD-L1, PD-1, CTLA-4, ICOS, TIM-3, LAG3, CD38, CD154, CCR7 ve HLA-DR ifade düzeyleri, çoğalma kapasiteleri ve canlılıkları akım sitometri ile saptandı. Kostimülasyon sinyallerinin T hücre yorulmasına olan etkileri ICOS-LG, PD-L1/PD-L2 ve CD80/CD86 bloklayıcı ajanlar ile test edildi. ELISA ile IL-2, IL-10, IL-4, TGF-β, IFN-γ ve TNF-α düzeyleri belirlendi. Fonksiyonel yorulmanın test edilmesi için yorulmuş (TIM-$3^{mo/hi}$) ve yorulmamış (TIM-$3^{-/low}$) Th alt-popülasyonları zenginleştirildi ve tekrar uyarıldı. AML:Th ko-kültürlerinde Th hücreleri üzerinde LAG3, TIM-3, PD-1, CTLA-4 moleküllerin belirgin artışı saptandı. Monosit ko-kültürlerde ise Th aktivasyonu ve proliferasyonu AML hücreleri ile elde edilen sonuçlara benzer iken yorulma belirteçlerinin düzeyi anlamlı olarak düşük kaldı. Bu yorulmuş hücreler düşük düzeylerde IL-2, IFN-γ ve TNF-α üretti. Bu hücrelerin yorulmaları önceki çoğalma düzeylerinden bağımsızdı. AML-kaynaklı kostimülatör sinyallerin aCD3 uyarımına kıyasla Th yorulması için daha kritik olduğu görüldü. Yorulma dışarıdan verilen IL-2 ile geri döndürülebiliyordu. Bu bulgular, AML hücrelerinin kostimülasyon aracılığı ile Th yorulmasına neden olduğunu göstermekte ve yeni bir immün kaçış mekanizmasına işaret etmektedir.

Anahtar kelimeler: ko-stimülasyon, ICOS-LG, T hücre yorulması, Akut miyeloid lösemi

Bu çalışma, Hacettepe Üniversitesi Bilimsel Araştırma Projeleri Koordinasyon Birimi tarafından desteklenmiştir (BAB, Destek No: THD-2015-6720).

ABSTRACT

Özkazanç D. The effect of inducible costimulatory ligand (ICOS-LG) expressing myeloid leukemia cells on helper T lymphocyte activation and exhaustion. Hacettepe University Institute of Health Sciences, Tumor Biology and Immunology Master of Science Program, Ankara, 2015. T cell exhaustion is characterized by progressive loss of cytokine production, decreased proliferation and resistance to reactivation especially upon continuous antigen stimulation. Despite being potent stimulators of helper T (Th) lymphocytes, AML cells employ intriguing mechanisms to limit anti-tumor responses. Thus, this study proposes an *in vitro* co-stimulation dependent Th cell exhaustion model that may represent a novel immune escape mechanism in AML. Firstly, ICOS-LG expression kinetics were evaluated on AML cell lines of different maturation status (HL-60, THP-1, U937, Kasumi-1, KG-1) in comparison to $CD14^+$ monocytes by flow cytometry under steady state and pro-inflammatory conditions. Then, $CD4^+$ T cells were co-cultured with AML cells or monocytes at different ratios and stimulated with various anti-CD3 concentrations. Media and aCD3 was regularly refreshed in extended culture periods. CD25, CD127, FoxP3, CD69, PD-L1, PD-1, CTLA-4, ICOS, TIM-3, LAG3, CD38, CD154, CCR7, HLA-DR expression, together with proliferation and viability were evaluated by flow cytometry. Assays were also performed under ICOS-LG, PD-L1/PD-L2 and CD80/CD86 blockade. IL-2, IL-10, IL-4, TGF-β, IFN-γ and TNF-α levels were measured by ELISA. Exhausted ($TIM\text{-}3^{mo/hi}$) and non-exhausted Th cells ($TIM\text{-}3^{-/low}$) were enriched and re-stimulated for functional exhaustion assays. In the co-cultures, Th cells possessed high levels of LAG3, TIM-3, PD-1, ICOS and CTLA-4. Th cells' proliferation and activation with AML cells or monocytes were similar; however, exhaustion was significantly higher in AML co-cultures. These exhausted cells produced lower IL-2, IFN-γ and TNF-α. Exhaustion was independent of Th cells' initial proliferative activity. Co-stimulatory signals derived from AML cells were more critical than aCD3 stimulation in Th cell exhaustion. Exhaustion could be reversed by exogenous IL-2. Our findings indicate a novel immune escape mechanism employed by AML cells that can induce a co-stimulation dependent Th cell exhaustion.

Key words: Co-stimulation, ICOS-LG, T cell exhaustion, Acute myeloid leukemia

This study was supported by Hacettepe University Scientific Research Projects Coordination Unit (BAB, Grant Number, THD-2015-6720).

CONTENTS

LIST OF ABBREVIATIONS

aCD3	anti-CD3 monoclonal antibody
AML	Acute myeloid leukemia
APC	Antigen presenting cells
BCL-XL	B-cell lymphoma-extra large
BCR-ABL	Breakpoint cluster region Abelson
BM	Bone marrow
BTLA	B and T lymphocyte attenuator
CD	Cluster of differentiation
CLL	Chronic lymphocytic leukemia
CML	Chronic myeloid leukemia
cMPO	Cytoplasmic myeloperoxidase
CRD	Cysteine-rich domains
CTLA-4	Cytotoxic T-lymphocyte antigen-4
CTLs	Cytotoxic T lymphocyte
DC	Dendritic cell
DR3	Death receptor-3
FACS	Fluorescence-activated cell sorting
Fas ligand	FasL
FBS	Fetal bovine serum
FLIP	FLICE-like inhibitory protein
FLT3	Fms-like tyrosine kinase 3
FoxP3	Forkhead box protein 3
gal-9	Galectin-9
GM-CSF	Granulocyte-macrophage colony-stimulating factor
HBV	Hepatitis B virus
HCV	Hepatitis C virus
HIV	Human immunodeficiency virus
HLA	Human leukocyte antigen
HVEM	Herpes virus entry mediator
ICOS	Inducible T cell co-stimulator
ICOS-LG	Inducible T cell co-stimulator ligand

IDO	Indoleamine 2,3-dioxygenase
IgSF	Immunoglobulin superfamily
IFN	Interferon
IL	Interleukin
iRs	Inhibitory receptors
JAK	janus-activated kinase
KIR	Killer inhibitory receptors
LAG3	Lymphocyte activation gene
LCMV	Lymphocytic choriomeningitis virus
LMP	Low molecular mass polypeptides
LSA	Leukemia-specific antigens
LSC	Leukemic stem cells
MDS	Myelodysplastic syndrome
MDSC	Myeloid-derived suppressor cells
MFI	Mean fluorescence intensity
MHC	Major histocompatibility complex
MLL	Mixed-lineage leukemia
MSC	Mesenchymal stem cells
Mϕ	Macrophage
NK	Natural killer
NKG2D	Natural-killer group 2 member D
NKp46	Natural killer cell p46-related protein
NO	Nitric oxide
pDC	Plasmocytoid dendritic cells
PD-1	Programmed-cell death-1
PD-L1	Programmed-cell death ligand-1
PI	Propidium iodide
PI3K	Phosphatidylinositol 3-kinase
PGE	Prostaglandin E
SCT	Stem cell transplant
SIV	Simian immunodeficiency virus
STAT	Signaling transducers and activators of transcription
TAM	Tumor-associated macrophages

TAP1	Transporter associated with antigen processing type 1
TCR	T cell receptor
TGF-β	Transforming growth factor beta 1
THD	TNF homology domain
TIL	Tumor-infiltrating lymphocyte
TIM-3	T-cell immunoglobulin and mucin domain-containing protein-3
TNFRSF	Tumor necrosis factor receptor superfamily
TRAIL	Tumor necrosis factor-related apoptosis-inducing ligand
Treg	Regulatory T cell
VEGF	Vascular endothelial growth factor
WHO	World Health Organization

FIGURES

TABLES

1. INTRODUCTION

Cancer arises in a form of nascent transformed cells. At physiological conditions, cancer immune surveillance system scans for and eradicates these transformed cells (1,2). However, tumor cells develop several strategies to evade immune recognition (3).

T cell exhaustion is one such mechanism. Tumor antigen-specific T cells often proliferate, but they remain at a low frequency and their functions are significantly modulated by the microenvironment (4). Under the influence of persistent antigen stimulation and local activatory and inhibitory signals, T cells adopt an exhausted phenotype (5,6). The exhausted T cells present progressive loss of cytokine production, decreased proliferation and resistance to reactivation. They are marked by expression of certain molecules that are called exhaustion-associated markers (7).

Acute Myeloid Leukemia (AML) cells substantially express high levels of co-stimulatory molecules, CD86 (B7.2) and ICOS-LG (8). These co-stimulatory molecule expressions determine the extent of T cell activation and survival. ICOS-LG and CD86 mediate efficient T cell responses, although $CD86^+$ AML patients exhibit poor prognosis and severe disease outcomes (9,10). ICOS-LG interacts with ICOS on activated T cells and is known to be expressed by myeloid derived cells such as monocytes and AML cells (10). In a study, the ICOS-LG expression levels were shown to be upregulated on monocytes upon treatment with pro-inflammatory cytokine, IFN-γ (9).

This study aims to establish an *in vitro* co-stimulation-dependent Th cell exhaustion model that may represent a novel immune escape mechanism in AML. ICOS-LG expression levels and their modulation on AML cell lines of different FAB classifications were determined upon exposure to IFN-γ. In order to establish an *in vitro* model, AML cells (HL-60 and THP-1) and/or monocytes were co-cultured with $CD4^+$ T cells at different cell ratios in the presence of different concentrations of anti-CD3 (aCD3) monoclonal antibody. This strategy enabled mimicking the TCR signal with aCD3 administration and co-stimulatory signals via modulation of AML cell ratios.

Additionally, co-cultures were regularly maintained with fresh media and aCD3 at a constant concentration to support viability of the co-cultured cells as well as to mimic persistent antigen stimulation. The expression of activation and exhaustion-associated markers, proliferation and cytokine production capacities of the co-cultured T cells were determined in order to evaluate the exhaustion state of Th cells in our model. Certain aspects of exhaustion were also confirmed in additional co-cultures performed with additional AML cell lines (KG-1, Kasumi-1 and U937). Then, the effect of co-stimulatory signals contributing to this phenotype was determined by blocking the major co-stimulatory pathways in the co-cultures. Lastly, these *in vitro* exhausted Th cells were functionally evaluated by restimulating the co-cultured Th cells in the presence of various agents.

Here, the viability and proliferation of T cells were substantially supported by the co-culture conditions. The co-cultured Th cells showed distinctive expression patterns for certain activation and exhaustion-associated markers compared to that of co-cultured with monocytes. This distinct pattern was also more evident as the ratio of AML cells were increased, while it was scarcely altered in aCD3 modulations. Hence, exhaustion state in this model majorly relied on co-stimulation signals in the expense of TCR signals. This was also supported by the upregulation of co-stimulatory receptors on Th cells and by the results of blockade of CD86 or ICOS-LG co-stimulatory pathways. IFN-γ, IL-2 and TNF-α levels were significantly diminished in the AML co-cultures, which indicated that exhaustion phenotype was induced in these co-cultures. The co-cultured T cells were recovered and isolated as two groups according to differential TIM-3 expression and restimulated with various agents. Accordingly, TIM-$3^{-/lo}$ Th cells demonstrated a higher proliferation rate than that of TIM-$3^{mo/hi}$ cells in all conditions. Thus, T cells were also confirmed to be functionally exhausted in this co-cultured model. Only, exogenous IL-2 could restore the proliferation activity of exhausted T cells.

In conclusion, this study proposes a newly established *in vitro* exhaustion model that indicates a novel immune escape mechanism

employed by AML cells that can induce a co-stimulation dependent Th cell exhaustion.

2. LITERATURE REVIEW

2.1. Leukemia

Leukemia is a malignant disease of blood-forming organs, which progresses by abnormal proliferation and development of leukocytes and their progenitors in bone marrow. Several factors are associated with the risk of developing leukemia. These include environmental and genetic factors; age, ethnicity, gender, virus infections, inherited syndromes (e.g., Down syndrome), cigarette smoking, exposure to certain chemical and ionizing radiation(11).

Leukemogenesis is a multifactorial process that involves several genetic mutations operating on hematopoietic precursors (12). The disease is mainly classified based on the type of white blood cells affected (lymphoid or myeloid) and manifestation characteristics of the disease (acute or chronic). Acute or chronic myeloid leukemia possess different rates of progression where the amount of tumor cells increases and heavily alters the patient survival. Not essentially every clonally expanding cell in bone marrow can be defined as leukemia. The presence of dysplasia in bone marrow and in peripheral blood may also address to myelodysplastic/myeloproliferative syndromes (13,14). Myelodysplastic syndromes (MDS) are generally identified as a heterogenous group of diseases characterized by active but ineffective hematopoiesis leading to pancytopenia (15). Acute myeloid leukemia (AML), chronic myeloid leukemia (CML) and MDS differ from each other in many aspects such as clinical variability or more importantly, cytogenetic abnormalities (16). Both MDS and AML are quite heterogenous diseases which lack one common molecular target, while BCR-ABL (Philadelphia chromosome) predominates the early phases and progression of CML (17).

CML is a form of leukemia in which the bone marrow makes too many white blood cells. It usually occurs during or after middle age, and rarely occurs in children. Differed by its quick progression, AML is a cancer of the blood and bone marrow which results from accumulation of abnormal blasts in the marrow. Its frequency peaks in early childhood and later adulthood.

MDS primarily affects the elderly since 40% of patients transform from MDS to AML (17).

2.1.1. Acute Myeloid Leukemia (AML)

In AML, hematopoietic progenitor cells fail to differentiate in the early phases of maturation, however they continuously overproliferate in the stem cell compartment. This results in the accumulation of non-functional blasts in the bone marrow niches. These immature blasts interfere with normal hematopoiesis which leads to the bone marrow failure and eventually, death. As one of the most aggressive forms of hematological malignancies affecting both the young and the old, it accounts for 85% of adulthood leukemia and 15% of childhood leukemia (18,19). AML has a variable prognosis, but particularly poor in patients over 55 years of age. The median age of patients is 65-70 (19).

The classification system in AML is primarily based on morphological and cytochemical criteria. So far, several molecular prognostic factors such as the adverse impact of a mutation in Fms-like tyrosine kinase 3 (FLT3) gene and duplication in myeloid/lymphoid or mixed-lineage leukemia (MLL) gene have been determined (20,21). Apart from this, various DNA double-strand breaks, translocations, point mutations and deletions are commonly seen in AML patients (22,23). Certain AML-associated abnormalities are presented by the 40% of the patients and other known chromosomal abnormalities can be found in 10% of the patients. Alternatively, AML patients can also present normal karyotype (24).

2.2. Cellular Differentiation Levels in AML

In 1970s, a group of leukemia experts divided AML into subtypes, according to the type of cell from which leukemia originates and the level of maturation. According to this French-American-British (FAB) classification of AML, blasts were categorized by their morphology and cytochemical staining (e.g., Wright-Giemsa, May-Grünwald Giemsa)(Table 2.1). Later, this classification felt behind the advances in technology and current clinical understanding of the disease. Thus, thereafter, this system gained new

perspectives and upgraded by World Health Organization (WHO) in 2001(25). This accounts for a milestone for clinicians since this system better defines the subgroups by their cytogenetic and molecular genetics abnormalities which determines the prognosis and treatment options.

Table 2.1. FAB classification of AML cells.

FAB subtype	Name
M0	Undifferentiated acute myeloblastic leukemia
M1	Acute myeloblastic leukemia with minimal maturation
M2	Acute myeloblastic leukemia with maturation
M3	Acute promyelocytic leukemia (APL)
M4	Acute myelomonocytic leukemia
M4 eos	Acute myelomonocytic leukemia with eosinophilia
M5	Acute monocytic leukemia
M6	Acute erythroid leukemia
M7	Acute megakaryoblastic leukemia

In the course of hematopoiesis, hematopoietic stem cells undergo several steps of maturation and differentiation under the influence of certain factors. Each step involves a cell expressing specific markers which can be used to determine its maturation and differentiation stage. The identification of CD34, CD117, CD33, CD15, CD4, CD11b, HLA-DR and cytoplasmic myeloperoxidase (cMPO) markers are one of the many gold standard factors that allow the researchers and clinicians to classify the maturation and differentiation status of these blastic precursors (26). For example, CD34 expression is linked to the immaturity of the blasts and a poor clinical outcome.

FAB classes are determined by the maturation and differentiation status and mainly classified as follows (27-29):

AML - M0 (undifferentiated): These blasts have basophilic granules. They stably express CD13, CD15 or CD33 and MPO. In a few reports, they were described to appear similar to M5 monoblasts, but this can be resolved by the lack of non-specific esterase activity.

AML - M1 (minimally differentiated): They appear to be either medium or large blasts, differential nucleocytoplasmic ratios and multinucleated cells with vacuoles. They have less granules than that of M0. They frequently express CD13, CD14, CD15, CD33 and CD34.

AML - M2 (differentiated): They have more granules, elevated MPO activities and abundant CD13 and CD15 expressions.

AML - M3 (promyelocytic leukemia): These blasts have dense cytoplasms with massive, red or purple granules. They tend to differentiate into basophils and neutrophils. They are widely negative for HLA-DR and CD34.

AML - M4 (myelomonocytic leukemia): They are able to differentiate to neutrophils, eosinophils or basophils. However, they are typically defined as monocyte-like cells. They are characterized by CD13, CD33, CD11b and CD14 expressions.

AML - M5 (monocytic/monoblastic leukemia): Monoblasts are basophilic cells, rich in cytoplasmic content and redundantly possess vacuoles. Monocytic leukemia cells have lower nucleocytoplasmic ratio, lobulated nucleus and are less basophilic. In some patients with acute monocytic leukemia, cells are described as macrophages or histiocytic cells. They are usually positive for CD11b and CD14.

AML - M6 (erythroid leukemia) and AML - M7 (megakaryoblastic leukemia): M6 subtype indicates MDS to leukemia transformation. They are marked by CD13, CD33, CD34, HLA-DR and MPO positivity. AML-M7 blasts are pleomorphic cells with lymphoblastic characteristics. They frequently express CD41, CD42 and CD61.

2.3. Immune System and AML

2.3.1. Tumor Immunology

Cancer arises as nascent transformed cells by a multistep process involving several genetic as well as non-genetic factors. Until it is clinically manifested, the immune system scans for and eradicates these transformed cells. This assassination mission, prosecuted by the cells of innate and adaptive immune systems, is termed *cancer immune surveillance*.

The cancer immune surveillance theory proposes that cancer prevalence would increase if the immune system fails to effectively function. By the time this theory was put forward, cancer was associated with an immune suppressive state or depicted as a complication of severe immunosuppression (30). Several studies showed the development of different malignancies in immunodeficiencies. A study in solid organ transplant recipients demonstrated an increased risk of developing cancers of both infection-associated and non-infectious causes (31,32). However, immunosuppression may prepare a fertile soil for cancer growth and survival in the body, but certain immune responses to common infectious agents are preserved in several cancer patients suggesting a complex interaction between the immune system and malignant process. These observations lead to various hypotheses on cancer immunity, among which *cancer immunoediting* is the most widely accepted.

Hence, it has been evidenced that immune system is able to recognize and destroy the cancer precursors; but it may also be deceived by the tumor cells which leads to malignant disease or metastasis. This ying-yang fashioned combination of host-protective and tumor-promoting functions of the immune system throughout tumor development has been termed cancer immunoediting and has been conceived as a dynamic process comprised of three phases: elimination, equilibrium and escape(Figure2.1) (3,33,34).

The elimination of the tumor cells is maintained by the immune surveillance of host-immunity. Nascent transformed cells are eradicated by the alliance of innate and adaptive immune cells. For this purpose, the host effector molecules such as interferons, perforin, Fas/Fas ligand (FasL), and

tumor necrosis factor-related apoptosis-inducing ligand (TRAIL); recognition molecules such as NKG2D; intact lymphocyte compartment in anti-tumor immunity work in concert to detect and efficiently eliminate the developing tumors (33,35,36).

The host effector molecules are endogenous molecules that mediate anti-tumor immunity. Both type I (IFN-α/β) and type II (IFN-γ) interferons are required to develop anti-tumor responses but they play distinct roles. IFN-γ targets tumor cells as well as hematopoietic cells; whereas, IFN-α/β targets primarily host cells. IFN-γ has direct effects on tumor cell immunogenicity and is critical in tumor recognition and elimination. Lately, two studies showed that type I IFNs initiate early anti-tumor responses and enhance the cross-presentation of tumor-antigens by CD8α/CD103^{+} dendritic cells (DC) to CD8^{+} T cells (37,38).

Perforin and Fas/FasL are other important host effector molecules involved in immune surveillance. Tumor elimination largely depends on cell-mediated cytotoxicity carried out by cytotoxic T lymphocytes (CTLs) and NK cells. These cells utilize either granule exocytosis or Fas pathway. The granule exocytosis pathway involves pore-forming protein (pfp) that direct granzymes and induce apoptosis. The latter initiates activation-induced cell death and lymphocyte-mediated killing. Moreover, ligation of TRAIL receptors leads to activation of caspase-3 and subsequently caspase-8 to induce apoptosis (39).

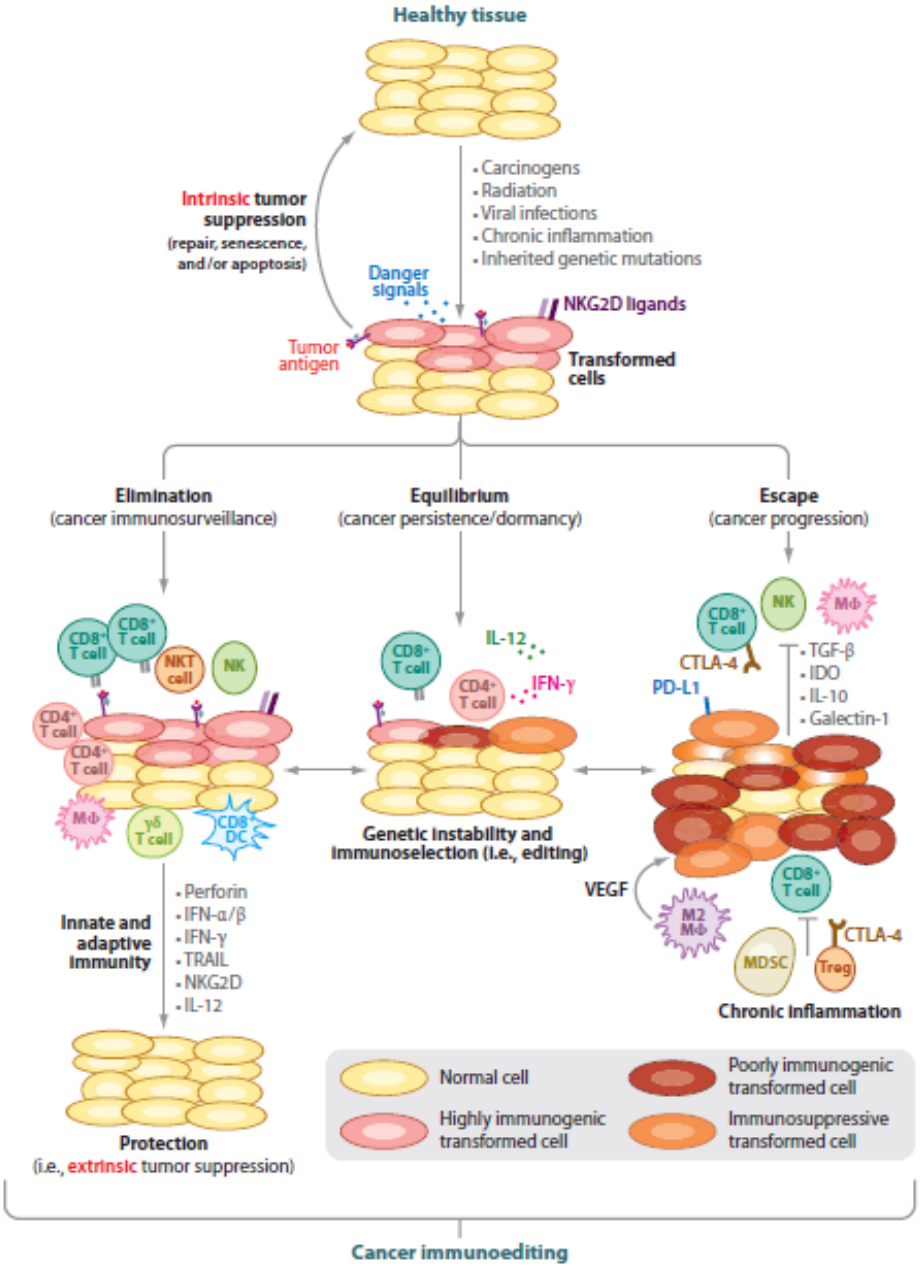

Figure 2.1. Major molecular and cellular interactions taking place during the three phases of cancer immunoediting process(36).

Elimination: immune system is evoked via NKG2D ligands andinitiates eradication of tumor cells. Innate and adaptive immune cells and factors (such as perforin, IFN-α/β etc.) recognize and destroy transformed cells. If anti-tumor responses fail, surviving tumor variants enter equilibrium phase, where adaptive immune cells ($CD8^+$ and $CD4^+$ T cells) prevent tumor outgrowth. If the variants acquire further mutations that facilitate evasion via mechanisms such as by expressing inhibitory surface molecules (PD-L1, CTLA-4), secreting factors to inhibit effector cell functions (VEGF, TGF-β, IDO etc.), by polarizing myeloid precursors into M2 macrophages (M2 Mϕ) or by accumulation of MDSCs that block T cell functions, then, clinically detectable malignancies are manifested.

Tumor elimination predominantly relies on innate immune system cells such as NK, NKT, γδ T cells, macrophages and DCs. They are activated by inflammatory cytokines secreted by tumor cells, macrophages and stromal cells neighboring the tumor. Immune cells that arrive to the tumor microenvironment produce other cytokines such as IL-12 and IFN-γ. The eradication of tumor cells through perforin-, FasL- and/or TRAIL-mediated killing by NK cells increases the availability of tumor antigens which provokes the adaptive arm of the immune system. NK cells promote the maturation of DCs and their migration to the tumor draining lymph nodes wherein the antigen presentation to naïve $CD4^+$ T cells becomes enhanced. Clonally expanded cytotoxic T lymphocytes (CTLs) and $CD4^+$ T cells migrate into the tumor site, where CTLs directly kill tumor cells and produce IFN-γ. IFN-γ fosters the immune responses, but also results in the selection tumor cells with reduced immunogenicity.

If anti-tumor immunity is unable to completely eliminate transformed cells, surviving tumor variants may enter into the ‘equilibrium’ phase; where cells and molecules of adaptive immunity keep the tumor growth under control. However, this continuous sculpting of tumor cells leads to the selection of immune resistant cells with the least immunogenicity. The resistant tumor cells are more capable of surviving in immunocompetent host. Thus, the equilibrium phase involves continuous elimination of tumor cells which favors the emergence of resistant tumor cells by immune selection pressure.

In the last phase, escape, the immune resistant tumor cells arisen during the equilibrium phase acquires additional mutations and evade from the immune recognition. As a matter of fact, cancer cells may adopt different strategies to escape from the immune surveillance. Because the transformed cells originate from “self” and since auto-reactive immune cells are either deleted or anergized for the sake of immune tolerance, they are not targeted by the immune system. The virus-associated cancers or tumors expressing immunogenic antigens adapt themselves to a less immunogenic phenotype by reducing the expression of tumor-associated antigens. Tumor cells can impair antigen processing and presentation pathways. Loss of TAP1, MHC

class I molecules, LMP2 and LMP7 and the development of IFN-γ or IFN-α/β insensitivity by tumor cells avoids T cell-mediated elimination (40-43). Tumor cells might lose their IFN-γ responsiveness, either by a mutation or epigenetic silencing of genes encoding IFN-γ receptor signaling, i.e. FNGR1, IFNGR2, janus-activated kinase1 (JAK1), JAK2 and signaling transducers and activators of transcription1 (STAT1)(44). Moreover, tumors can become invisible to the cells of innate immune system through the loss of ligands for NKG2D, or through the reduction of pro-inflammatory danger signals to impair DC maturation (45,46).

In addition, some tumors may become resistant to the death mechanisms employed by the immune system or gain insensitivity to death signals to evade immune-mediated cell killing by upregulating anti-apoptotic molecules such as FLIP, BCL-XL (47,48). Tumor cells gain mutations that inactivate death receptors, including TRAIL receptor and Fas (49,50).

The secretion of soluble factors, the expression of inhibitory molecules or tolerizing cells developed in the tumor microenvironment forms an immune suppressive milieu. TGF-β secretion by tumor cells inhibits the activation of DC, and directs inhibition of T cell and NK cell functions(51). Additionally, IL-10 in the tumor microenvironment suppresses DC function and alters T cell responses toward type II phenotype in favor of tumor cells (52). However, the function of IL-10 is yet ambiguous, since there is also evidence on its role in augmenting tumor destructive capacity of immune cells (53). Tumor cells can also actively and directly perpetuate suppression via inhibitory-ligand expression on their surfaces. Inhibitory molecules such as PD-L1(B7-H1), HLA-G, HLA-E do so by interacting with their cognate receptors on T cells(54-56). HLA-E or HLA-G can also induce tolerance in antigen-presenting cells, thereby inhibiting the NK-mediated cell killing (55).

A variety of immunosuppressive cells such as regulatory lymphocytes, myeloid-derived suppressor cells (MDSC), plasmacytoid DC (pDC), tumor-associated macrophages (TAM) can suppress immune functions. Regulatory T (Treg) cells inhibit CTL function with distinct mechanisms, including IL-10 and TGF-β production, CTLA-4 and PD-L1 expression, and IL-2 decay (57). Furthermore, TGF-β produced by tumor cells can convert effector T cells into

Tregs so that even the immune cells recently infiltrated the microenvironment become suppressed (58). In addition to Tregs, MDSCs are also responsible for ineffective immunity in cancer. Their expansion is supported and elaborated by soluble factors such as GM-CSF, IL-1β, VEGF or PGE_2 secreted by the tumor (59). MDSCs are a heterogenous population of myeloid progenitor cells and immature myeloid cells that can inhibit lymphocyte function by a number of mechanisms. These include the production of immunosuppressive cytokines, the inhibition of T cell activation by altering TCR complex, the induction of Tregs (60-62). pDC subsets are another important immunosuppressive group. Especially in ovarian cancer, tumor cell products are known to activate pDCs, which are, then, induce expansion of IL-10-producing $CD8^+$ Tregs (63). Many tumors promote polarization of monocytes to M2-like macrophages. These polarized tumor-associated macrophages (TAMs) are influenced by IL-4 and IL-13 and can impede anti-tumor responses through production of IL-10 and TGF-β (64).

All in all, the balance between the immune-stimulatory conditions and the inhibitory mechanisms determines the rate of the tumor progression and tumors' capacity to avoid immune responses.

2.3.2. Immune Responses in AML

Both innate and adaptive immune cells are able to recognize AML cells, eliminate or maintain equilibrium for preventing tumor growth. However, AML is able to generate an immunosuppressive environment in the bone marrow (BM) wherein strong immune responses are profoundly deregulated (Figure2.2). Indeed, leukemic blasts in patients with AML can outgrow and overwhelm autologous or allogenic immune responses through various mechanisms. Such are expression of anti-inflammatory metabolic enzymes (e.g. IDO, arginase, nitric oxide (NO)), secretion of inhibitory cytokines or active suppression of immune cells through receptor–ligand interactions.

NK Cell Responses to AML

Innate immunity in the anti-leukemia responses is particularly governed by NK cells. Having a specific role in the innate immune system, NK cells exert direct anti-tumor activity via cytotoxicity and cytokine-secretion and summoning DCs and other immune cells to the tumor microenvironment, in order to support adaptive arm of the anti-tumor responses (65). In order to recognize the malignant or infected cells, NK cells express various activating and inhibitory receptors, and natural cytotoxicity receptors, in addition to co-stimulatory molecules. Briefly, these receptors are able to respond to cellular stress and self-major histocompatibility (MHC) class I and related molecules. The balance between activating and inhibitory NK cell receptors is especially deterministic for NK cell activity. When inhibitory killer inhibitory receptors (KIR) on NK cells engage to MHC class I ligands, cell-mediated cytotoxicity is prevented. If a cell alters or losses MHC class I expression, the inhibition state is lifted. NK cell activation can also be inhibited by the loss of an activating ligand on a cell's surface. Thus, tumor cells can adopt these mechanisms to evade NK-mediated destruction.

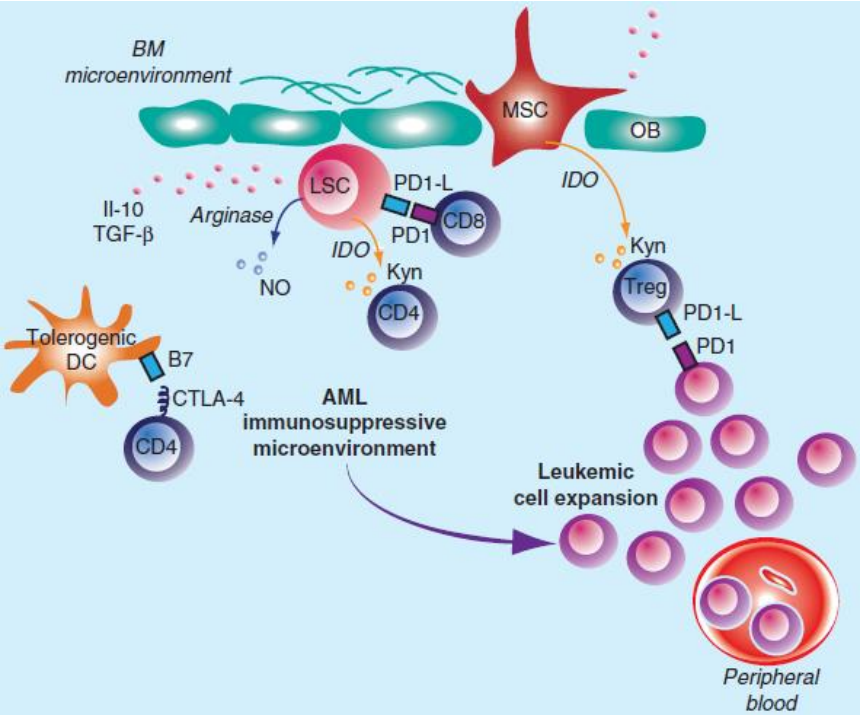

Figure 2.2. Major immunosuppression mechanisms in AML (66).

Leukemic stem cells (LSC) either themselves or with the help of other regulatory immune cells (Tregs, tolerogenic mesenchymal stem cells (MSC) and DCs) create an immunologically dysregulated environment which is also supported by the expression of other factors such as co-inhibitory ligands cytokines and metabolic enzyme expression.

In a clinical research on HLA-mismatch stem cell transplant (SCT) receiving AML patients, it was shown that allogeneic SCT can induce strong alloimmune responses together with efficient eradication of AML cells and reduce the risk of relapse (67,68). Accordingly, when allogeneic cells with a mismatch self-MHC class I molecules is given to a patient with AML, NK-mediated alloreactivity can occur. This observation notes the importance of NK cells for innate immunity against AML.

AML cells are able to escape from NK immune surveillance through various mechanisms. These include NK cell abnormalities, immune suppression and interactions with other immune cells. AML modulates the expression of activating and inhibitory molecules in its favor to escape. Downregulation of the activating molecules (NKp30, NKp44, NKp46) or

unfavorable KIR phenotype (KIR2DL2); AML resistance increased by downregulating the activatory ligand expression on its surface (NKG2D-L) or upregulating the immunosuppressive cell surface protein (CD200) or defects in cell-killing mechanisms (TRAIL, Fas-mediated killing) by high decoy or low receptor expressions; by suppression of NK cells by DC cells, by Tregs through TGF-β expression (69-79).

T cell Responses to AML

T cells are established key players in the immune surveillance of AML. Leukemic blasts from AML patients express several known leukemia-specific antigens (LSA) which can induce T cell responses. These antigens are self proteins that are either in abnormal quantities (over-expressed), post-translationally modified or truncated as a result of mutations or chromosomal abnormalities. Frequently identified LSAs are epithelial tumor antigen MUC1 and myeloperoxidase and proteinase 3 (80,81). However, AML cells utilize several mechanisms to escape from adaptive immunity. Catabolism of small molecules such as tryptophan and arginine by AML cells, the help of other cells in the microenvironment and expression of co-stimulatory molecules by AML cells are established mechanisms.

Indoleamine 2,3-dioxygenase (IDO) functions in the tryptophan kynurenine metabolism. Tryptophan starvation due to its consumption by IDO inhibits T cell activation whereas tryptophan catabolites such as free oxygen radicals support T cell proliferation and survival (82). As for AML cells, IDO is constitutively expressed, which employ an immunosuppressive environment for T cell responses. It was also shown *in vitro* that IDO supports conversion of $CD4^+CD25^-$ cells into $CD4^+CD25^+$ Tregs which deteriorate T cell immunity (83).

A similar immunological tolerance is induced in the tumor microenvironment by myeloid-derived suppressor cells (MDSCs) through arginine metabolism. MDSCs, especially in case of solid tumors, are known to act as immune depressants. One of the immune suppression mechanisms exerted by MDSCs from arginase I expression (84,85). A resembling

mechanism is also employed by AML cells as an immune escape mechanism (85).

T cell functions are directed by co-stimulatory molecules which are either activatory or inhibitory. As tricky as it gets, AML blasts are known to promiscuously express potent co-stimulatory molecules such as CD86 and inducible T cell co-stimulator ligand (ICOS-LG) that can induce efficient T cell activation (8,10,86). Surprisingly, a number of independent studies demonstrated that $CD86^+$ and/or $ICOS\text{-}LG^+$ AML cells are correlated with negative prognosis and poor clinical outcomes (8,10,86). This controversy was elucidated in an *in vitro* study on helper T cell responses against AML cells. It was suggested that $CD86^+$ AML cells provoke PD-L1 and PD-L2 as an adaptive resistance against anti-tumor responses by the upregulation of inhibitory molecules (87).

Accordingly, recent studies have provided that one of the mechanisms by which tumor cells evade immune surveillance by the regulation of immunological checkpoint receptors such as programmed death-1 (PD-1) and cytotoxic T-lymphocyte antigen-4 (CTLA-4). Normally, the interaction of PD-1 and CTLA-4 expressed by activated T cells with their ligands PD-L1 (B7-H1)/PD-L2 (B7-DC) and CD80/CD86 (B7-1/B7-2), respectively, on APCs and non-hematopoietic stromal cells maintains peripheral tolerance and facilitates cessation of immune responses (88). However, cancer cells such as AML blasts are also able to express PD-L1 and CTLA-4 ligands so that they can conceal the efficient induction of anti-tumor T cell responses (89). In fact, the inhibition of PD-1/PD-L1 in several murine models resulted in elevated anti-tumor immunity and reduced tumor growth (5,90-92). In a murine model of AML, PD-L1 expressing blasts are able to promote immune escape which leads to AML progression. Although further investigation is needed on CTLA-4, its expression on AML cells points out a similar mechanism to PD-1. CTLA-4, which is expressed on activated T cells and a subset of Tregs, reduces T cell effector functions upon ligating to its ligands CD80/CD86 (88). Intriguingly, a recent report on a cohort of AML patients, demonstrated a single-nucleotide polymorphisms CT60, located in the

3’untranslated region of the *CTLA-4* gene, was associated with a higher rate of leukemic relapse and a lower overall survival (93).

2.4. Co-stimulatory Signals in T Cell Activation

Inflammatory responses are exerted under the control of accessory receptors expressed on the immune cells. Naïve T cells rely on three distinct signals for their activation and function (94,95). Antigen recognition occurs through the interaction of T cell receptor (TCR) and its cognate antigen peptide in the context of MHC molecules on antigen presenting cells (APCs)(88). This accounts for the initiator signal, the *first* signal. The *second* signal is provided by co-stimulatory molecules upregulated on activated APCs that indulges survival, proliferation and differentiation of T cells during activation. The *third* skews the differentiation towards a particular type of effector T cell and is maintained by cytokines secreted derived from the activated APCs.

Co-stimulatory receptors direct T cell function and determine their fate. In the absence of co-stimulation, T cell activation halts and T cell goes to anergy. This emphasizes a pivotal need for secondary supporting signals for T cell activation (96).

The repertoire of T cell co-signalling receptors are usually defined as cell-surface molecules that can transduce signals into T cells to positively (via co-activatory receptors) or negatively (via co-inhibitory receptors) fine-tune TCR signaling. These co-signalling molecules are frequently versatile and able to respond to changes in the tissue environment. Their cognate co-signalling ligands and counter-receptors have been identified on various cell types, but they are critically expressed on APCs asthe primary inducers of T cell activation and differentiation (97).

Most of the co-signalling molecules are of tumor necrosis factor receptor superfamily (TNFRSF) and of immunoglobulin superfamily (IgSF). TNFRSF receptors are composed of one or more extracellular cysteine-rich domains (CRDs), but their ligands contain a conserved extracellular TNF homology domain (THD). Some of the best known TNFRSF receptors with co-stimulatory functions are HVEM, death receptor-3 (DR3; TNFRSF25),

CD40 (TNFRSF5) and lymphotoxin-β receptor (LTBR; TNFRSF3).On the other hand, the TNFSF receptors found on Th cells are restricted. The IgSF family plays a non-redundant central role in the cross-talk between T cells and APCs. Among IgSF co-signalling families, CD28 – B7 include the most well-recognized receptor-ligand couples which have significant impact on T cell responses.

2.4.1. CD28 - B7 Receptor – Ligand Family

The CD28 family primarily favors the binding of the members of B7 molecules except for two cases; the co-inhibitory receptor B and T lymphocyte attenuator (BTLA) binds to the TNFSFR member herpes virus entry mediator (HVEM), and B7-H6 binds to the natural killer cell p30-related protein (NKp30) of the natural cytotoxicity receptor family (98).

Certain B7 family members are also capable of dual function. When engaged to their specific receptors, CD80 (B7-1) and CD86 (B7-2) can either activate or inhibit T cell activation. While ICOS-LG sends supporting signals as a co-activatory molecule; whereas, B7-H1, B7-H4 and B7-DC act as co-inhibitory molecules. There are also some ligands such as B7-H3 whose function is either not clear or may display bimodal (both activatory and inhibitory) activity.

B7 family ligands are critical molecules that regulate T cell responses. CD80, CD86, ICOS-LG (B7-H2), PD-L1 (B7-H1) and PD-L2 (B7-DC) are the well-characterized members of the B7 family molecules. These molecules can either boost T cell activation through interacting with co-activatory receptor or dampen T cell responses, upon interacting with co-inhibitory receptors (99).

In the immunological synapse, CD28 which is constitutively expressed on naïve $CD4^+$ and $CD8^+$T cells interacts with CD80 and CD86. This provides essential co-stimulatory signals for T cell activation, proliferation and survival (100). CTLA-4, co-inhibitory receptor, is induced on activated T cellto suppress T cell responses (Figure2.3). As CTLA-4 expression becomes elevated, CD28 is downregulated by trans-endocytosis. On the other side, CD86 is constitutively expressed on the APCs and only lowered to some

extent but it never diminishes. Activated APCs induce transcription, translation and transportation of both CD80 and CD86 to the cell surface. Retrograde signaling from CTLA-4-bound CD80 and CD86 may induce the expression of indoleamine 2,3 dioxygenase (IDO) to suppress activation of conventional T cells and to promote regulatory T cell functions.

The surface interactions between the co-signalling receptors activate several signaling events. The downstream signaling pathways of the TCR and co-signalling molecules may overlap. CD28 and ICOS co-stimulatory signaling pathways such an example. CD28 has YMNM and PYAP motifs in its cytoplasmic tail (101). The proximal YMNM motif associates with phosphatidylinositol 3-kinase (PI3K) which induce targeting of AKT to activate various distal signal transduction (101). The interaction between CD28-PI3K-AKT pathways promotes T cell proliferation and survival. Additionally, these two motifs of CD28 are also important counterparts required for interleukin-2 (IL-2) production (102). ICOS contains a unique YMFM SH2-binding motif that recruits subunits of PI3K (103). ICOS signaling via PI3K and the induction of IL-4, IL-10 and IL-21 expression are critical for ICOS mediated development of type 2 helper T cell (Th2) responses (104). Nevertheless, because ICOS lacks PYAP motif, it fails to trigger IL-2 production as efficient as CD28 (102). Furthermore, ICOS induces IL-4 production through C-MAF pathways (105).

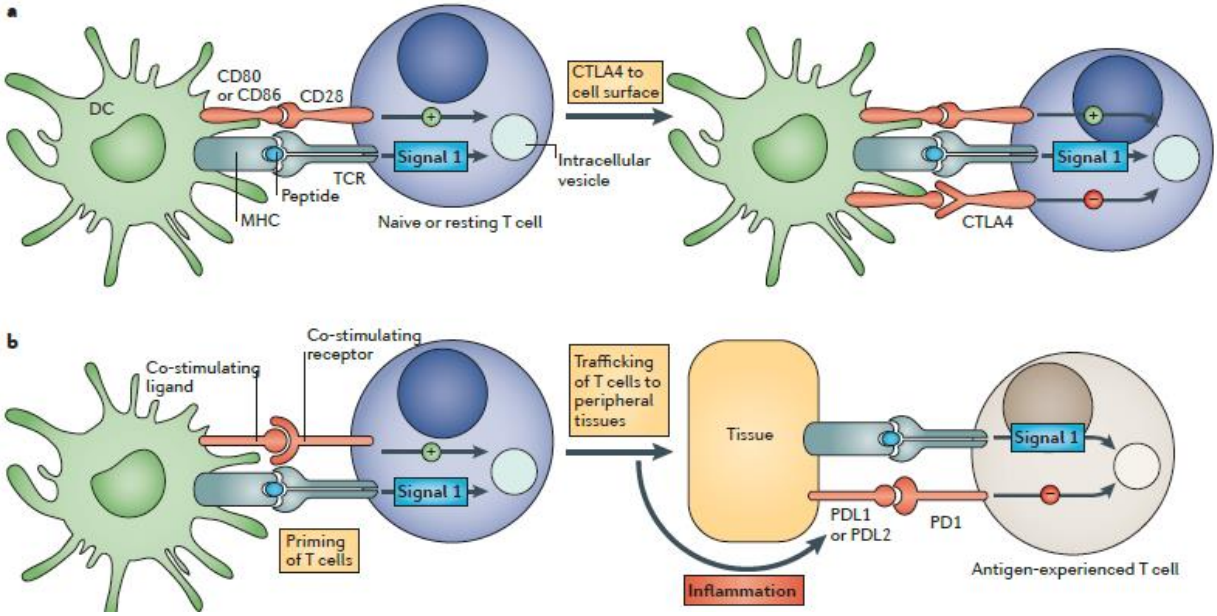

Figure 2.3. The CD28-B7 interactions in the immunological synapse (5).

a. CD28-CTLA-4 interaction is regulated on a time-dependent manner and adjusted in accordance with the amplitude of the initial TCR signal. CTLA-4 is sequestered in intracellular vesicles and at the time of initial encounter with the antigen via strong TCR (and CD28) signal, CTLA-4 is deposited on the T cell surface. CTLA-4 functions to dampen the overall signals which maintain a consistent level of T cell activation. **b.** In contrast to CTLA-4, the role of PD-1 is rather to regulate inflammatory responses by effector T cells recognizing antigen in peripheral tissues. Activated T cells upregulate PD-1and continue to express it in tissues. In response to inflammatory signals in the tissues induce expression of PD-1 ligands, which downregulate the T cell activity to hinder collateral tissue damage.

ICOS-LG is promiscuously expressed on B cells, macrophages, and certain non-lymphoid tissues (epithelia and endothelial cells). Upon binding to its receptor ICOS on B and T cells, co-activatory signals are produced. ICOS/ICOS-LG interaction induces $CD4^+$ T cell activation, differentiation and regulation. In a study by Yao et al., it was also shown that ICOS-LG has an affinity for binding CD28 and it is able to induce sufficient signal for T cell activation (106). ICOS usually favors Th2 cell proliferation and supports their functions. However, ICOS may also mediate differentiation of other types of T helper cells (Th1, Th17, TFH and Treg) under certain circumstances (103,104). *In vivo* studies on ICOS proved that it supports cytokine production of both Th1 and Th2 cells during initial stimulation and effector phases (107).

There are two critical co-inhibitory receptors, CTLA-4 and PD-1, upregulated on activated T cells. PD-1 predominantly regulates effector T cell activity within tissues and tumors, while CTLA-4 primarily regulates T cell's activation (Figure 1.3).

CTLA-4, is expressed exclusively on T cells where it regulates the amplitude of early stages of T cell activation. CTLA-4 counteracts the activity of CD28. The highly conserved MYPPPY motif of the proline-rich FG loop of CD28 and CTLA-4 is detrimental for binding the FG loop of CD80 and CD86, and analogous FDPPPF motif on ICOS essential to bind to ICOS-LG. The exact mechanisms of CTLA-4 are still ambiguous, yet, CTLA-4 is known to have a higher overall affinity for both ligands. Thus, it outcompetes CD28 in binding to CD80 and CD86, in addition to deliberately sending inhibitory signals to T cell(108). Among many potential signaling pathways, phosphatase SHP2 appears to be very important in counteracting kinase signals that are induced by TCR and CD28 (100).

In contrast to CD28 and CTLA-4, PD-1 lacks a well-organized FG loop and proline-rich XXPPPXX motif present in CD28, CTLA-4 and ICOS (109).Therefore, PD-1 interacts with FG loops of PD-L1 and PD-L2 through residues that are disseminated on the IgV domain. Engagement of PD-1 by one of its two ligands, PD-L1 and PD-L2, PD-1 inhibits kinases that are involved in the inhibition of T cell activation majorly through SHP2 (54,110-114). Thus, its primary mission is to limit the excess activity of T cells in response to infections and to limit autoimmunity (114,115).However, this translates into a critical resistance mechanism in the tumor microenvironment (116). PD-1 expression on activated $CD4^+$ and $CD8^+$ T cells was shown to create an immune suppressive environment through interacting with its ligands on peripheral tissues, activated T and B cells, monocytes and DCs(95). It is also highly expressed on Tregs (117).

2.5. T cell Exhaustion

In the course of viral infections, antigen-specific naïve $CD8^+$ T cells undergo activation, massive proliferation followed by cellular changes where T cells acquire effector functions such as production of antiviral cytokines

(such as IFN-γ and TNF-α) and elevation of cytotoxicity (118,119). At approximately 90-95% of the effector T cell population dies by apoptosis, the survivors differentiate into long-term memory T cells. Although memory $CD8^+$ T cells downregulate some effector functions and adopt a resting phenotype, they retain their high proliferation capacity and expand dramatically upon re-infection (118,119). In addition, the memory $CD8^+$ T cell population can persist in the long-run, even in the absence of antigen, and sustain homeostatic self-renewal primarily maintained through IL-7 and IL-15 (119-121).These properties of memory cells generate protective immunity even long after the virus has been cleared.

While these cascade of events are often caused by acute infections or by vaccination, during chronic infections or cancer, $CD8^+$ T cell responses are impaired and virus-specific $CD8^+$ T cells fail to differentiate into memory cells(122). Chronic antigen stimulation causes deterioration of T cell responses drawing a picture of ‘exhausted’ virus-specific $CD8^+$ T cells with limited effector functions. T cell exhaustion was first described in mice with chronic lymphocytic choriomeningitis virus (LCMV) infection (123,124). Although functional effector cells are initially generated, these functions are eventually lost in a hierarchical manner as the pathogen persists(125). Certain properties such as IL-2 production, cytotoxicity and proliferation are forfeited early, while TNF-α production is diminished later (Figure2.4) (125). Finally, at an advanced stage of exhaustion, IFN-γ production is lost (125). In a severe exhaustion scenario, together with high levels of antigen and absence of $CD4^+$ T cell help antigen-specific $CD8^+$ T cells are identified with completely impaired effector functions or they can be even physically deleted (125-129).

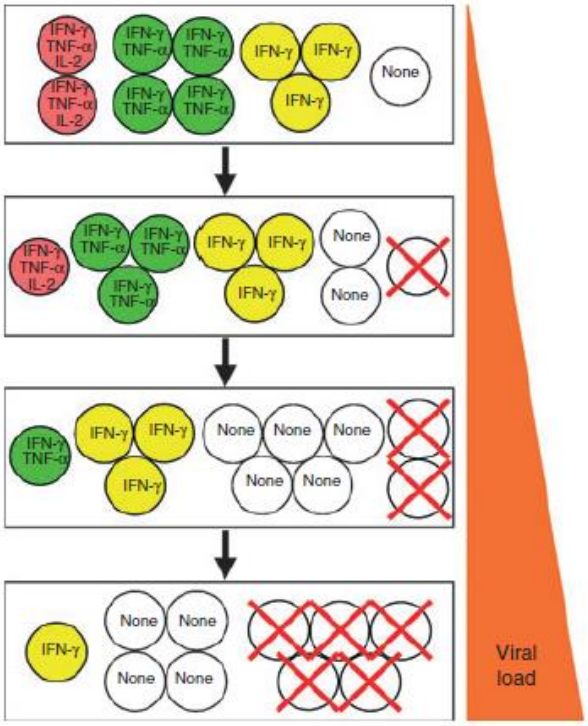

Figure 2.4. T cell exhaustion characteristics (130).

Exhaustion develops progressively and in a stepwise manner. As the viral load is enhanced over time, reductions in the functional potential of the population occur.

Exhaustion phenomenon has emerged on a subset of T cells with unique characteristics from the other differentiated subsets (i.e. effector or memory T cells), as well as T cell populations of different states (i.e. anergic, senescent or stem-like T cells) (6,7,131). What is more, recent studies have begun to shape the exhaustion profile not only by the definition of cellular differentiation state, by phenotype or by function but also through the usage of state-of-the-art molecular and transcriptional profiling. Thus, now it is possible to distinguish T cells with exhausted phenotype.

2.5.1. T cell Exhaustion and Activation Markers

T cell exhaustion is mainly constituted by immunoregulation in which soluble factors (e.g., IL-10), immune regulatory cells (e.g., regulatory T (T_{reg}) cells), and inhibitory receptors (e.g., programmed cell death 1 (PD-1)) play

fundamental roles. The latter is especially significant to pinpoint due to the central role of inhibitory receptors (iRs) on adaptive immunity, including self-tolerance and autoimmunity (132). Even though there are some shared expressions of certain iRs, they can be transiently found on effector T cells during activation. Exhausted T cells are marked by the stable expression of multiple iRs such as PD-1, CTLA-4),T-cell immunoglobulin and mucin domain-containing protein-3 (TIM-3), CD160, 2B4 (CD244), lymphocyte activation gene 3 (LAG3), and, B and T-cell lymphocyte attenuator (BTLA) on both $CD8^+$ and $CD4^+$ T cells (133,134).

T cell biology relies on a broad range of co-stimulatory and co-inhibitory signals integrating in the complex T cell signaling network which stoichiometrically directs the T cell into priming, activation, differentiation, and memory responses(135). However, the exact role of several iRs in this complex system is yet to be elucidated.

The signals triggered by PD-1 and PD-L1, is one of the most outstanding pathways in exhaustion. PD-1 is the most well-identified inhibitory molecule upregulated on exhausted T cells upon persistent antigenic stimulation but only transiently expressed on effector T cells during acute infections and is absent on memory T cells (136). Moreover, it is associated with disease progression and immune dysfunction (136). Thus, this molecule is widely targeted in the clinical studies and recent data have highlighted that blockade of this pathway resuscitate virus-specific $CD8^+$ T cell responses lowering the viral load in a chronic infection setting(137). In addition, T cell exhaustion associated with high levels of PD-1 expression often occurs during chronic infections (such as human immunodeficiency virus (HIV)(138-140), hepatitis B virus (HBV)(141), hepatitis C virus (HCV)(142), simian immunodeficiency virus (SIV)(143)) where interfering with the PD-1/PD-L1 interaction can restore T cell responses, *in vitro*. Having the brake released upon blockade, T cells overcome the exhaustion by enhancing the proliferation of $CD8^+$ and $CD4^+$cells and boost cytokine production (140). Notably, PD-1 blockade plays a critical role in limiting the effectiveness of antigen-specific T cells both in viral infections and in cancers (132,133).

Although PD-1 is the best characterized receptor in T cell exhaustion, several other receptors of CD28 family member have been shown to impair T cell functions such as CTLA-4 (144). It is denoted that exhausted antigen-specific $CD8^+$ T cells have elevated CTLA-4 mRNA, however, blockade of CTLA-4 has a minor effect on viral load or T cell responses during persistent infections (137,145).Additionally, there was no synergistic effect of co-blokade with CTLA-4 and PD-1(145).

Another important receptor to sustain sufficient protective T cells responses is TIM-3. It is a type I membrane glycoprotein expressed on terminally differentiated Th1 cells and innate immune cells (146-148). Ligation of TIM-3 on T cells to its only confirmed ligand, Galectin-9 (gal-9), inhibits Th1 responses which are crucial to infection, autoimmunity, peripheral tolerance, and inflammation (148-150). A study conducted by Nagahara et al. showed a dual role of TIM-3 signalling pathway mediating pro-inflammatory cytokine production in naïve dendritic cells (DC) and monocytes (151). They are especially shown to function as both co-stimulatory and co-inhibitory molecule. On the other hand, TIM-3 has a strong correlation to PD-1 co-expression and its expression shows a parallel between the exhausted state and disease severity during many cases of persistent stimulation (148,152-154). In line with co-expression, blockade of these surface molecules rescues T cell effector functions; cell cycle progression, sustained cytokine expression and cytotoxicity (152,155). In fact, dual manipulation on both of these co-inhibitory molecules was more effective for the recovery of the exhausted antigen-specific $CD8^+$ T cells (156).

The correlation between the co-expression and exhaustion phenotype is not merely limited to PD-1 and TIM-3. The presence of various iRs marks antigen-specific $CD8^+$ T cells which undergo a ‘deep-exhaustion’ state under the influence of a number of negative signals followed after T cell activation. A milestone research by Blackburn et al. investigated the effect of co-expression of several of these iRs on exhaustion in the course of chronic infection (157). Here, many other markers such as CD160, 2B4, LAG3 were found to contribute to $CD8^+$ T cell exhaustion (157).

For some receptors, especially for CD160 and 2B4, the mechanism of signaling is quite ambiguous and whether the receptor is an activator or an inhibitor has not been clearly elucidated. CD160, a glycosylphosphatidylinositol-anchored member of the immunoglobulin superfamily, is found on cytotoxic lymphocytes and on a portion of unstimulated $CD4^+$ T cells (158). CD160 is recently identified as ligand for herpes virus entry mediator (HVEM) molecule. BTLA is another cognate ligand for HVEM. The engagement of HVEM to CD160 or BTLA delivers co-inhibitory signals (158). Blocking the interaction between HVEM and CD160/BTLA results in a stronger T cell activation and indicates a regulatory mechanism in $CD4^+$ T cell activation (158).

Besides PD-1 and 2B4, LAG3 remains to be highly expressed on virus-specific $CD8^+$ T cells during chronic infection (7). LAG3 is a key molecule in immune checkpoint that mediates T cell activation and homeostasis. In addition, both *in vivo* and *in vitro* blockings showed that absence of LAG3 causes naïve $CD4^+$ T cells to adopt a Th1 phenotype(159). LAG3 is also co-expressed with PD-1 on antigen-specific lymphocytes and notably, dual blockade leads to more robust immune responses than that obtained with single treatment. Thus, LAG3 is another important co-inhibitory molecule in T cell homeostasis and a synergistic cooperation between LAG3 and PD-1 operates on potent T cell responses (116).

Although over-expression of particular iRs which are considered to be the molecular signature of exhausted T cells, Legat et al. proposed a link between iR expression and the activation and differentiation status of T cells (Figure 2.5)(134). Accordingly, several of these molecules show distinct expression patterns depending on T cells' differentiation stages (134). All in all, it makes the differentiation and activation stages appear to be important concepts to evaluate in the exhaustion phenomenon. Following the receipt of activation signals, T cells induce the expression of specific markers that indicate their activation and/or differentiation status. Most of these activation markers display transient expression dynamics.

CD69, a 22.5kD type II transmembrane homodimeric glycoprotein, is transiently expressed on T cells as early as 2 hours post-activation and is

subsequently downregulated approximately 55-60 hours following activation (160,161). Thus, CD69 expression is widely used as an indicator of early activation. On the other hand, CD25, the 55kD low affinity IL-2 receptor α chain, a type I transmembrane glycoprotein appears at 13-25 hours post-activation and remains on the surface at high levels (162,163). Thus, its expression coincides to later phases of activation. Moreover, receptors for T cell-tropic cytokines such as IL-2 (CD25) and IL-7 (CD127) expressed by $CD4^+$ T cells can be used for distinguishing into sub-populations. For instance, $CD127^+CD25^{low/-}$ subsets indicate IL-2-producing naïve and central memory T cells; $CD127^-CD25^-$ subsets include effector T cells expressing perforin and IFN-γ; while, $CD127^{low}CD25^{high}$ subsets point out FoxP3-expressing regulatory T cells (164). CD127 receptor is the α chain of IL-7R. Engagement to IL-7 enhances TCR-mediated signaling, and thus, primes the newly activated T cell for proliferation and IL-2 production (165).

iR:	Changes of iR expression				iR+ cells show less cytokine production than iR− counterparts, considering:		
	With differentiation	With activation[a]	In normal LN[b]	In TILN[b]	Total cells (≈artifact[c])	Subsets (i.e., corrected for differentiation)	Anatomical location
PD1	Increased (+ in effectors)	+++	Presence of PD1hi	Presence of PD1hi	Opposite!: IR+ = slightly more cytokines	No	Trend in LN
CTLA-4	(Absent in steady state)	++++	Increased	Increased	Yes (slightly)	Yes in non-naive/CM	Yes in HD PBMC; trend in all other locations
TIM-3	Increased in N and EMRA	+++	Similar	Can be increased	Trend	No	Trend in patient blood and TILN
LAG-3	(Absent in steady state)	++++	Similar	Can be increased	NA	NA	NA
CD160	Increased (+ in EMRA)	Stable	Increased	Similar	Yes (note very low fraction of iR+)	Yes	Yes in blood; trend in LN
2B4	Increased (progressive+)	Stable or –	Similar	Decreased	Opposite!: IR+ = more cytokines	No (iR+ slightly more functional)	All locations similar
KLRG1	Increased (progressive+)	Stable or –	Similar	Decreased	Opposite!: IR+ = more cytokines	No (iR+ slightly more functional)	All locations similar
BTLA	Decreased (progressive –)	Stable or +	Slightly increased	Slightly increased	Yes	No	All locations similar

Figure 2.5. Expression of certain iRs and their link to cytokine production in $CD8^+$ T cells, relating to differentiation, activation, and anatomical location (134).

Additionally, CD25 and CD127 expressions are characterized in a subset of $CD4^+$ T cells; Tregs. This subset is commonly identified by high CD25 surface expression and/or intracellular expression of forkhead box P3 (FOXP3) transcription factor (166,167). FOXP3 is especially significant for development and function of suppressor cells (166,167). Also, these Tregs express $CD127^{low/-}$ discriminating them from the conventional T cells (164,168). The expression of CD127 is inversely correlated with FOXP3 expression and with the suppressive function of $CD25^{high}$ Tregs.

Having received enough activation signals, T cells express certain surface molecules that are only specific to activated cells. Besides CD69 and CD25 mentioned above, CD154 (CD40L) is primarily expressed on activated T cells of early-onset acting as a co-stimulatory molecule easing the cell-to-cell communication in adaptive immunity. Other co-stimulatory molecules such as CD80, ICOS are promiscuously found on activated T cells. These molecules have counterparts, such as CTLA-4, PD-1, PD-L1 that are co-inhibitory molecules also expressed on activated T cells much later than the co-stimulatory molecules. This fashion enables T cells to be negatively regulated to keep them away from constitutive activation.

Adding more to the list, HLA-DR and CD38 markers can also be used as representatives of early activation and differentiation of T cells (169). CD38 is known to be the marker of early differentiation and activation of T lymphocytes (170). Activated T lymphocytes are not only identified by CD38 expression but also in combination with HLA-DR. In fact, these so-called activation antigens are often found in chronic diseases, especially in HIV-infected T lymphocytes. Both $CD4^+$ and $CD8^+$ T cells showed HLA-DR and CD38 expression significantly higher than that of in symptomatic and asymptomatic HIV-infected subjects (171).

2.5.2. T cell Exhaustion in Cancer

Functional exhaustion is not limited to chronic infections, but may also arise in a similar setting of persistent antigenic stimulation that is also postulated in cancer (Figure 2.6). Tumor antigen-specific T cells often proliferate, but they remain at a low frequency and their functions are

significantly modulated by the microenvironment (4). Together with the long-term exposure to tumor antigens, T cells adapt an exhausted phenotype under the influence of local activatory and inhibitory signals (5,6).

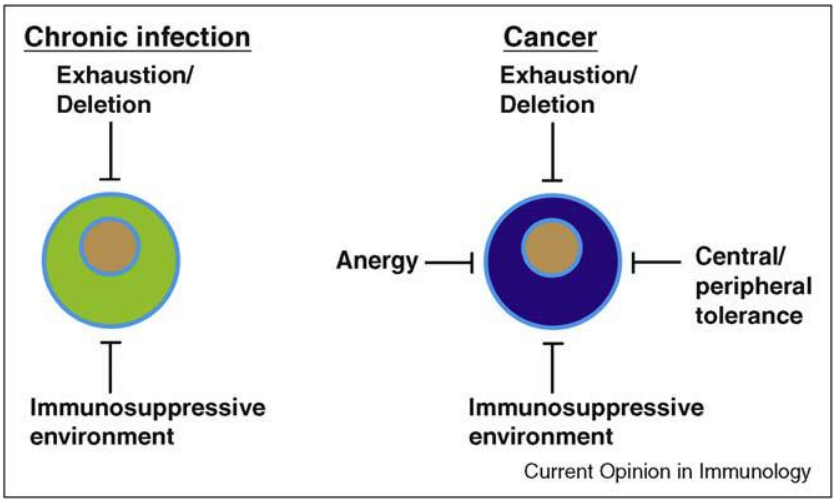

Figure 2.6. Behavior of T cells under the conditions of chronic infection and cancer (172).

Cancer and chronic infections can be perceived as analogs since they have common features such as providing a continuous source of antigens and forming an immune modulatory microenvironment. However, viral antigens are easily processed and thus, highly immunogenic; whereas, tumor antigens are self-molecules that are poor immunogens. Moreover, high-avidity T cells that might have possessed the capacity to recognize tumor antigens are deleted as a part of thymic selection process. Due to low immunogenicity of tumor antigens and the inadequate number of tumor-reactive T cells, cancer cells are able to escape from the immune surveillance. In order to overcome these two obstacles, one strategy was to adoptively transfer *in vitro* stimulated and expanded tumor-specific T cells to enable tumor elimination. It was reported that central memory tumor-reactive $CD8^+$ T cells exhibited a far more effective anti-tumor activity than effector memory T cells (173). Also, IL-2-induced tumor-specific $CD8^+$ T cells manifested more potent effector functions *in vivo* than their counterparts treated with IL-5 (174). Eventually, unless an army of well-educated T cells

are prepared to combat for tumor clearance, the present tumor-infiltrating lymphocytes will only be kept silenced by the microenvironment.

Strategies involving adoptive transfer of tumor-reactive $CD8^+$ cytotoxic lymphocytes (CTLs) expanded and differentiated *in vitro* received by lymphopenic hosts was shown to augment anti-tumor immunity in animal models and patients with cancer. However, a different strategy on adoptive transfer was developed using $CD4^+$ T cells since they are essential to support CD8 T cell functions. Additionally, $CD4^+$ T cells secrete a multitude of cytokines that either directly exert effector functions or prompt other immune cells. Activated $CD4^+$ T cells express important ligands (e.g., CD40L) to interact with B cells, dendritic cells (DCs) and $CD8^+$ T cells. Hence, this approach made it possible to eradicate large, established and vascularized tumors (175-177). Surprisingly, despite the efficacy of adoptive T cell transfer strategies employing helper T cells, tumor recurrence surpasses. This can only be explained by prevalence of the immunosuppressive environment exerted by the increase in Tregs, loss of antigen expression and amplified inhibitory ligand expression by tumor cells (54,178,179).

Similar to virus-specific T cells, tumor-reactive T cells exposed to high levels of tumor antigens undergo both phenotypic (upregulation of inhibitory molecules such as PD-1, CTLA-4, LAG3 and TIM-3) and functional modifications (depletion of effector cytokines). Thus, exhaustion profiles of the two chronic inflammatory diseases notably resemble each other. For instance, in metastatic melanoma patients, $CD4^+$ TILs were shown to upregulate PD-1 and majority of $CD8^+$ TILs were CTLA-4^+, which was predominantly expressed by PD-1^+ $CD8^+$cells (180,181). Additionally, PD-1^+ $CD8^+$ TILs were mostly $CD25^-$ and $CD127^-$, albeit HLA-DR^+, denoting that they had diminished capacity to proliferate, differentiate into memory cells and produce cytokines (181). $CD4^+$ TILs were also lacked CD25, but overexpressed CTLA-4 (181). In a different study on human metastatic melanoma, again, $CD8^+$ TILs were shown to upregulate PD-1 and the number of cytokine-producing cells was increased upon PD-1 blokade (111). Besides PD-1 and CTLA-4, LAG3 was also found on majority of $CD8^+$ TILs in cancer patients and in mouse tumor models (182,183). In mice bearing solid

tumors (colon adenocarcinoma, mammary adenocarcinoma and melanoma), both $CD4^+$ and $CD8^+$ TILs displayed co-expression of PD-1 and TIM-3. Majority of $CD8^+$ TILs were $TIM\text{-}3^+PD\text{-}1^+$ in all forementioned models and virtually all $TIM\text{-}3^+$ TILs co-expressed PD-1 (184). Additionally, in a murine model of colon adenocarcinoma, $PD\text{-}1^+$ single positive TILs that did not express TIM-3 produced the highest levels of IFN-γ among all TIL populations. Since this particular population was also actively produced IL-2 and TNF-α, $TIM\text{-}3^+PD\text{-}1^+$ population might represent the most exhausted TILs in this cancer model. This pattern of co-expression is also found on $CD8^+$ T cells of mice with advanced acute myelogenous leukemia (AML)(185). In this AML model, the number of $TIM\text{-}3^+$ $PD\text{-}1^+$ $CD8^+$ T cells increased as the disease progressed. Combined treatment anti-PD-L1 and TIM-3Ig significantly reduced the tumor load and with increased the survival rate of mice. In contrast, chronic lymphocytic leukemia (CLL) exhibits a slightly different exhaustion profile. $CD8^+$ T cells from CLL patients showed a marked expression of CD244, CD160 and PD-1, but a stable expression of certain exhaustion markers such as CTLA-4, TIM-3 and LAG3. Cytokine production was another unusual trait of $CD8^+$ T cells in CLL. It was intriguing that these cells had increased production of IFN-γ and TNF-α together with reduced IL-2 production (186,187).

3. MATERIALS AND METHODS

This work was done in Hacettepe University Cancer Institute, Department of Basic Oncology Laboratories through February 2014 – April 2015. It was approved by the Local Non-invasive Clinical Research Ethics Committee at Hacettepe University (Doc. Nr.: 16969557 – 1200).

3.1. Materials used in this research

The chemicals and biological materials used in this study and their suppliers are listed below:

Phosphate buffered saline (PBS) tablet, 2-mercaptoethanol, Diethyl pyrocarbonate (DEPC), Lipopolysaccharide (LPS), Trypan blue, Ionomycin (Sigma-Aldrich Co., USA); 10x Tris-borate-EDTA (TBE) buffer (Dr. Zeydanlı, Turkey); Seakem® Le Agarose (Lonza, USA); Ethanol (AppliChem, Germany); L-glutamine, Penicillin-streptomycin, RPMI-1640 (Lonza, Switzerland); Fetal bovine serum (FBS) (Biological Industries, Israel); Primer oligonucleotides (Alpha DNA, Canada);10x Taq buffer $(NH_4)_2SO_4$, $MgCl_2$ (25 mM), dNTP mix (2mM), Taq DNA polymerase, Oligo $(dT)_{18}$ primer, Deionized nuclease-free water, 5x RT reaction buffer, dNTP mix (10mM), Ribonuclease inhibitor, Reverse transcriptase, 50 bp DNA ladder, 6x Loading dye (Thermo Scientific, USA); QuantiTect SYBR Green PCR Kit (QIAGEN, Netherlands); *Ficoll* 1.077 (Biochrome AG; Germany); Carboxyfluoresceinsuccinimidyl ester (CFSE) (Invitrogen, USA); rhICOS-Fc chimera, rhCTLA-4-Fc chimera, rhPD-1-Fc chimera, rhIFN-γ, rhIL-2 (R&D Systems, USA); Phorbol 12-myristate 13-acetate (PMA; Cell Signaling, USA); Non-essential amino acids (HyClone™, GE Healthcare, United Kingdom); 10X Bovine serum albumin (BSA) (Fermentas, Lithuania);FACS Flow, Cell wash (BD Biochemicals, USA); Anti-human CD3 monoclonal antibody (clone: HIT3a), LEAF™ purified anti-human CD28 antibody (clone: CD28.2), LEAF™ purified mouse IgG1 isotype control antibody (clone: MOPC-21), Annexin V-FITC apoptosis detection kit, Propidium iodide staining solution, Cell proliferation dye eFlour 670 (RedCFSE), Legend Max™ human IL-10, TNF-α, TGF-β, IL-4, IL-2 ELISA kits with pre-coated plates (eBiosciences, USA); Dimethyl sulphoxide

(DMSO)(OriGenBiomedical AB, Sweden);Cell culture flasks, Falcon tubes, sterile strainers (Corning, USA); 96-well plates, Serological pipettes (Costar, USA).

3.2. Buffers and solutions

PBS solution: 1x PBS solution was freshly prepared by dissolving 1 tablet in 500 mL of distilled water as directed by the manufacturer. Then, the solution was bottled and sterilized utterly by autoclaving.

TBE buffer: 1x TBE buffer was diluted from 10x TBE buffer with distilled water.

FBS (heat-inactivated): FBS was thawed at 4˚C or at room temperature. Then, it was incubated at 56˚C for 30 minutes. Aliquots of 50 mL heat-inactivated serum were prepared and stored at -20˚C.

Complete RPMI-1640 cell culture medium: In order to obtain a complete culture medium, 55 mL (final concentration~ 10%) heat-inactivated FBS, 5.5 mL (final concentration~ 1%) L-glutamine, and 5.5 mL (final concentration~ 1%) penicillin and streptomycin were added into 500 mL RPMI-1640 medium and mixed well. Only for Kasumi-1 cell line, the final concentration of FBS was increased to 20%. The complete culture media were stored at 4˚C.

Preparation of recombinant protein solutions: rhICOS-Fc chimera, rhCTLA-4-Fc chimera, rhPD-1-Fcchimera, and rhIFN-γ were obtained in lyophilized form from the manufacturer and reconstituted at recommended concentrations in sterile PBS or PBS containing 0.1% BSA, as described below. Aliquots of all recombinant protein solutions were stored at -80˚C.

rhICOS-Fc chimera was reconstituted at 100 µg/mL in sterile PBS. Working solution of 1.5 µg/mL was prepared in sterile PBS and aliquoted for further use.

rhCTLA-4-Fc chimera was reconstituted at 500 µg/mL in sterile PBS containing 0.1% BSA. Working solution of 0.5 µg/mL was prepared in sterile PBS from stock solution of 25 ng/µL and was aliquoted.

rhPD-1-Fc chimera was reconstituted at 100 µg/mL in sterile PBS. Working solution of 1.5 µg/mL was prepared in sterile PBS and aliquoted.

rhIFN-γ was reconstituted at 0.2 µg/mL in sterile, deionized H_2O (dH_2O) and stored at -86˚C. Working solution of 200 U/mL was prepared freshly in serum-free RPMI-1640 and used immediately.

rhIL-2 was reconstituted at 100 µg/mL in sterile 100 mM acetic acid containing at least 0.1% BSA. Working solution of 0.25ng/mL was aliquoted in sterile PBS for further use.

LPS solution: 1 mg LPS was weighted under sterile conditions and dissolved in serum-free RPMI-1640 medium at 10 µg/mL final concentration. Then, working solutions of 100 µg/mL concentration was prepared in RPMI-1640 and aliquoted. Stock and working solutions were stored at -20˚C.

Carboxyfluoresceinsuccinimidyl ester (CFSE): 50 µg of CFSE powder was dissolved in 18 µL sterile DMSO to obtain 5 mM stock solution and stored at -86˚C.

Cell proliferation dye eFlour670 (Red-CFSE): Lyophilized red-CFSE was dissolved in sterile DMSO in order to obtain 5mM working solution and stored at -86˚C as instructed by the manufacturer.

Phorbol 12-myristate 13-acetate (PMA) solution: Supplied as a 200 µM stock in sterile DMSO from the manufacturer, a working solution of 5 ng/mL were prepared in serum-free RPMI-1640, aliquoted, and stored at -20˚C.

Ionomycin solution: Ionomycin powder was dissolved in sterile DMSO at a concentration of 10 mg/mL. Aliquots of 0.5 µg/mL working solution were prepared in serum-free RPMI-1640 and stored at -20˚C.

Anti-human CD3 monoclonal antibody solution: Anti-CD3 mAb was obtained at 1 mg/mL concentration. It was diluted in serum-free RPMI-1640 in order to obtain a working solution of 2 µg/mL. Aliquots were stored at -20˚C.

Preparation of aCD3-bound plates: Anti-CD3 mAb of 1 mg/mL was diluted in sterile PBS to obtain a stock solution of 5 µg/mL and stored at -20˚C. A working solution of 0.25 µg/mL was prepared freshly in sterile PBS prior to use. Bottom of each well subject to CD3 coating was covered with 50 µL working solution. The plate was tightly sealed with parafilm and incubated at 4˚C overnight. Prior to use, the remaining antibody solution was removed

and the wells were rinsed with 200 µL of sterile PBS. Just before seeding the cells, the plate was placed in incubator for 5 minutes at 37˚C.

Trypan blue solution: 40 mg trypan blue powder was dissolved in 99.8 ml saline or PBS to obtain 0.4% solution. The solution was filtered using 0.22 um sterile filters.

3.3. Cell culture and purification

3.3.1. Culture of cell lines and cells isolated from peripheral blood

HL-60 and Kasumi-1 (ATCC, LGC Promochem, USA), U937 and KG-1 (courtesy of Dr. Yulia Nefedova, H. Lee Moffitt Cancer Center, FL, USA), and THP-1 (a kind gift from Dr. Nesrin Özören, Bogazici University, Turkey) cell lines were cultured in complete RPMI-1640 in suspension. These AML cell lines have been classified into different French – American – British (FAB) groups according to the morphology and immunophenotype (Table 3.1). Cell lines were maintained with fresh medium twice or thrice a week, just before attaining the maximum cell densities as recommended by the original supplier (ATCC, LGC Promochem, USA). Peripheral blood mononuclear cells (PBMCs) or the specific subset of cells isolated amongst the PBMCs were also cultured in complete RPMI-1640 medium (see Section 3.3.3 for PBMC isolation). All the cells were incubated under standard conditions (37˚C and 5% CO_2) in a humidified incubator (Thermo Scientific, Hera Cell 150i, USA).

Table 3.1. FAB classifications of AML cell lines used in this study.

AML Cell Line	FAB Classification
KG-1	M0/1 (188,189)
Kasumi-1	M2 (190)
HL-60	M2/3 (189,191)
U937	M4/5 (192-194)
THP-1	M4/5 (194,195)

Thawing cryopreserved cell lines: A small beaker (50 mL) was filled with 20-25 mL dH_2O and placed into water bath at 37˚C. When the water became warm enough, the cryovial freshly recovered from the liquid nitrogen tank was seated into the beaker for a quick thawing. Complete medium was used to mix the cells gently and transfer them to a 50 mL Falcon tube. Then, the mix was centrifuged (Jouan CR3, UK)(5 minutes, 1800 rpm) to remove the residual cryo media containing DMSO. After discarding the supernatant, the pellet was resuspended in 10 mL fresh complete medium and transferred into a T-25 culture flask. Having being incubated (at 37˚C) for several days, the cells were transferred into a T-75 culture flask.

Subculturing of the AML cell lines: The subculturing methods were adapted specifically for each AML cell line. As soon as the cell cultures reached to a density over 60%, unless they were used in further procedures, the cells were subcultured. Leaving about 7-9 mL of a total volume of 21 mL cell mix in the flask, the rest of the mix was replaced with 10-12 mL fresh medium.

Cell counting: For an accurate cell count, a uniform suspension containing single cells is necessary. For this purpose, the cell suspension was gently dispersed by pipetting up and down and around 10 mL of the mix was transferred to a 50 mL tube. The cover slip and the Fuchs-Rosenthal cytometer (0.200 mm tiefe depth) (Hausser Scientific, USA) were utterly cleaned with 70% ethanol solution. 10 µL cell suspension was combined with 10 µL 0,4% trypan blue solution. If uniform enough, this mix was transferred to one of the Fuchs-Rosenthal chambers allowing the chamber to be filled by capillary action. Under a light microscope (40x), the cytometer was seen to have 16 small squares divided by bold grids as shown in Figure 3.1. Four of these 16 squares were randomly chosen and the cells scattered between the grids were counted and a cell concentration was calculated according to Formula 3.1.

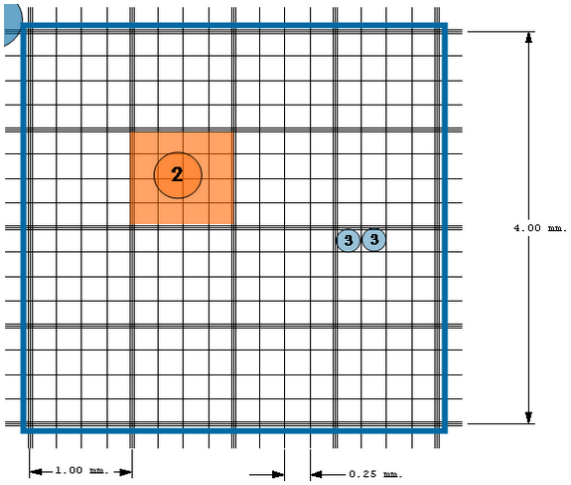

Figure 3.1. A closer look into Fuchs-Rosenthal cytometer (celeromics, Fuchs-Rosenthal Chamber Formulae, UK). Each small square is measured 0.25 mm and one side of each square is 1.00 mm (Total of 16 squares having a side of 1 mm).

(3.1)

$$\text{Area} = 1\ \text{mm} \times 1\ \text{mm} = 1\ \text{mm}^2$$

$$\text{Volume} = 1\ \text{mm}^2 \times 0{,}1\ \text{mm} = 0{,}1\ \text{mm}^3 = 1 \times 10^{-4}\ \text{mL}$$

$$\text{Cell Concentration} = \frac{\text{Total cell count} \times 10^4}{\text{Number of counted squares}} \times \text{Dilution factor}$$

3.3.2. Stimulation of cultured cells for ICOS-LG expression

AML cells or PBMCs were counted and seeded in complete medium. IFN-γ (200 U/mL) or LPS (1 µg/mL) were added to the corresponding cell cultures and incubated for various periods of time (4, 8, 16, 32, 64 and 128 hours) (Figure 3.2).Cells were collected at the end of each time point and taken for analysis.

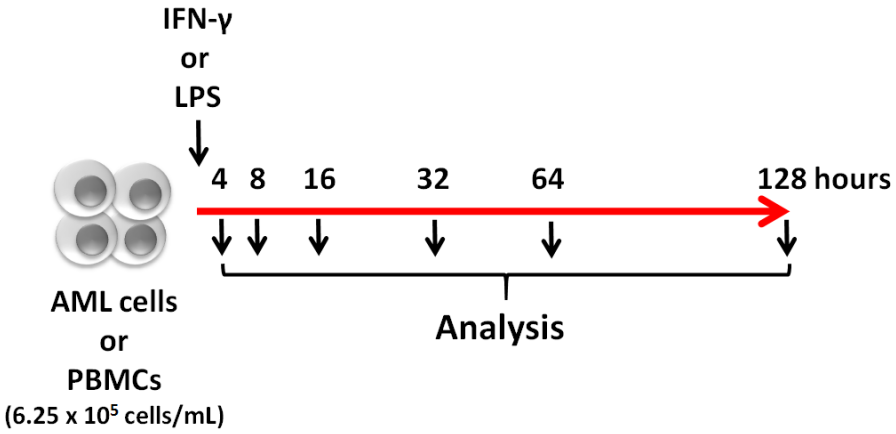

Figure 3.2. A schematic description of experimental set up for the stimulation of AML cells or PBMCs with IFN-γ or LPS.

3.3.3. Cell isolation and sorting

Isolation of mononuclear cells from peripheral blood: PBMCs were isolated from the blood obtained from healthy volunteers. Blood samples were collected into EDTA-containing tubes and were 1:1 mixed with serum-free RPMI-1640. Ficoll (3 mL, 1.077 g/mL) was added to the bottom of a 15 mL Falcon tube. The blood sample was gently layered onto Ficoll with a constant pace. The tube was centrifuged (25 minutes, 400x g) and the layer containing PBMCs were collected by using a Pasteur pipette. The cells were transferred to a 50 mL Falcon tube, washed with 1x PBS solution and centrifuged (5 minutes, 1800 rpm). Supernatant was discarded and pellet was resuspended in complete RPMI-1640. The cells of interest were labeled with appropriate antibodies (see Table 3.2) and then, sorted from the PBMCs by fluorescence-activated cell sorting (FACS) (FACSAria II, BD Biosciences, USA) as explained below.

Table 3.2. Antibodies used for sorting.

Antibody (Mouse anti-human)	Clone	Manufacturer	Fluorochrome	Final concentration in 100 µL (µg/mL)
CD4	L200	BD Biosciences, USA	APC	9.0
CD13	L138		PE	19.0
CD14	M5E2		FITC	7.0
TIM3	F38-2E2		PE	4.5

Purification of $CD4^+$ T cells and $CD14^+$ monocytes: Since it was difficult to obtain copious amount of monocytes for the co-culture experiments, monocytes were first enriched by incubating PBMCs in a complete medium in a T-75 culture flask for 2-3 hours at standard conditions. Adhered cells were recovered for monocyte-enriched fraction; whereas, the cells in suspension were recovered for T cell isolation; then, the cells were thereafter and centrifuged in 1800 rpm for 5 minutes. For the isolation of $CD4^+$ T cells and $CD14^+$ monocytes, they were resuspended in 1 mL PBS and labeled with anti-CD14-FITC, anti-CD13-PE and anti-CD4-APC monoclonal antibodies (mAb) and incubated at room temperature for 20 minutes in dark. Then, 2 mL full RPMI was added into the tubes and filtered using 70 um sterile strainers to remove any aggregates. For FACS, $CD4^+$ T cells and $CD14^+$ monocytes are gated as shown in Figure 3.3. The resulting purified $CD14^+$ monocytes and $CD4^+$ T cells were resuspended in appropriate volumes of complete media and maintained in the co-cultures (Section 3.3.4).

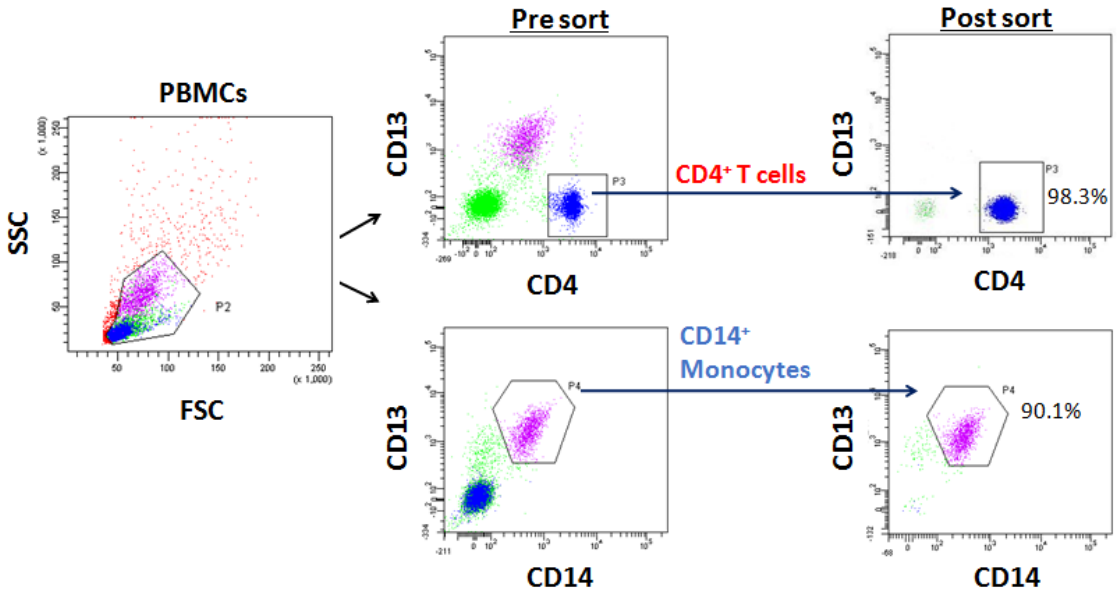

Figure 3.3. Isolation of $CD4^+$ T cell (P3) and $CD14^+$ monocyte (P4) populations from PBMCs by FACS. The first panel (on left) was designed considering the granularity (SSC) and size (FSC) of the PBMCs. The cells of interest (lymphocytes and monocytes) were gated as P2 on the panel. This gate was further channeled into a different panel for detecting CD13, CD4, and CD14-positive populations. Then, the sort efficiency was determined with post-sort reading in the cytometer.

Enrichment of $TIM3^{mo/hi}$ and $TIM3^{-/lo}$ cells from the co-cultures: The cells in the co-cultures (co-culture method is explained in 3.3.4) were harvested from the 96-well culture plates. The cells were collected in a 50 mL Falcon tube, centrifuged (5 minutes, 1800 rpm) and the supernatant was discarded; pellet was resuspended with 1 mL PBS. For the isolation of $TIM3^{mo/hi}$ and $TIM3^{-/lo}$ $CD4^+$ T cells, the mix was labeled with anti-CD4-APC and anti-TIM3-PE mAbs at room temperature for 20 minutes in dark. Then, 2 mL full RPMI was added into the tubes and filtered from 70 um sterile strainers.For FACS, $TIM3^{mo/hi}$ and $TIM3^{-/lo}$ $CD4^+$ T cells are gated as shown in Figure 3.4.

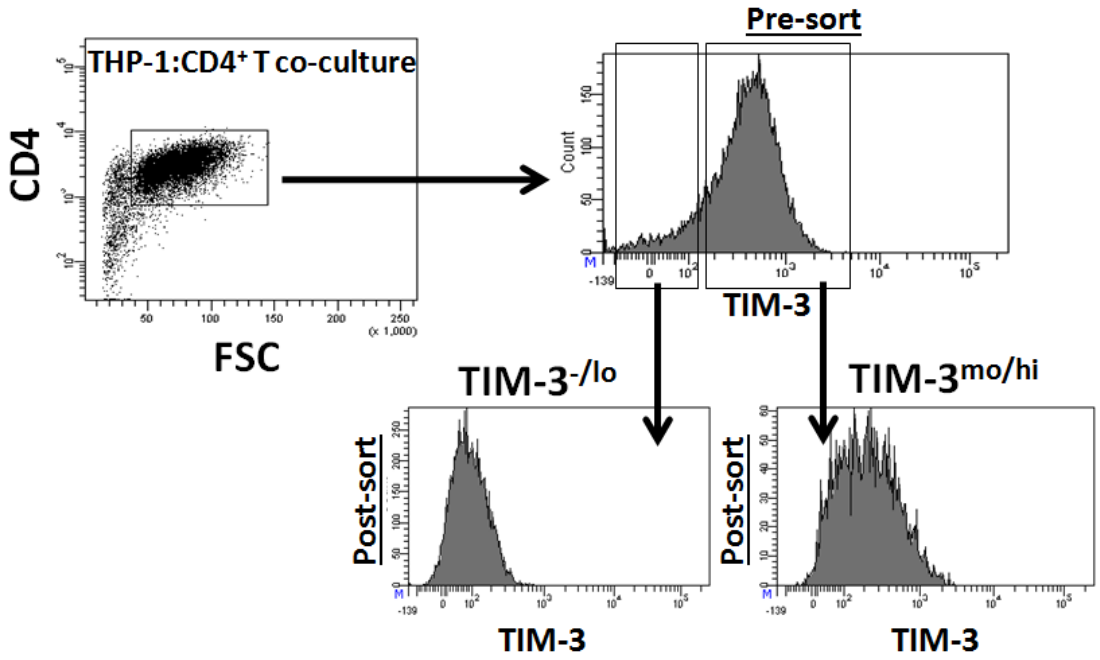

Figure 3.4. Enrichment of TIM3$^{mo/hi}$ and TIM3$^{-/lo}$ CD4^{+} T cell populations from THP1 and CD4^{+} T cell co-cultures by FACS. Co-cultured cells were first gated on a scatter plot for CD4 and size (FSC). These cells were further channeled into TIM3 expression panel. TIM3 negative/low (lo) and moderate (mo)/high (hi) populations were gated and sorted. Following FACS, the resulting populations were tested on flow cytometer.

Fluorescence-activated cell sorting (FACS):

In order to purify a certain population of cells, one has to set the flow cytometer for sort procedure. Cytometer was initially tested for accurate drop delay with BD FACS Accudrop Beads (BD Biosciences, USA). As a sorting strategy, the cells of interest were initially selected to be composed of singlets and then, gated based on side scatter (SSC) versus forward scatter (FSC) properties. Then, CD4^{+}CD13^{-} T cells and/or CD14^{+}CD13^{+} monocytes were gated (Figure 3.3).

For the recovery of CD4^{+} T cells from co-cultures (back-sort), a generic gate was drawn for FSC versus CD4. Then, CD4^{+}TIM3$^{mo/hi}$ and CD4^{+}TIM3$^{-/lo}$ populations were gated (Figure 3.4). Isolation of the targeted cell types was performed by FACS (FACSAria II, BD Biosciences, USA) and FACS Diva software.

Purity of isolated cells was analyzed by post-sort analyses on flow cytometry. The cells obtained from sorting with a cell purity ≥96% for T cells,

≥90% for monocytes were used in further experiments. TIM3$^{mo/hi}$ and TIM3$^{-/lo}$ populations were determined in the enrichment procedures with FACS. A loss in the fluorescence intensity especially in TIM3-positive population was observed since the cells were not relabeled prior to post-sort analyses.

3.3.4. Establishment of co-cultures

AML cell lines (HL-60, THP-1, Kasumi-1, KG-1, U937) were counted and seeded uniformly into a round bottom 96-well culture plate. CD4$^+$ T cells obtained by FACS were firstly stained with red-CFSE (as described in Section 3.4) and then, co-cultured with AML cells at different ratios or with different concentrations of aCD3 (Hit3a) mAb, as explained in detail below.

As a general procedure designed to obtain exhausted T cells, the medium and anti-CD3 (aCD3) antibody were refreshed every 24 hours in order to maintain adequate amount of supplements and TCR stimulation. Anti-CD3 was maintained at a constant concentration during refreshments. Briefly, 100 µL media from each well was carefully removed from the top of the well, leaving the cells at the bottom. Then, a mixture of fresh media and aCD3 (100 µL) was carefully added into each well. At the end of 96 hour-incubation, supernatants were collected from the co-cultures and cells were harvested for further analyses (Figure 3.5).

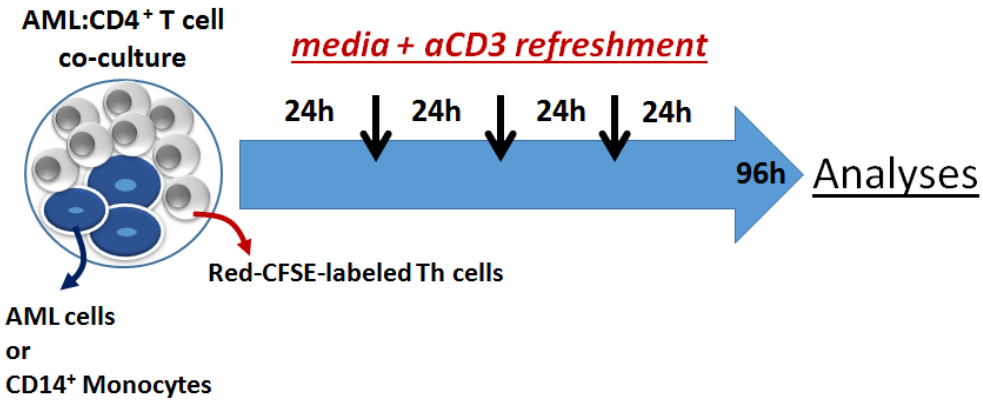

Figure 3.5. Experimental plan of the co-cultures for exhaustion induction. AML cells or CD14$^+$ monocytes were co-cultured with red-CFSE-labeled CD4$^+$ T cells. Co-cultures were supplemented with media and anti-CD3 mAb refreshments every 24 hours. At the end of 96 hours, co-cultured cells were harvested for analyses.

Modulation of co-culture ratios: AML cell lines (HL-60 or THP-1) were counted and seeded into round bottom 96-well plates at AML to $CD4^+$ T cell ratios of 0.25:1, 2:1, 4:1 as shown in Figure 3.6. Obtained by FACS, $CD4^+$ T cells were stained with red-CFSE (as described in Section 3.4) and stimulated at a final concentration of 25 ng/mL anti-CD3 mAb and supplemented with fresh medium and anti-CD3 mAb every 24 hours. The co-cultures were incubated (37˚C, 5% CO_2) for 96 hours.

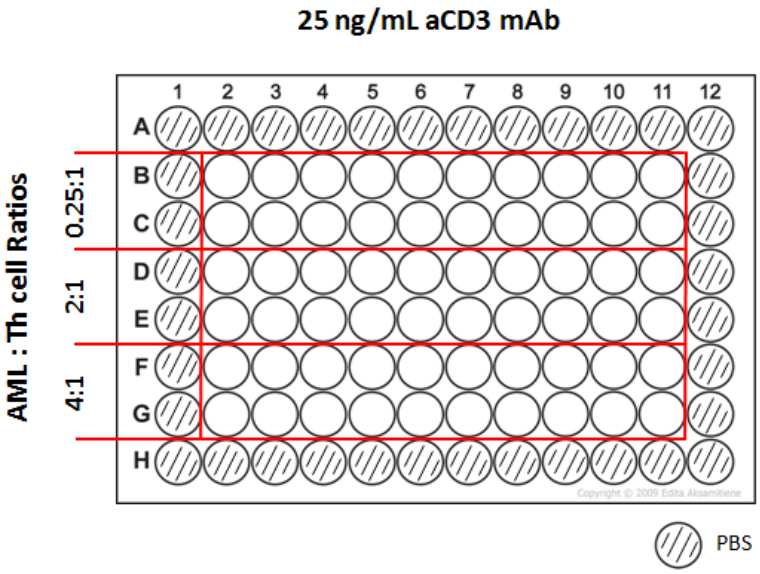

Figure 3.6. Schematic presentation of a 96-well plate prepared for AML:$CD4^+$ T cell co-cultures established at different cell ratios. (1 = 2.5 x 10^4 cells)

Modulation of anti-CD3 mAb stimulation: AML cell lines (HL-60 or THP-1) were counted and seeded into round bottom 96-well plates at a constant AML to $CD4^+$ T cell ratio of 2:1 as shown in Figure 3.7. Obtained by FACS, $CD4^+$ T cells were stained with red-CFSE (as described in Section 3.4) and stimulated at different concentrations of anti-CD3 mAb (100, 50, 25, 12.5, 6.25 ng/mL). Refreshment of the culture medium and anti-CD3 mAb was done every 24 hours in the appropriate concentrations keeping the starting (initial) concentration of anti-CD3 mAb constant. The co-cultures were incubated (37˚C, 5% CO_2) for 96 hours.

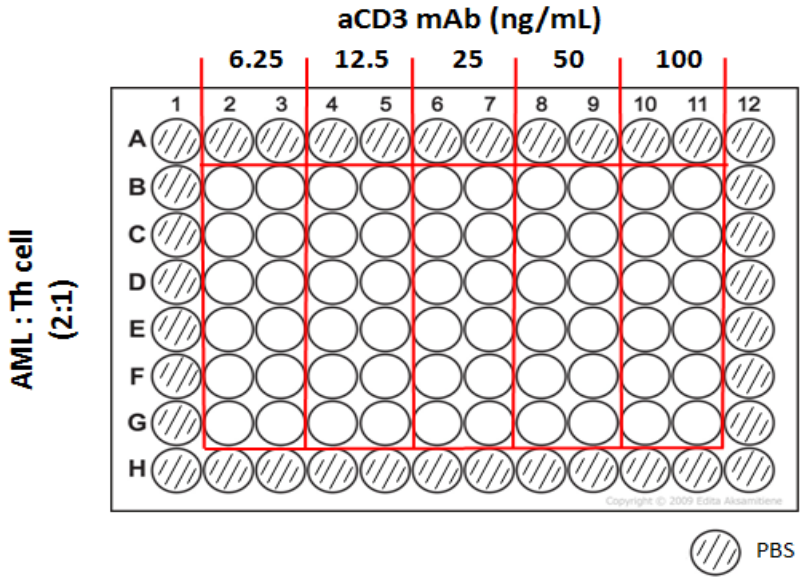

Figure 3.7. Schematic presentation of a 96-well plate prepared for AML:$CD4^+$ T cell co-cultures established with different anti-CD3 mAb concentrations.(1 = 2.5 x 10^4 cells**)**

Modulation of co-stimulatory signals in the co-cultures (refreshments with ICOS-Fc, PD-1-Fc, CTLA-4-Fc chimeric proteins): After THP-1 cells were seeded into 96-well plates, ICOS-Fc (1.5 µg/mL), PD-1-Fc (1.5 µg/mL), CTLA-4-Fc (0.5 µg/mL) recombinant chimeric proteins were added to each well. Then, $CD4^+$ T cells were added into each well in order to establish co-cultures. These co-cultures were prepared with a constant AML to $CD4^+$ T cell ratio of 2:1 and with 25 ng/mL anti-CD3 mAb. During 96-hour-incubation period, refreshments with media containing these recombinant proteins and aCD3 mAb were provided every 24 hours as described above in Section 3.3.4. All components were maintained at constant concentrations during refreshments.

3.3.5. Restimulation of T cells obtained from the co-cultures

In order to obtain $CD4^+$ T cells enriched in $TIM3^+$ and $TIM3^-$ populations, initially, THP-1 cells were co-cultured with $CD4^+$ T cells at 2:1 ratio and stimulated and refreshed with 25 ng/mL anti-CD3 mAb for 96 hours. Then, co-cultured $CD4^+$ T cells were back-sorted into two sub-populations as $TIM3^{-/lo}$ and $TIM3^{mo/hi}$ using FACS (as explained in Section 3.3.3). Back-sorted T cells were, stained with green-CFSE (as described in Section.3.4) and seeded ($2.5x10^4$/well) into 96-well plates. Both $TIM3^{-/lo}$ and $TIM3^{mo/hi}$ populations were stimulated with 5 ng/mL PMA and 0.5 µg/mL ionomycin; plate-bound aCD3 and 2 µg/mL of soluble anti-CD28 mAb; PBMCs (6250 cells/well, giving 0.25:1 PBMC:$CD4^+$ T cell ratio) and plate-bound anti-CD3; 0.25 ng/mL rhIL-2; or with plate-bound anti-CD3, soluble CD28 and rhIL-2. After 2 and 24 hours of incubation, supernatants were harvested from the PMA/ionomycin-induced cells. At the end of 96-hour incubation, the cells' proliferation stimulated with the agents except for PMA/ionomycin was analyzed by flow cytometry. PMA/ionomycin stimulations for 2 and 24 hours were analyzed by ELISA.

3.4. T cell proliferation with CFSE assay

Tracing the proliferation of $CD4^+$ T cells with eFluor670 (Red-CFSE) : After attaining $CD4^+$ T cells in suspension using FACS, the cells

were centrifuged (5 minutes, 1800 rpm). Supernatant was discarded and the cells were washed with PBS for two times in order to remove any remaining serum. The pellet was resuspended with serum-free medium ($1x10^6$ cells/mL). Red-CFSE was added into the cell suspension at a final concentration of 5 µM. Stirred slowly, the mix was incubated (at room temperature, for 10 minutes in dark. Then, 4-5 mL complete medium was added onto the mix and placed on ice for 5 minutes. The cells were washed with complete medium and centrifuged (5 minutes, 1800 rpm). Washing step was repeated for 3 times. After that, the cells were resuspended with complete medium and used in further experiments. Analyses were performed to measure the dilution of CFSE dye by flow cytometry (as described in Section 3.5).

Tracing the proliferation of restimulated $TIM3^{-/lo/+/hi}CD4^+$ T cells with CFSE (Green-CFSE): After enriching the $TIM3^-$ and $TIM3^+$ cells from the co-cultures by using FACS, the two populations were centrifuged (5 minutes, 1800 rpm). Having discarded the supernatants, the cells were resuspended with serum-free media ($1x10^6$ cells/mL). The cells were incubated in water bath (37˚C, 5 minutes) and then, CFSE (1 µL/mL) was added at a final concentration of 5 µM. Stirred slowly, the cells were incubated (37˚C, 15 minutes). Onto the cells, 40-45 mL of ice-cold complete media was poured and incubated for 5 minutes on ice. The cells were washed one more time with complete media and centrifuged. Then, the pellet was resuspended in appropriate amount of complete media ($2.5x10^4$ cells/100 µL) and used in further experiments. Analyses were performed to measure the dilution of CFSE dye by flow cytometry (as described in Section 3.5).

3.5. Flow cytometry

Immune-phenotyping: The cells either freshly obtained, or co-cultured or stimulated with various agents were collected, washed with PBS and the pellets were resuspended with appropriate volumes of 1xPBS and mixed by vortexing. 100 µL of the mix was uniformly distributed to the flow cytometry tubes and monoclonal antibodies were added by pipetting. List of

antibodies used is given in Table 3.3. Following incubation at 4˚C for 30 minutes in dark, the cells were washed with 1.2 mL PBS and centrifuged (5 minutes, 1800 rpm). Supernatant was discarded. 100 µL of 1X PBS was added onto the cell pellet and mixed by vortexing. Cells were gated and analyzed on a FACSAria II flow cytometer (BD Biosciences, USA). Since the isotype antibody is non-specific for the molecule of interest, the percentage of positive cells was calculated by comparison with the appropriate isotype-matched control antibodies (Table 3.4).

Table 3.3. Antibodies used for flow cytometric analyses.

Antibody	Clone	Manufacturer	Fluorochrome	Final concentration in 100 µL (µg/mL)
CD4	L200	BD, USA	APC	10
CD4	SK3	Biolegend, USA	APC	2
CD13	L138	BD, USA	PE	10
CD14	M5E2		FITC	10
CD25	M-A251		FITC	10
CD38	HIT2		FITC	10
CD69	FN50		FITC	10
CD80	2D10	Biolegend, USA	PE	2
CD86	IT2.2		PE	2
CD127	hIL-7r-M21		PE	2
CD152 (CTLA-4)	L3D10		PE	2
CD154 (CD40L)	24-31		FITC	2
CD197 (CCR7)	150503	BD, USA	PE	10
CD274 (PD-L1)	MIH1		PE	10
CD275 (ICOS-L)	9F.8A4	Biolegend, USA	PE	2
CD278 (ICOS)	C398.4A		FITC	2
CD279 (PD-1)	EH12.2H7		PE	2
FoxP3	236A/E7		APC	2
HLA-DR	G46-6	BD, USA	FITC	10
LAG3	FAB2319F	R&D Systems, USA	FITC	10
TIM3	F38-2E2		PE	2

Table 3.4. Isotype control antibodies used for the assessment of positive cells during flow cytometric analyses.

Antibody	**Clone**	**Manufacturer**	**Fluorochrome**	**Final concentration in 100 µL (µg/mL)**
IgG1, Κ	MOPC-21	Biolegend, USA	APC	10
IgG1/G1	X40/X40	BD, USA	FITC/PE	10
IgG1/G2a	X40/X39		FITC/PE	10
Armenian Hamster IgG	HTK888	Biolegend, USA	FITC	2

Proliferation Analysis: Since red-CFSE emits at 670 nm, it was analyzed through FL4 (APC) channel, positive cells were gated and the proliferation capacities were evaluated. Because the intracellular CFSE becomes diluted as the cell divides, low and high proliferating cells can be easily gated based on the CFSE intensity (Figure 3.8). Mean fluoresencence intensity (MFI) values were also determined by FACSDiva software (BD Biosciences, USA).Proliferative activity of the cells was determined by the calculation of CFSE dilutions according to Formula 3.2.

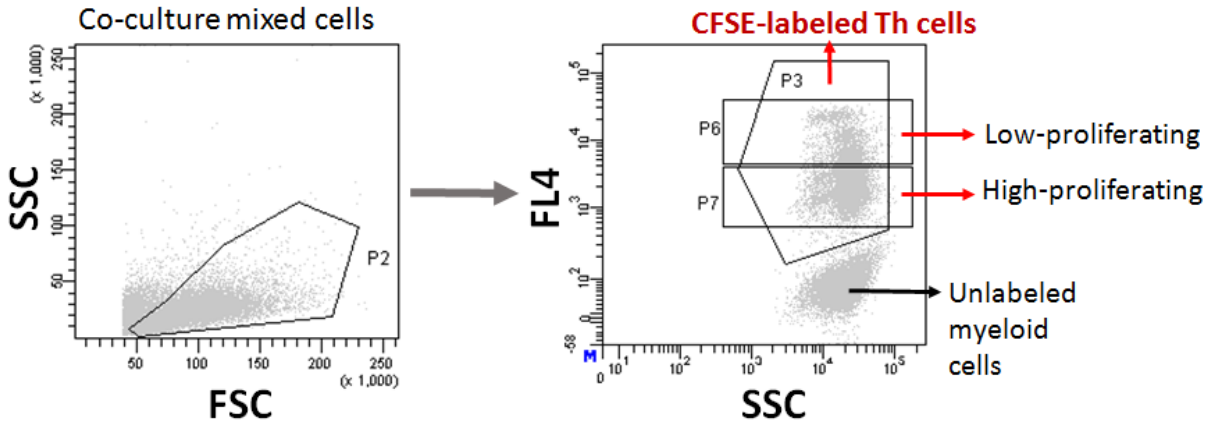

Figure 3.8. Gating strategy for red-CFSE-labeled T cells and discrimination of low and high proliferating populations. The first panel (left) was designed considering the granularity (SSC) and size (FSC) of the cells recovered (P2) from the co-cultures. The cells were further channeled into the next panel (right), where red-CFSE-labeled cells were gated in P3. This gate was further elaborated into P6 and P7 gates, in order to select low-proliferating and high-proliferating cells, respectively.

(3.2)

$$\text{CFSE Dilution} = \frac{\text{Initial CFSE MFI}}{\text{Final CFSE MFI}}$$

Determination of cell viability by annexin V–propidium iodide (PI) staining: The cells recovered from the co-cultures were washed with cold 1XPBS by gently and centrifuged (5 minutes, 1800 rpm). The pellet was resuspended in 100 µL Binding Buffer (1x)(eBiosciences, USA) by gently pipetting. 5 µL Annexin V-FITC and 5 µL PI were added by gently pipetting and incubated for 15 minutes in dark at room temperature. After adding 100 µL of Binding Buffer (1x), the cells were analyzed by flow cytometry.

Intracellular staining: The cells were washed with 1xPBS and centrifuged (5 minutes, 1800 rpm). Supernatant was discarded and onto the remaining pellet Cytofix/Permeabilization solution (1x, BD Biosciences, USA) was added. The cells were incubated at 4˚C for 30 minutes in dark and washed with 1.2 mL 1x Permeabilization Buffer and centrifuged (5 minutes, 1800 rpm). This step was repeated for two times. The cells were

resuspended in 150 µL 1xPermeabilization Buffer and anti-FoxP3 monoclonal antibody (Table 3.3) was added by gently pipetting. After incubation at 4˚C for 30 minutes in dark, the cells were washed with 1.2 mL 1xPBS and centrifuged (5 minutes, 1800 rpm). The pellet was resuspended with 100 µL 1xPBS and analyzed on flow cytometer.

3.6. Enzyme-linked immunosorbent assay (ELISA)

Supernatants from the co-cultures established with $CD4^+$ T cells and AML cells (HL-60, THP-1) or $CD14^+$ monocytes from the co-cultures of AML cells (HL-60, THP-1) with $CD4^+$ T cells in the presence of blocking chimeric proteins rhICOS-Fc, rhCTLA-4-Fc, rhPD-1-Fc and control IgG were harvested and centrifuged at 1800 rpm for 5 minutes at 4˚C. Supernatants were collected on ice and stored at -80˚C. Prior to use, the samples were brought to room temperature and vortexed briefly before pipetting into ELISA plates. The reagents were also brought to room temperature 15 minutes before using.

IL-2, TNF-α, IFN-γ, IL-10, IL-4 and TGF-β were detected by commercial ELISA kits (Biolegend, USA) according to the manufacturer's instructions. Briefly, the ELISA plates were provided in the kit as coated with the appropriate antibodies. Each kit included a lyophilized standard which was reconstituted by the addition of a volume of Assay Buffer (provided in the kit) indicated on the vial label in order to obtain the standard stock solution. The reconstituted standard was allowed to wait at room temperature for 15 minutes and briefly vortexed before use. This top standard solution was used to perform serial-dilutions in different tubes by using Assay Buffer as a diluent. Each tube was mixed thoroughly before use. 1X Assay Buffer was used as the zero standard (0 pg/mL). All ELISA procedures shared a common wash step with 1x Wash Buffer diluted freshly from 20x concentrate with deionized water. The plates were initially prepared by washing for four times with at least 300 µL of 1x Wash Buffer per well. These wash steps and the following interval wash steps followed by a firm tapping of the plates on absorbent paper to remove the residual buffer. Then, the subsequent procedures specific for each assay were followed according to the

manufacturer's manual. Into each well that will contain either standard or samples were 50 µL Assay Buffer was added. Starting from the standard solutions, 50 µL standards and samples were added into appropriate wells. Each plate was sealed and incubated at room temperature for 2 hours while shaking at 200 rpm. The plates were, then, washed with 1X Wash Buffer for four times. 100 µL of Detection Antibody was added to the appropriate wells, sealed and incubated at room temperature for 1 hour while shaking at 200 rpm. The plate was washed for four times and then, 100 µL of Avidin-HRP solution was added. The plate was sealed and incubated at room temperature for 30 minutes while shaking at 200 rpm in dark. After being washed for five times, 100 µL Substrate Solution was added and incubated for 15 or 20 minutes in the dark. The reaction was stopped by adding 100 µL Stop Solution into each well. In order to quantify the amount of cytokine secretion, the plates were processed with an optical reader (Microplate spectrophotometer, SpectraMax Plus, Molecular Devices, USA) at 450 nm and 570 nm, the absorbance at 570 nm was subtracted from the absorbance at 450 nm. Standard curves were drawn for each cytokine (Figure 3.9) and OD values were calculated by using SoftMax® Pro Microplate Data Acquistion and Analysis Software (Molecular Devices, LLC., USA).

A)

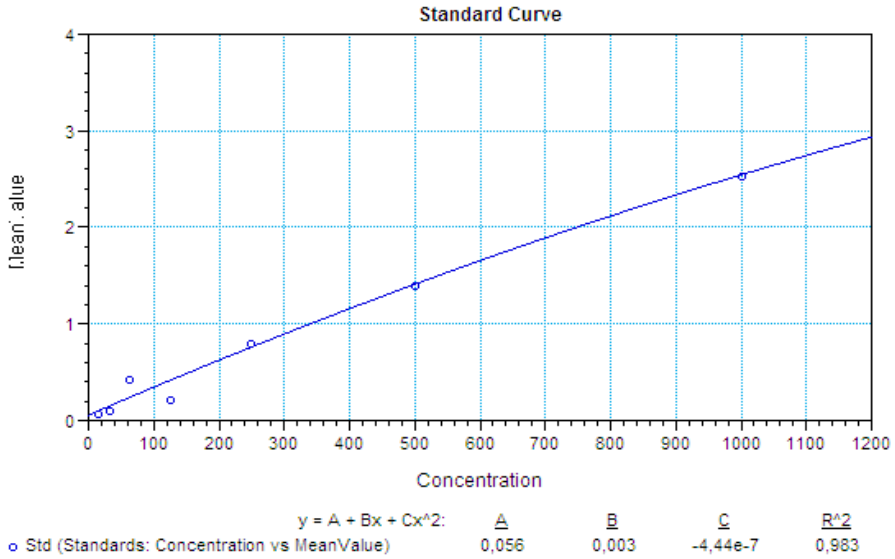
Standard Curve
MeanValue
Concentration
y = A + Bx + Cx^2: A B C R^2
Std (Standards: Concentration vs MeanValue) 0,056 0,003 -4,44e-7 0,983

B)

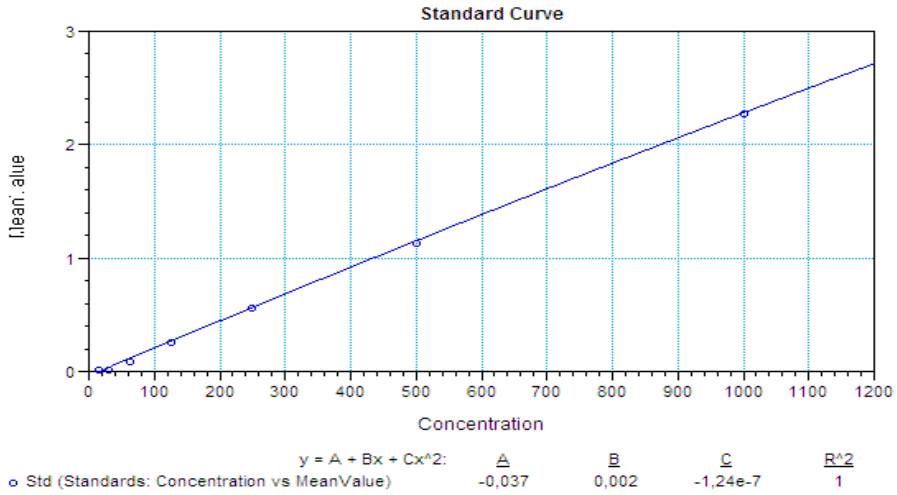
Standard Curve
MeanValue
Concentration
y = A + Bx + Cx^2: A B C R^2
Std (Standards: Concentration vs MeanValue) -0,037 0,002 -1,24e-7 1

C)

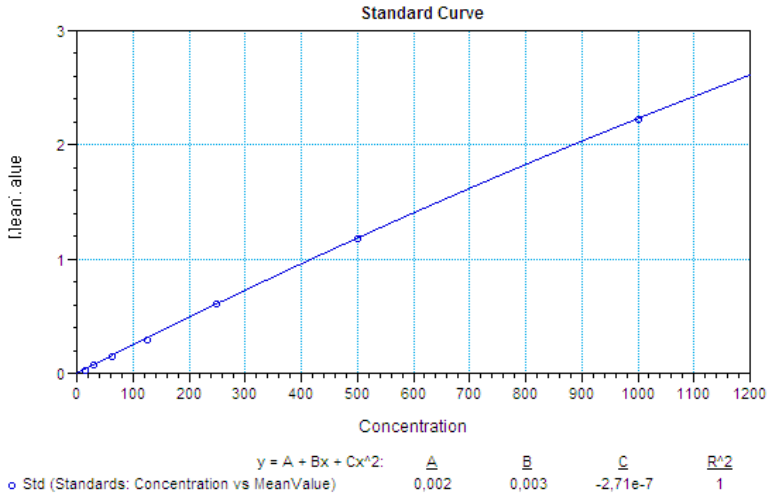
Standard Curve
Mean value
Concentration
y = A + Bx + Cx^2:
A
B
C
R^2
Std (Standards: Concentration vs MeanValue)
0,002
0,003
-2,71e-7
1

D)

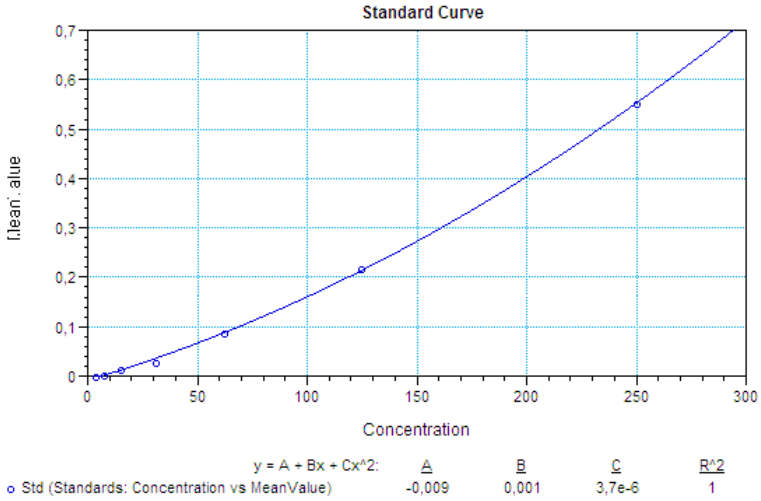
Standard Curve
Mean value
Concentration
y = A + Bx + Cx^2:
A
B
C
R^2
Std (Standards: Concentration vs MeanValue)
-0,009
0,001
3,7e-6
1

E)

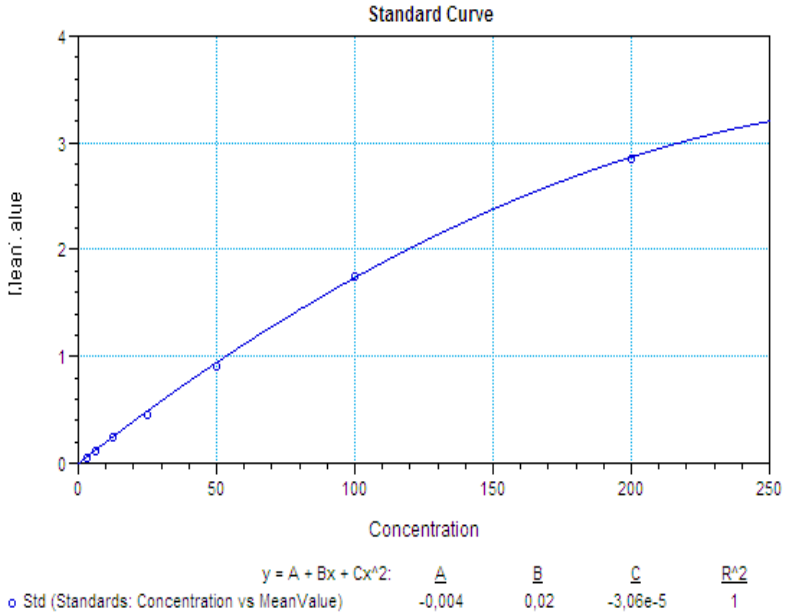

F)

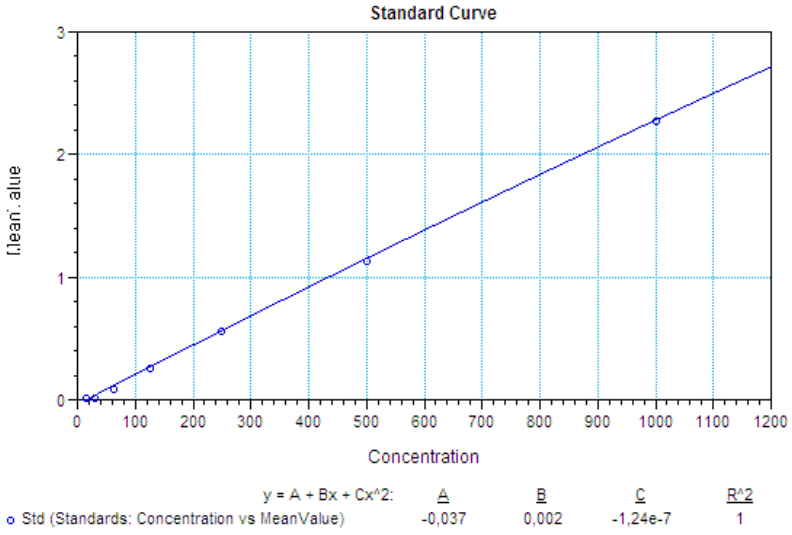

Figure 3.9. Standard curves drawn for A) IL-2, B) TNF-α, C) IFN-γ, D) IL-10, E) IL-4, F) TGF-β ELISAs.

3.7. Molecular Techniques

3.7.1. Total RNA Isolation

In order to isolate total RNA from cell cultures QIAmp® RNA Blood Mini Kit (QIAGEN, Germany) was used. Briefly, cells were centrifuged (5 minutes, 1800 rpm), supernatant was discarded and 350 µL of buffer RLT containing 10% β-mercaptoethanol was poured onto the pellet. The mix was pipetted harshly up and down and vortexed to burst out the all the cells. 350 µL of 70% ethanol was added and the mixture was transferred to a QIAmp spin column followed by a quick centrifuge (20 seconds, 10000 rpm). After discarding the flow-through 700 µL buffer RW1 was added and centrifuged (20 seconds, 10000 rpm). The flow-through was discarded and 500 µL buffer RPE was added to the column. Then, the column was centrifuged (20 seconds, 10000 rpm) and the flow-through was discarded. 500 µL buffer RPE was added to the column and centrifuged (4 minutes, 13000 rpm). The column was placed in a new collection tube and centrifuged (1 minutes, 13000 rpm). The column was, then, transferred to a 1.5 mL DNase-RNase-free microcentrifuge tube. 30 µL RNase-free water was added directly onto the center of the column (membrane) and centrifuged (1 minutes, 10000 rpm). Isolated RNA samples were stored at -86˚C.

3.7.2. RNase-free DNase treatment

In order to remove residual genomic DNA in the RNA samples, RNA Clean & Concentrator kit (Zymo, USA) was used. 20 µL DNase-RNase-free water, 5 µL DNase I Buffer (10x), 3 µL recombinant DNase I (2 U/µL) was added and mixed gently with RNA. This mix was incubated at 37˚C for 45 minutes. Two volumes of RNA Binding Buffer was added to the samples. Then, one volume of 70% ethanol was added to the mix and it was transferred to the Zymo column and centrifuged (1 minute, 13000 rpm). 400 µL RNA Prep Buffer was added and centrifuged (1 minute, 13000 rpm). After discarding the flow-through, 700 µL RNA Wash Buffer was added and centrifuged (30 seconds, 13000 rpm). This wash step was repeated with 400

µL Wash Buffer and centrifuged for 2 minutes at 13000 rpm. The column was, then, transferred to a RNase-free tube and eluted with appropriate volume of DNase-RNase-free water. The water was added directly onto the center of the column matrix, incubated (1 minute, room temperature) and centrifuged (30 seconds, 13000 rpm). RNA samples were stored at -86˚C. The absence of residual DNA in RNA samples was determined with PCR (Section3.7.5). For the samples giving positive reaction, the DNase treatment was repeated.

3.7.3. Spectrophotometric analysis of RNA

The concentration and quality of the isolated RNA were measured with an UV spectrophotometer (NanoDrop ND-1000, USA) at 260 nm, 230 nm, and 280 nm. Quality of nucleic acids was determined by using A260/A280 and A260/A230 ratios. These ratios for RNA purity are accepted to be qualified in the range of 1.9 - 2.0.

3.7.4. cDNA synthesis by reverse transcription

Single chain complementary DNA (cDNA) was synthesized from total RNA by using RevertAid™ First Strand cDNA Synthesis Kit (Fermentas, Lithuania). cDNA synthesis reaction components and conditions are shown in Table 3.5. cDNA products were stored at -20°C.

Table 3.5. Components and conditions used in cDNA synthesis.

Component	Volume (µL)	Final Concentration
RNA	890 µg	0.1 µg/µL
Oligo(dT)$_{18}$ Primer (0.5 µg/µL)	1 µL	0.025 µg/µL
Deionized dH$_2$O	Complete to 12 µL	
Incubation		**65°C, 5 min**
RT Reaction Buffer (5x)	4 µL	1x
dNTP mix (10 mM)	2 µL	1 mM
Ribonuclease Inhibitor (20 U/µL)	1 µL	1 U/µL
M-MuLVReverseTranscriptase(200 U/µl)	1 µL	10 U/µL
Incubation		**70°C, 10 min**
Final Volume	20 µL	

3.7.5. Polymerase chain reaction (PCR)

Prior to use, all reagents were thawed at room temperature and mixed by gently vortexing except for DNA polymerase. ICOS-LG and β-actin, as a house keeping gene, primers are used for gene expression analyses by PCR (see Table 3.6).

Table 3.6. Primer sequences and related information used in gene expression analyses.

	Forward Primer (5'-3')	Reverse Primer (5'-3')	Product Size	Gene Bank. No.
ICOS-LG	aggaagtcagagcgatggtag	tggtaggtcaccacggttttcg	130 bp	NM_015259.4
β-actin	ctggaacggtgaaggtgaca	aagggacttcctgtaacaatgca	139 bp	BC013835

A master mix was prepared in a 1,5 mL tube on ice. The mix contained distilled water (dH_2O),Taq buffer, $MgCl_2$, dNTP mixture, forward and reverse primers and *Taq* DNA polymerase enzyme, which was added into the mix at the very last (see Table 3.7). The master mix was, then, briefly centrifuged and distributed equally into each PCR tube on a cold block. cDNA (template DNA) sample was appended into each tube, gently mixed, and placed into the thermal cycler plate (Arktik Thermal Cycler,Thermo Scientific, USA). General conditions used for PCRs are given in Table 3.8 and Table 3.9.

Table 3.7. Standard PCR components, volumes and final concentrations.

Component	Volume (µL)	Final Concentration
dH_2O	30.7	
Taq Buffer with $(NH_4)_2SO_4$ (10x)	5.0	1x
$MgCl_2$(25mM)	5.0	2.5 mM
dNTP mix (2mM)	5.0	0.2 mM
Forward Primer (5µM)	1.5	0.15 µM
Reverse Primer (5µM)	1.5	0.15 µM
Taq DNA Polymerase (5U/µL)	0.3	0.03 U/µL
Template cDNA	1.0	
Final Volume	50.0	

Table 3.8. Thermal cycler program for β-actin PCR.

Initial denaturation	95˚C	3 min	
Denaturation	94˚C	30 sec	35 cycles
Annealing	60˚C	30 sec	
Extension	72˚C	30 sec	
Final extension	72˚C	5 min	

Table 3.9. Thermal cycler program for ICOS-LG PCR.

Initial denaturation	94˚C	30 sec	
Denaturation	94˚C	30 sec	38 cycles
Annealing	60˚C	30 sec	
Extension	72˚C	20 sec	
Final extension	72˚C	5 min	

3.7.6. Real-time PCR (RT-PCR)

Real-time PCR analyses were performed on ICOS-LG gene, together with the reference house keeping gene, β-actin.

The ingredients were thawed at room temperature and mixed by vortexing. DNA master SYBR mix (QIAGEN, Netherlands), $MgCl_2$, forward and reverse primers (Table 3.6) and distilled water (dH_2O) was added into a tube on ice to obtain a master mix (Table 3.10). The mix was briefly centrifuged and distributed uniformly into PCR tubes on a cold block and cDNA was added into each. Then, the tubes were placed into the real-time PCR instrument (Corbett Rotor-Gene 6000, Netherlands). The annealing temperatures were set as described in Table.3.11. The results were analyzed according to Formula 3.2.

Table 3.10. Real-time PCR components, volumes and final concentrations.

Component	Volume (µL)	Final Concentration
DNA Master Syber Green Mix (10x)	2.0	1X
$MgCl_2$(25mM)	2.0	2.5 mM
Forward Primer (5µM)	0.2	0.05 µM
Reverse Primer (5µM)	0.2	0.05 µM
ddH_2O	14.6	
Template cDNA	1.0	
Final Volume	20.0	

Table 3.11. Real-time PCR conditions.

Initial denaturation	95˚C	2 min
Annealing	60˚C	10 min
Extension	60˚C	20 sn
Final extension	95˚C	10 min

(3.3)

$$\Delta Ct_{treated} = Ct\ (ICOS\text{-}LG - IFN\text{-}\gamma\ treated) - Ct\ (\beta\text{-}actin - IFN\text{-}\gamma\ treated)$$

$$\Delta Ct_{control} = Ct\ (ICOS\text{-}LG - control) - Ct\ (\beta\text{-}actin - control)$$

$$\Delta\Delta\ Ct = \Delta Ct_{treated} - \Delta Ct_{control}$$

$$Normalized\ target\ gene\ expression\ level = 2^{-(\Delta\Delta Ct)}$$

3.7.7. Agarose gel electrophoresis

In order to prepare 1% or 2% (w/v) agarose gel, 1 gr or 2 gr agarose was weighted and mixed with 100 mL 1XTBE buffer. Agarose was melted in microwave oven (Imperial, USA). After moderate cooling, 10 mg/mL ethidium bromide was added (250 µg/mL) and poured into a gel casting tray equipped with a comb. After gelling, the comb was removed, gel was put inside the tank, and 1XTBE was added over the gel to completely cover it. PCR

products (20 µL) was mixed with 6XDNA loading dye (Thermo Scientific, USA) (final concentration 1X) and loaded into wells. To observe PCR product size, 0.5 µg DNA size marker (Fermentas, Lithuania) was loaded (Figure 3.10). The gel electrophoresis was run under 120V constant voltage. At the end of the run, PCR products were observed under UV light using Kodak gel Logic 1500 digital imaging system (Carestream Health Inc., USA).

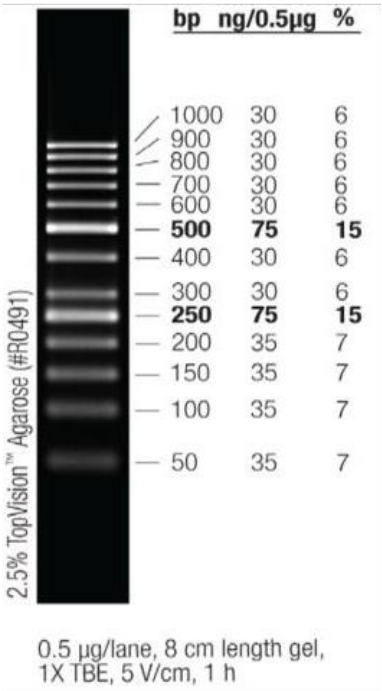

Figure 3.10.50 bp DNA size marker (Fermentas, Lithuania).

3.8. Statistical analysis

Statistical analyses were carried out by using Microsoft Office Excel 2007 program. All values were expressed by arithmetic mean ± standard deviation (SD). Statistical difference between experimental groups was determined using Student's paired or unpaired *t-test* or ANOVA and Chi-square, where appropriate. Differences were regarded as statistically significant when $P \leq 0.05$.

4. RESULTS

4.1. ICOS-LG expression on AML cell lines

ICOS-LG surface expression on AML cell lines (HL-60, THP-1, U937, Kasumi-1 and KG-1) at different maturation stages were investigated by flow cytometry (Figure 4.1). $CD14^+$ monocytes found in freshly obtained PBMCs were used as controls. Representative results for HL-60, THP-1, U937, Kasumi-1 and monocytes are shown in Figure 4.1A. ICOS-LG expression percentages and MFI values in these cells are shown in Figure 4.1B and Figure 4.1C, respectively. ICOS-LG was expressed prominently on HL-60 (93.7±2.0%), THP-1 (91.1±4.1%) and Kasumi-1 (92.7±4.7%). On the other hand, U937 (63.4±3.1%) and KG-1 (32.0±3.6%) cells did not show a uniform positivity for ICOS-LG. This co-stimulatory molecule determined to be the lowest on $CD14^+$ PBMCs (46.5±5.6%). Except for KG-1 (FAB M0-M1) cell line, ICOS-LG expression showed a decreasing tendency as the differentiation status (i.e. FAB stage for AML cell lines) of these myeloid cells is increased. This observation was also evidenced with ICOS-LG MFI values (Figure 4.1C). These results underlined that ICOS-LG can be promiscuously found on AML cells under steady state conditions.

4.2. Modulation of ICOS-LG expression on AML cells upon exposure to IFN-γ

The pro-inflammatory cytokine IFN-γ is known to be a potent stimulator of maturation and differentiation for several cells including immune cells and malignant cells (196). IFN-γ is especially critical for anti-tumor responses. Since it has been widely detected on most of the AML cells, the effect of IFN-γ on ICOS-LG expression was investigated.

The AML cell lines were stimulated with standard dose of IFN-γ (200 U/mL) for 16 and 64 hours and the expression kinetics of ICOS-LG and monocytic differentiation status (CD14 expression levels) were determined by flow cytometry (Figure 4.2A) (197). $CD14^+$ PBMCs were used as controls and also stimulated with IFN-γ or LPS (100 μg/mL) (Figure 4.2). The percentages

and MFI values for CD14 expression are shown in Figure 4.2A and Figure 4.2B, respectively.

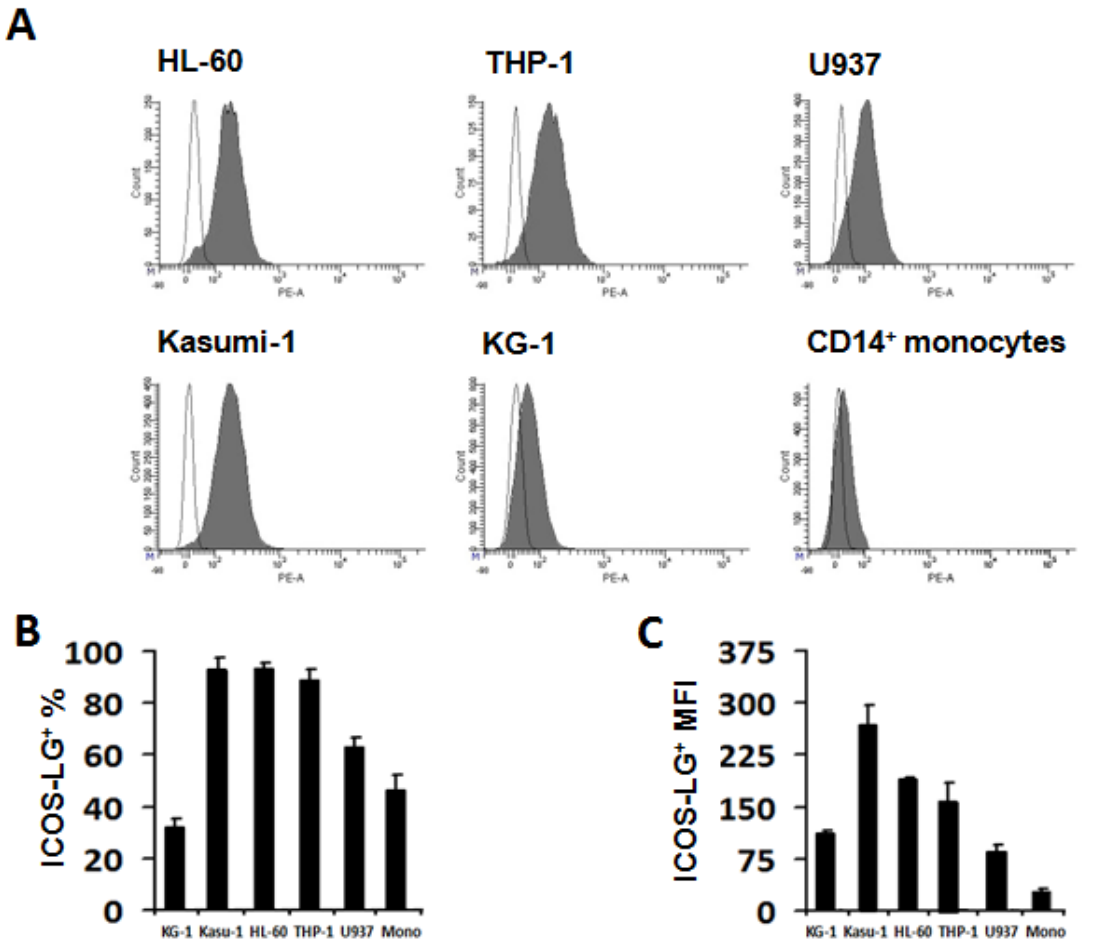

Figure 4.1. ICOS-LG expression on AML cell lines. A) Representative histograms of ICOS-LG expression on myeloid cells determined by flow cytometry. Empty histograms belong to isotype controls, filled histograms show specific staining with ICOS-LG antibody. The percentage (B) and MFI (C) values of ICOS-LG on AML cell lines and $CD14^+$ PBMCs. (Mono, monocytes), (n≥3).

Upon treatment, AML cells displayed a gradual increase in CD14 expression. While it was increased drastically on KG-1 (at 0 h, 9.7±1.4; 16 h, 37.6±7.1; 64 h, 62.6±3.3) and HL-60 (at 0 h, 15.3±4.2; 16 h, 46.4±11.5; 64 h, 77.5±8.0), the more mature cells THP-1 and U937 were already positive for CD14. Kasumi-1 was the least responsive cell line to IFN-γ in terms of CD14, since it did not show a stable expression as the exposure time to IFN-γ was

increased. Expectedly, as the maturation stage of the myeloid cells used increased, their CD14 upregulation capacity was enhanced. Even monocytes responded well to IFN-γ and to LPS, to a certain extent, and upregulated CD14 levels. This was clearly demonstrated at the cellular level using CD14 MFI values (Figure 4.2B). Collectively, CD14 was increased on all AML cell lines upon exposure to IFN-γ. IFN-γ treatment was effective enough to induce maturation and differentiation of these AML cells for a period of time.

ICOS-LG expression on all IFN-γ-induced AML cells and monocytes were increased in 16 hours (KG-1, 46.4±11.3%; Kasumi-1, 94.4±3.9%; HL-60, 96.0±1.8%; THP-1, 86.0±3.8%; U937, 90.1±8.7%; $CD14^+$ PBMC, 97.8±1.6%)(Figure 4.2C). While its expression was still high on KG-1 and $CD14^+$ PBMCs at 64 hours, rest of the AML cells tend to downregulate ICOS-LG either significantly or not (Figure 4.2C and Figure 4.2D). Representative CD14/ICOS-LG flow cytometry dot-plots of IFN-γ-induced AML cells and PBMCs were shown in Figure 4.3. ICOS-LG expression kinetics were also investigated at mRNA level. Upon treatment with IFN-γ for 4, 8, 16, 32, 64 and 128 hours, gene expression levels in HL-60, THP-1 and U937 were determined by RT-PCR.

ICOS-LG mRNA level was slightly changed in HL-60 cells with IFN-γ treatment; whereas, it was considerably elevated in both THP-1 and U937 for the first 8 hours but exhibited a decreasing trend at longer incubation periods. The decrease was quite rapid in U937, at 16 h. ICOS-LG mRNA level in Kasumi-1 was elevated approximately 3-fold at 16 h and scarcely changed at 64 h. KG-1 showed 1-fold decrease after 16 h and stabilized for next 48 h (Figure 4.F).

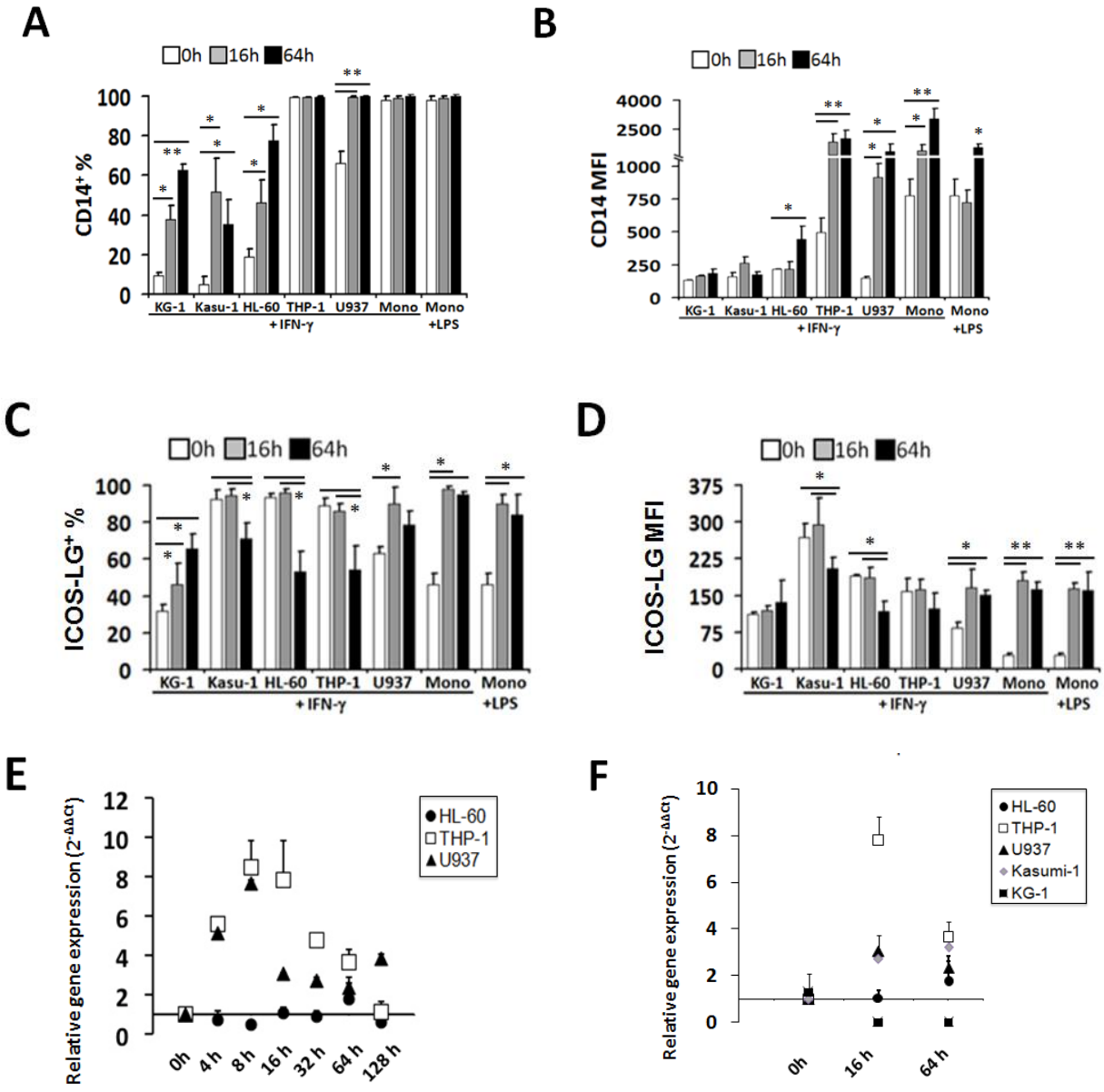

Figure 4.2. Expression of CD14 as a myeloid maturation marker and ICOS-LG upon exposure to IFN-γ.

A) Percentages and B) MFI values of CD14 on AML cell lines and monocytes (Mono.) at 0, 16 and 64 hours. C) Percentages and D) MFI values of ICOS-LG on AML cell lines and monocytes at 0, 16 and 64 hours. E) Relative gene expression ($2^{-\Delta\Delta Ct}$ values) of IFN-γ-induced HL-60, THP-1 and U937 cells for 4, 8, 16, 32, 64 and 128 hours. F) Relative gene expression ($2^{-\Delta\Delta Ct}$ values) of IFN-γ-induced HL-60, THP-1, U937, Kasumi-1 and KG-1 cells for 16 and 64 hours. A $2^{-\Delta\Delta Ct}$ value = 1 represents equal amount of gene expression between control and IFN-γ-treated cells (n≥3, **P*<0.05, ***P*<0.001).

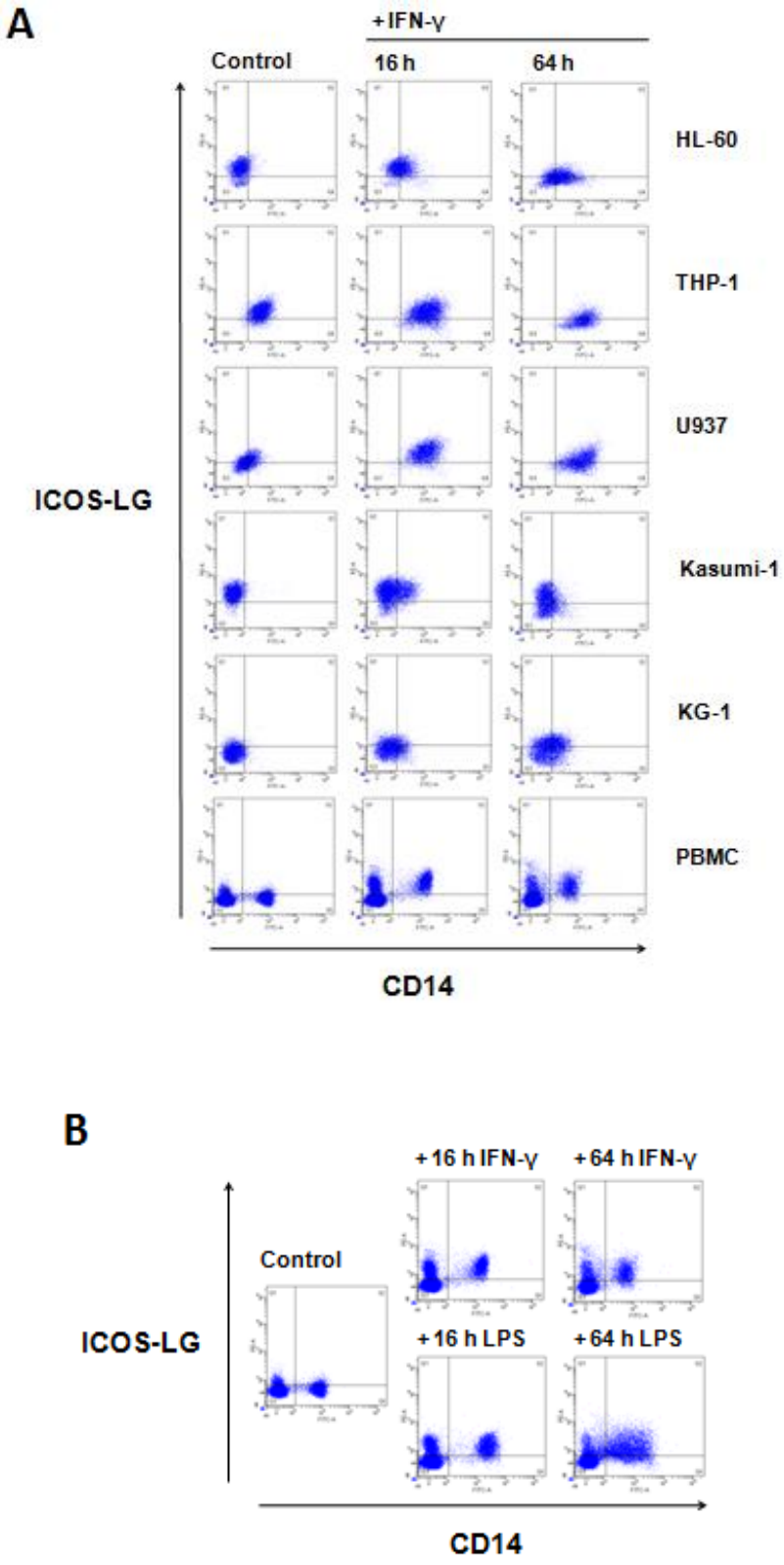

Figure 4.3. Representative flow cytometry dot-plots showing the expression of ICOS-LG and CD14 on HL-60, THP-1, U937, Kasumi-1, KG-1 and PBMCs. B) Representative flow cytometry dot-plots of PBMCs induced with IFN-γ (200 U/mL) or LPS (100 µg/mL) for 16 and 64 hours.

In vitro stimulation with IFN-γ was able to induce maturation and simultaneously modulate ICOS-LG expression on AML cells. This modulation was distinctive in each AML cell in close correlation with their monocytic differentiation stages. THP-1, stably expressing high levels of CD14, as a monocytic cell line and others such as HL-60 and KG-1 manifesting an inducible CD14 expression upon IFN-γ treatment were demonstrated. Because a detailed ICOS-LG kinetics showed a significant modulation of ICOS-LG expression in HL-60 and THP-1 in extended IFN-γ treatment, the two were preferentially selected to establish an exhaustion model attributing to the effects of ICOS-LG modulation on AML cells.

4.3. Modeling the T helper cell exhaustion in the co-cultures with AML cells

In order to establish an *in vitro* exhaustion model, AML cells were co-cultured with purified $CD4^+$ T helper cells for 96 hours in the presence of soluble anti-CD3 monoclonal antibody (aCD3) (refer to Section 3.3.4 for detailed description of co-cultures). For the co-cultured T cells, soluble aCD3 was used as a potent stimulator of T cell receptor (TCR) by which T cells attained activation and survival signals (96). Together with AML cells, this co-culture model allowed T cells to receive both activatory signals by aCD3 through TCR signaling and co-stimulatory signals through CD86 and ICOS-LG on AML cell (87,198).

In order to establish a Th cell exhaustion model *in vitro*, certain experimental approaches were employed:

i. The effect of TCR stimulation mimicked by aCD3 was tested by titrating aCD3 concentrations. HL-60 or THP-1 cells were co-cultured with $CD4^+$ T cells at a ratio of 2:1 in the presence of different aCD3 concentrations (6.25, 12.5, 25, 50, 100 ng/mL).

ii. The effect of co-stimulatory signals provided by AML cells was modulated by using different co-culture ratios. HL-60 or THP-1

cells were co-cultured with $CD4^+$ T cells at the ratios 0.25:1, 2:1, 4:1 in the presence of a standard 25 ng/mL aCD3 concentration.

iii. T cells were also co-cultured with $CD14^+$ monocytes freshly obtained from healthy volunteers as a control.

iv. Prior to co-culturing, $CD4^+$ T cells were stained with red-CFSE dye for tracking their proliferation rates. This dye can be clearly monitored on flow cytometry with 670-nm excitation and emission filters (Figure 4.4A). Stained T cells were easily discriminated from myeloid counterparts and low- and high-proliferating subpopulations were gated. Accordingly, CFSE dilution calculated less than five (<5) was categorized as low-proliferating cells whereas average CFSE dilution was about 15 in high-proliferating T cells (Figure 4.4B).

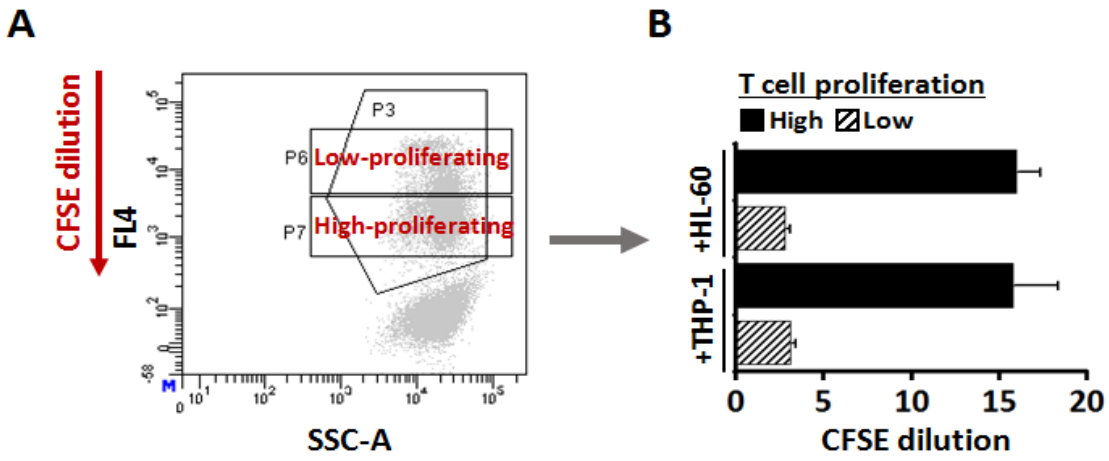

Figure 4.4. Gating strategy and CFSE dilutions of $CD4^+$ T cells in the co-cultures. A) T cells that were labeled with red-CFSE were gated in P3. Low- and high-proliferating cells were gated in P6 and P7, respectively. B) CFSE dilutions were calculated for $CD4^+$ T cells co-cultured with HL-60 and THP-1 using the formula given in Section 3.5, (n≥3).

v. Co-cultures were maintained for 96 hours in order to maintain an efficient interaction between the cells and to constitute the required activatory signals for T cell exhaustion. Because this period may jeopardize viability of the co-cultured cells, the media and aCD3 was freshly supplemented every 24 hours. Refreshments not only supported the viability of the cells, but also mimicked the persistent antigen stimulation known to be required during exhaustion process.

At the end of 96-hours of incubation with refreshments, in the co-cultures either with HL-60 or THP-1 AML cells or with normal monocytes Th cell proliferation was highly supported. In addition, almost all the T cells (≥95%) was proliferated under every co-culture condition applied (Figure 4.5). Thus, there was no difference between T cell proliferation rates in the co-cultures established. Accordingly, a general co-culture condition with a T cell:myeloid cell ratio of 2:1 and aCD3 concentration of 25 ng/mL was settled on.

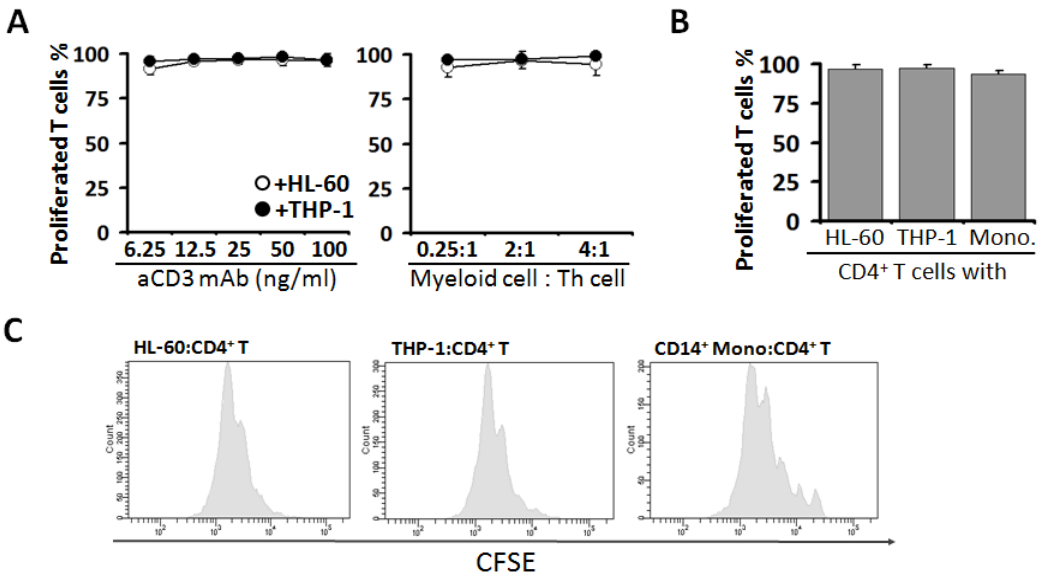

Figure 4.5. The percentages of proliferated $CD4^+$ T cells in HL-60 or THP-1 co-cultures

(A) containing different concentrations of aCD3 (left-panel) or different AML:$CD4^+$ T cell ratios (right-panel). B) T cell proliferation in the co-cultures with HL-60, THP-1 or monocytes at 2:1 ratio in the presence of 25 ng/mL aCD3. C) Representative flow cytometry histograms of T cell proliferation in AML or $CD14^+$ monocyte co-cultures, (n≥3).

HL-60, THP-1 or monocytes were co-cultured with Th cells at a standard T cell:AML cell ratio of 2:1 in the presence of 25 ng/mL aCD3. At the end of 96 h co-culturing, T cells' viability was not hampered in the co-cultures as evaluated by Annexin V-PI staining (Figure 4.6). PI-negative cells were >95% whereas approximately 10-15% of the cells determined to be at early apoptosis (Annexin V-positive).

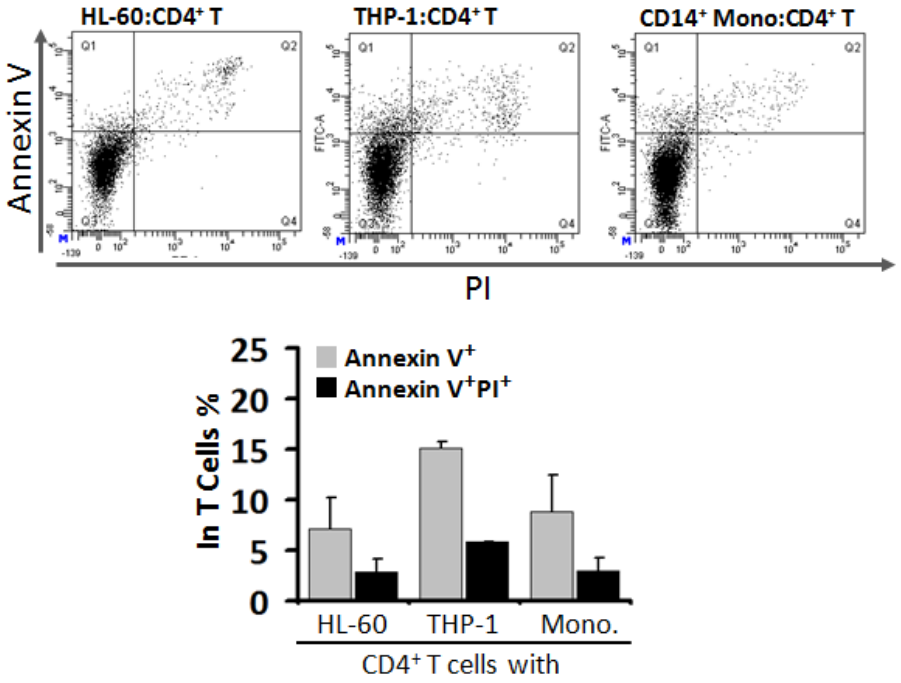

Figure 4.6. Annexin-PI staining for $CD4^+$ T cells co-cultured with HL-60, THP-1 or $CD14^+$ monocytes. Analyses were performed after gating the red-CFSE-stained Th cells, (n≥3).

According to these results, this *in vitro* model supported the proliferation of T cells and did not damage the viability thereof. The proliferation rates were independent from aCD3 concentrations or AML cell ratios.

4.3.1. The effect of aCD3 stimulation on T cell activation/exhaustion markers

HL-60 or THP-1 cells were co-cultured with $CD4^+$ T cells in the presence of different aCD3 concentrations (6.25, 12.5, 25, 50, 100 ng/mL) with a constant AML to T cell ratio of 2:1. The expression of CD25, CD127, CCR7, ICOS, CTLA-4, PD-1, TIM-3, LAG3, HLA-DR, CD154, CD69, PD-L1 and CD38 markers which are related to T cell activation and/or exhaustion was evaluated by flow cytometry at the end of 96-hour co-culture period (Figure 4.7).

More than 80% of the Th cells expressed CD25, CCR7, CTLA-4, PD-1, ICOS and TIM-3 in both HL-60 and THP-1 co-cultures at 96 h. CD127

expression on Th cells ranged between 30-40% in both co-cultures. $LAG3^+$ Th cells remained as a minority in THP-1 co-cultures, while it was more widely expressed in HL-60 co-cultures. HLA-DR seemed to be slightly decreased at the increasing concentrations of aCD3 in HL-60 co-cultures; whereas, it was vaguely increased on T cells in THP-1 co-cultures, but did not reach to the level of statistical significance (Figure 4.7). For CD154, a similar reduction trend was observed in HL-60 co-cultures and slightly upregulated in THP-1 co-cultures, as aCD3 concentration was increased, again it did not reach to the level of statistical significance. There was no significant change in CD69 expression for HL-60 co-cultures depending on changing aCD3 concentrations. PD-L1 expression was clearly increased directly proportional to the elevated concentrations of aCD3 in both HL-60 and THP-1 co-cultures. CD38 expression ascended from 50% to 80% in HL-60 co-cultures, but, remained around 80% in THP-1 co-cultures (Figure 4.7). The representative flow cytometry histograms of the markers PD-1, CTLA-4, TIM-3, LAG3 and ICOS which in the literature are strongly acknowledged to be associated with T cell-exhaustion and co-stimulation are shown in Figure 4.8.

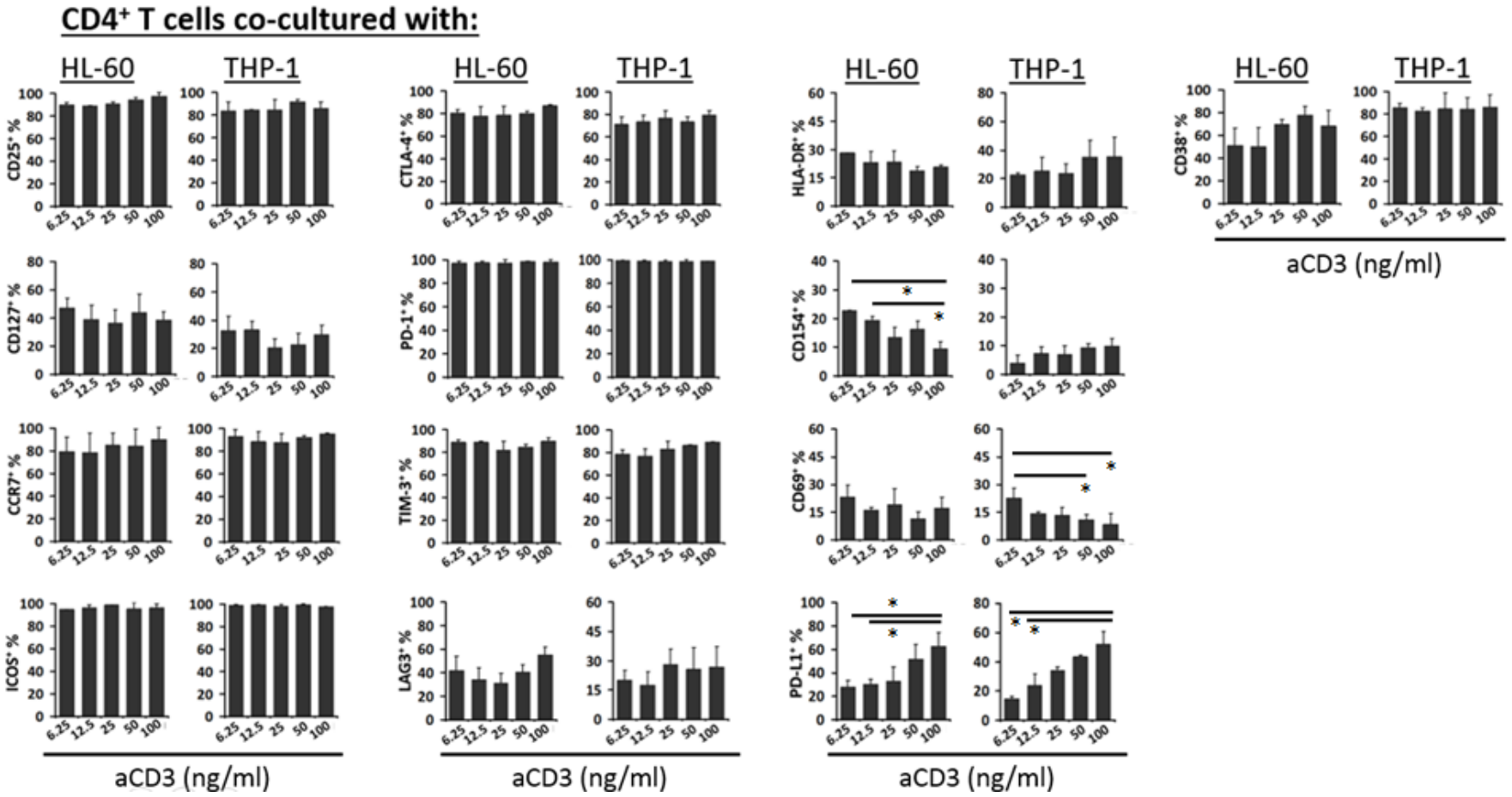

Figure 4.7. The effect of stimulation with various concentrations of aCD3 on activation/exhaustion markers expressed by CD4$^+$ T cells co-cultured with HL-60 or THP-1 cells at 2:1 AML: T cell ratio for 96 h (*P<0.05, **P<0.001, n≥3).

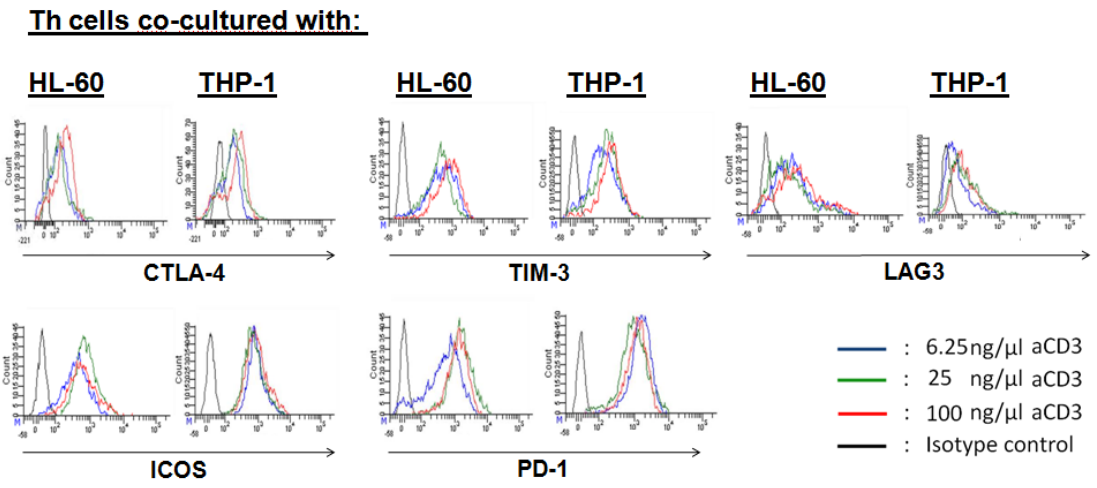

Figure 4.8. Representative histograms for CTLA-4, TIM-3, LAG3, ICOS and PD-1 expression on $CD4^+$ T cells co-cultured with HL-60 or THP-1 with three different concentrations of aCD3 for 96 h.

In order to check if the expression of these markers was differing between the high- and low-proliferating Th cell subpopulations, additional analyses were performed according to the gates shown in Figure 4.4. Between the high- and low-proliferating cells, there was hardly any difference on co-cultured T cells for various markers except for CD69 (Figure 4.9). The amount of CD69 expressing low-proliferating T cells was especially surpassing that of high-proliferating cells in both HL-60 and THP-1 co-cultures.

All in all, in this co-culture system, different concentrations of aCD3 did not critically alter the amount of Th cells carrying activation/exhaustion markers.

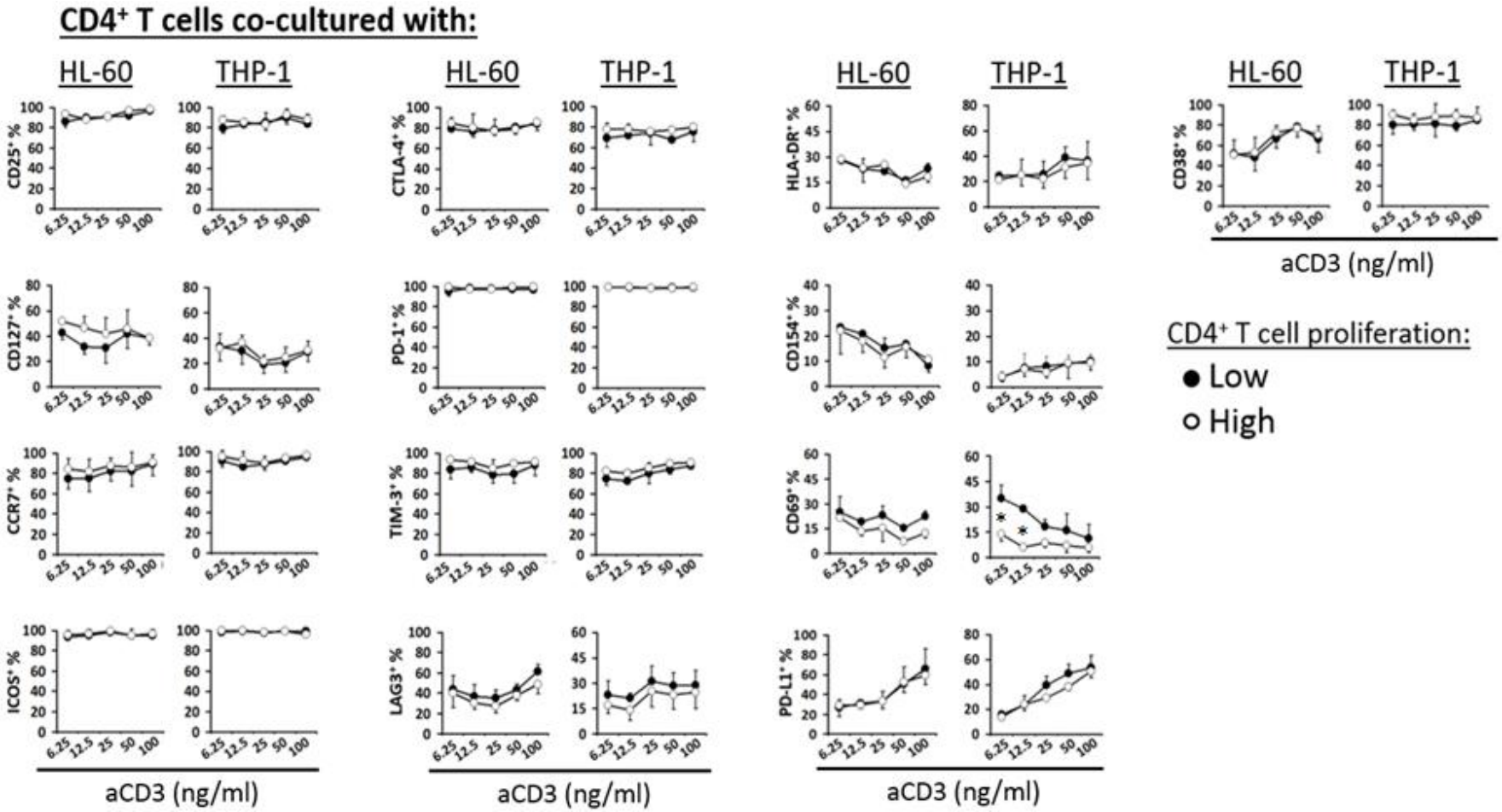

Figure 4.9. The effect of stimulation with various concentrations of aCD3 on activation/exhaustion markers expressed by high- and low-proliferating CD4$^+$ T cells co-cultured with HL-60 or THP-1 cells at 2:1 AML: T cell ratio for 96 h (*P<0.05, n≥3).

4.3.2. The effect of AML cell ratio on Th cells' activation/exhaustion markers

HL-60 or THP-1 cells were co-cultured with $CD4^+$ T cells at different AML to T cell ratios (0.25:1, 2:1, 4:1)with 25 ng/mL aCD3 mAb to maintain TCR stimulation (signal 1). As it was previously shown, the co-stimulatory molecules expressed by AML cells provide secondary signals required for T cell responses. Thus, by changing the ratio of AML cells in the co-cultures, the magnitude of co-stimulation can also be modulated indirectly (87). The expression of CD25, CD127, CCR7, ICOS, CTLA-4, PD-1, TIM-3, LAG3, HLA-DR, CD154, CD69, PD-L1 and CD38 on Th cells were evaluated with flow cytometry at the end of 96-hour co-culture period (Figure 4.10).

The percentages of Th cells carrying CD25, CCR7, ICOS, PD-1, PD-L1 and CD38 molecules were only slightly varied when the ratio of AML cells was changed. CD127 and CD69 employed a decreasing trend when AML cell ratios were elevated (0.25:1, 33.5±10.4%; 2:1, 25.6±11.2%; 4:1, 20.6±10.8% and 0.25:1, 33.4±9.1%; 2:1, 28.0±10.0%; 4:1, 23.7±9.8%, respectively) in HL-60 co-cultures. Similarly, in THP-1 co-cultures, CD127 and CD69 showed a decreasing trend (0.25:1, 26.1±9.5%; 2:1, 17.1±3.5%; 4:1, 13.1±9.2% and 0.25:1, 15.0±8.4%; 2:1, 9.9±4.8%; 4:1, 6.9±2.7%, respectively). On the other hand, CTLA-4, TIM-3, LAG3, HLA-DR and CD154 expressions were significantly escalated as the amount of AML cells increased in the co-cultures (Figure 4.10). This was demonstrated either with HL-60 or THP-1 co-cultures. Co-culturing with HL-60 gave more clear results compared to that of established with THP-1. In general, the percentage of Th cells positive for a specific marker did not significantly change as the ratio of THP-1 cells was increased from 2:1 to 4:1. This illustrated that activation/exhaustion state of co-cultured cells were dependent on AML cell ratios, in other words co-stimulatory signals. Most of the co-cultured T cells became positive for CTLA-4, ICOS and PD-1 co-stimulatory receptors; moreover, TIM-3 and LAG3, expression appeared to be critically regulated by the presence of AML cells, and AML-derived co-stimulatory signals (Figure 4.11).

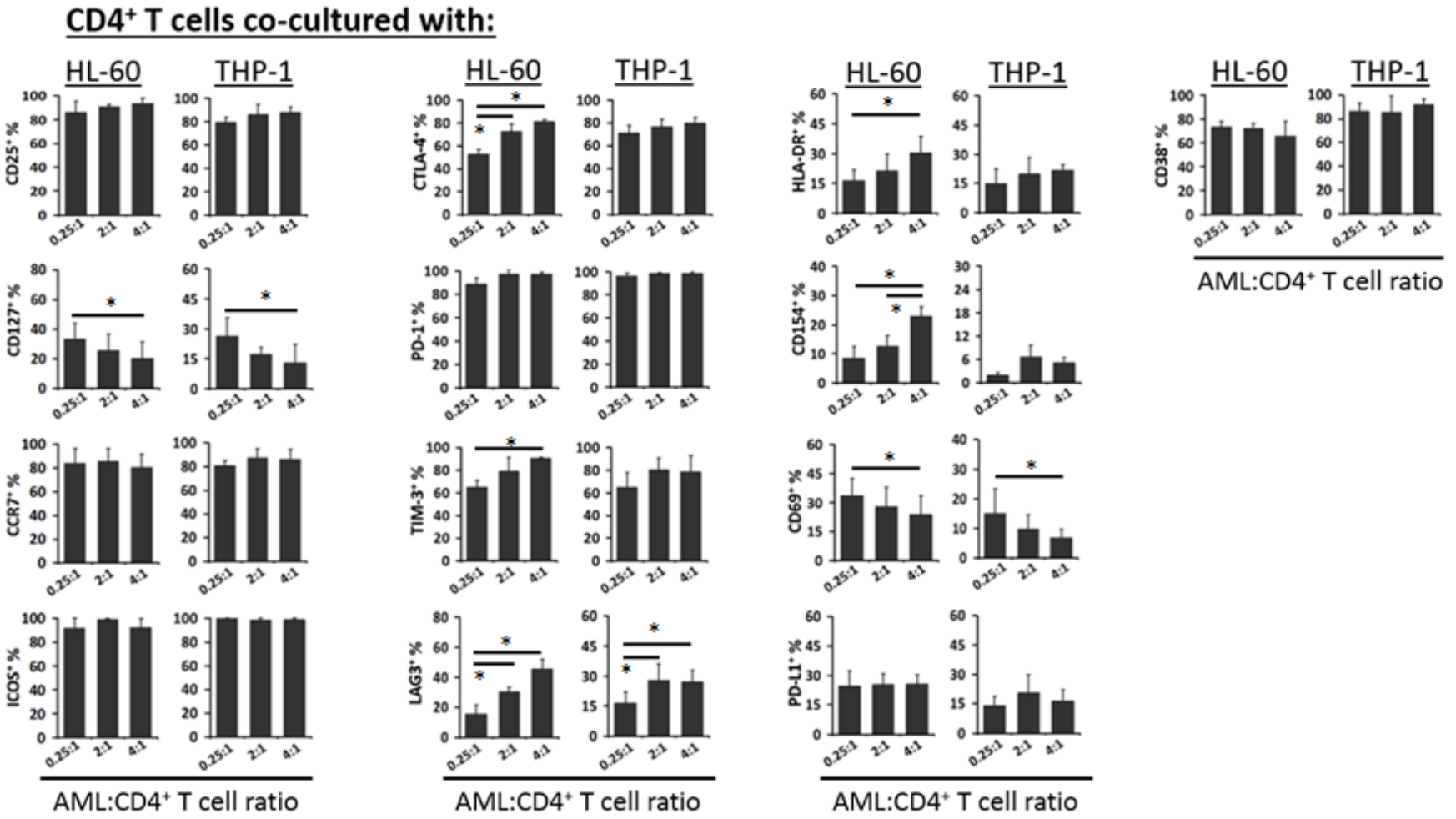

Figure 4.10. The effect of stimulation with various AML cell ratios on the activation/exhaustion markers expressed by $CD4^+$ T cells co-cultured with HL-60 or THP-1 in the presence of 25 ng/mL aCD3 concentration for 96 h (*P<0.05, **P<0.001, n≥3).

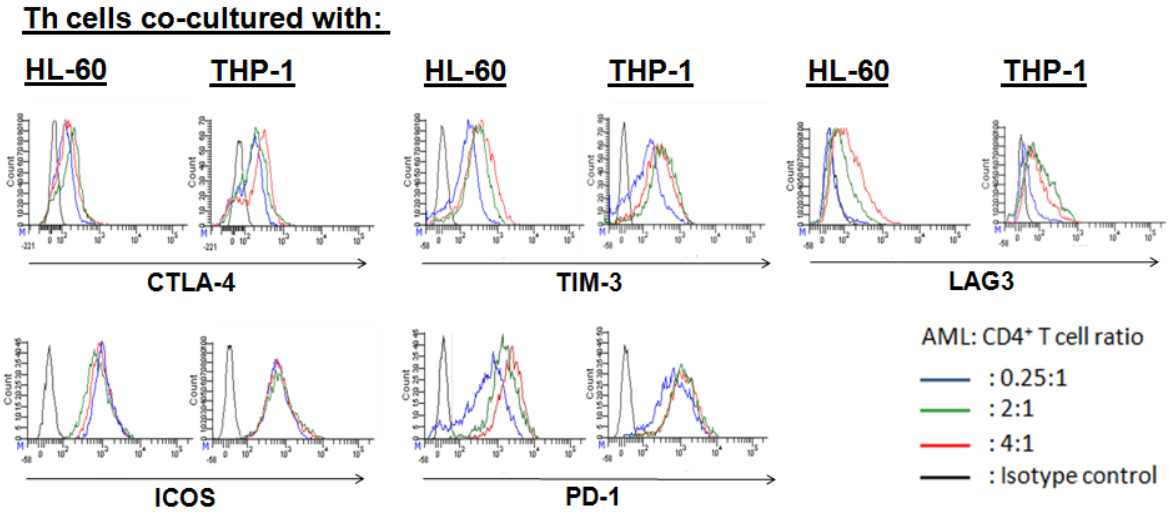

Figure 4.11. Representative histograms for CTLA-4, TIM-3, LAG3, ICOS and PD-1 on $CD4^+$ T cells co-cultured with HL-60 or THP-1 at AML:T cell ratios 0.25:1, 2:1, 4:1 for 96 h.

The effect of AML cell ratio was also measured on high- and low-proliferating T cells (Figure 4.12). While most of the expressions drew a similar pattern between the two groups, LAG3, PD-L1 and CD69 were more frequent on the low-proliferating T cells. However, both low- and high-proliferating Th cells showed parallel responses in terms of the markers analyzed in the co-cultures established with increasing ratios of AML cells (Figure 4.12).

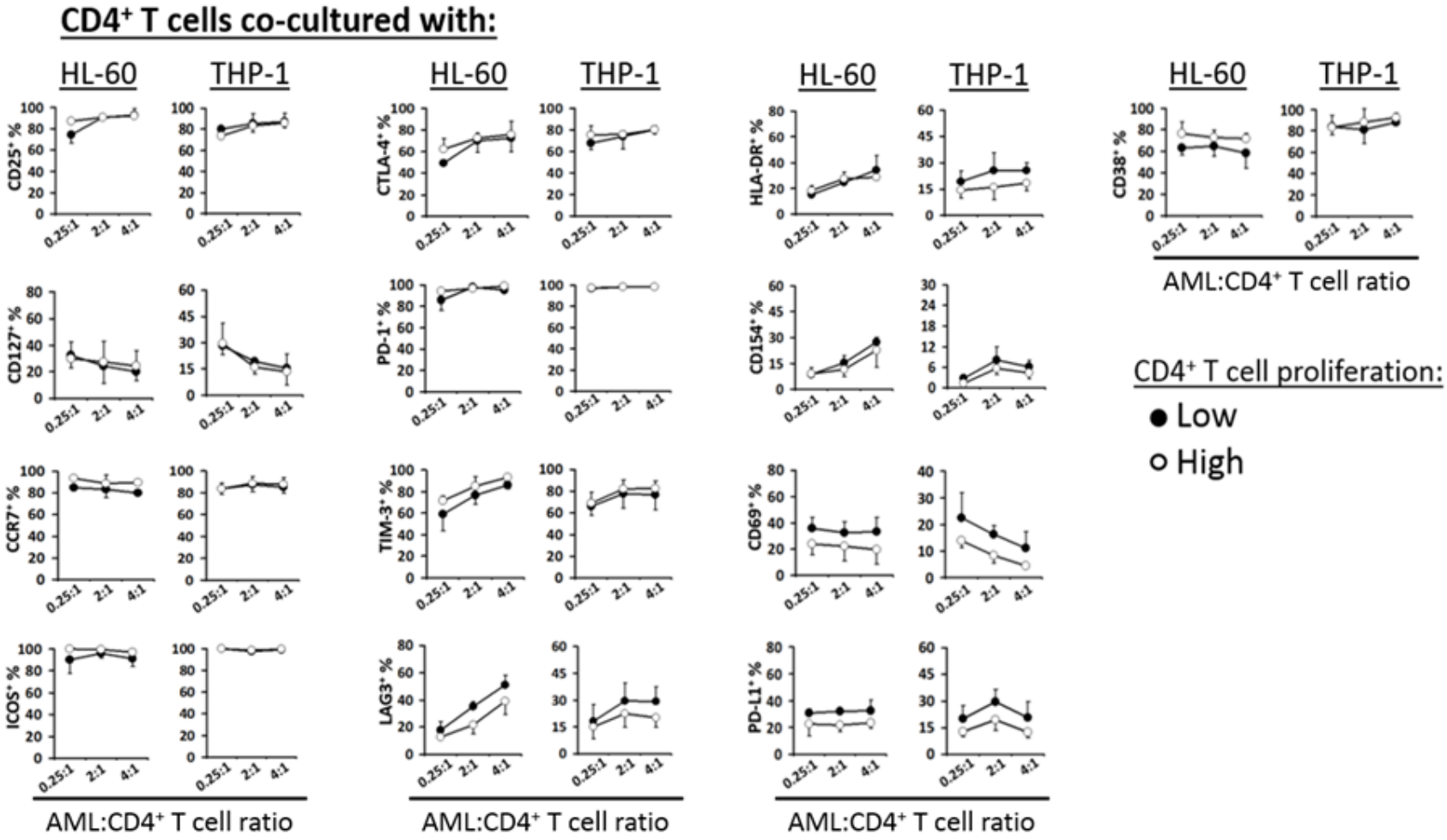

Figure 4.12. The effect of stimulation with various AML cell ratios on the activation/exhaustion markers expressed by high- and low-proliferating $CD4^+$ T cells co-cultured with HL-60 or THP-1 cells in the presence of 25 ng/mL aCD3 concentration for 96 h (n≥3).

4.3.3. Determination of the markers' expression kinetics during early-activation

In order to discriminate between the activation and exhaustion state of T cells and to differentiate activation markers from potential exhaustion-associated markers, their expression kinetics were determined on 6, 12, 24, 96 hours of co-cultures (Figure 4.13A). Freshly obtained naïve $CD4^+$ T cells were used as 0 hour control group.

The early-onset upregulation of CD69, CD127 and CD154 by 12 hours showed that most of the co-cultured T cells were activated as early as 12 hours. CD25, CD38, TIM-3, LAG3, ICOS, CTLA-4, PD-1, PD-L1 and HLA-DR expressions were prominently detected at 24 hours. While $CD4^+$ T cells behaved similar in both HL-60 and THP-1 co-cultures, for CD154 and HLA-DR, they were intriguingly different in their expression patterns. The percentage of CD154 carrying T cells started to increase significantly as early as 6 hours and reached its maximum at 12 hours in HL-60 co-cultures. In the course of 24 hours, only a minority of T cells co-cultured with THP-1 expressed CD154 and showed hardly any change during the co-culture period of 24 hours. Upon co-culturing with THP-1, T cells demonstrated a significantly increasing trend for HLA-DR expression; however, HL-60-co-cultured T cells did not upregulate this molecule in the course of 24 hours.

Because exhaustion progresses over time, the chronic stimulation in the co-cultures was maintained as long as 96 hours. A comparison between marker expressions at 24 hours and 96 hours of co-culturing are shown in Figure 4.13B. At the end of 96 hours, the percentage of T cells carrying certain markers was strikingly lowered in the co-cultures. Positivity for CD69 and CD127 positivity was dropped from approximately 85% to 20% and 53% to 21%, respectively. More importantly, there was a remarkable increase on TIM-3, LAG3, ICOS, CTLA-4 and PD-1 expressions. The change in $TIM\text{-}3^+$ and $LAG3^+$Th cell percentages were especially high in both co-cultures. TIM-3 was measured 33.8±7.4% by 24 hours and elevated up to 79.0±12.2% by 96 hours in the HL-60 co-cultures; similarly, it was 42.2±8.3% by 24 hours and elevated up to 80.6±10.1% by 96 hours in the THP-1 co-cultures. An

analogous but a moderate increase was observed on LAG3 expression (Figure 4.13B). Representative flow cytometry overlay histograms for LAG3 and TIM-3 exhaustion-associated molecules' on Th cells co-cultured for 24 and 96 hours are illustrated in Figure 4.13C.

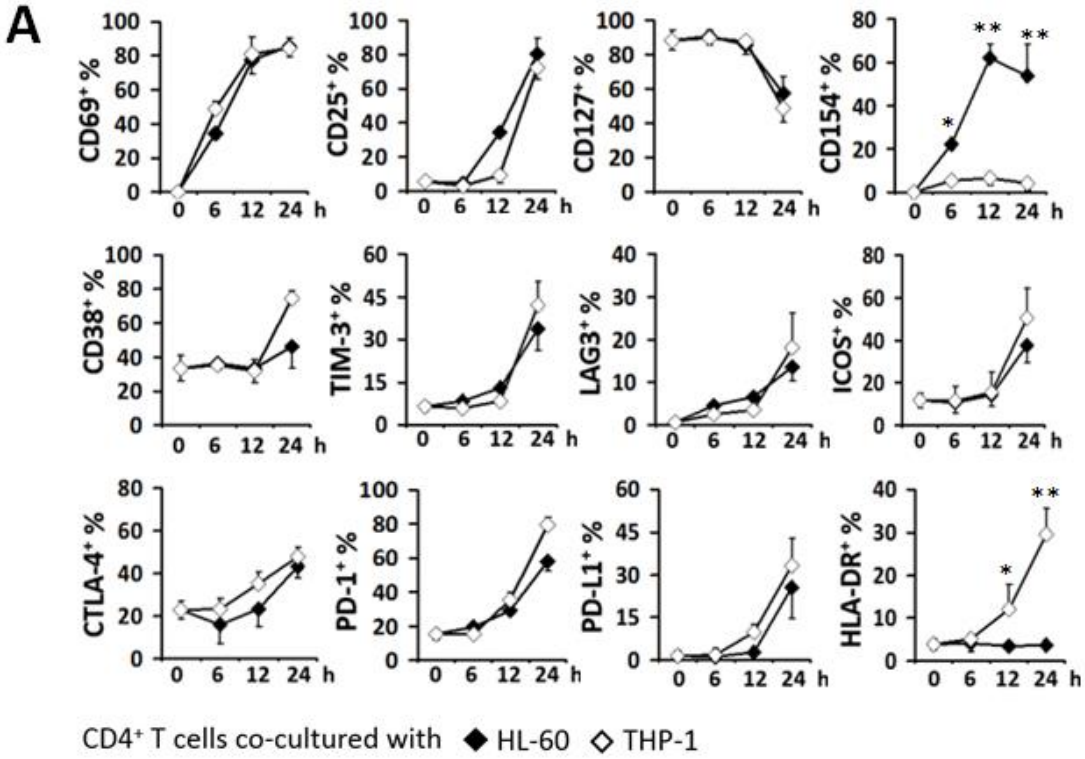

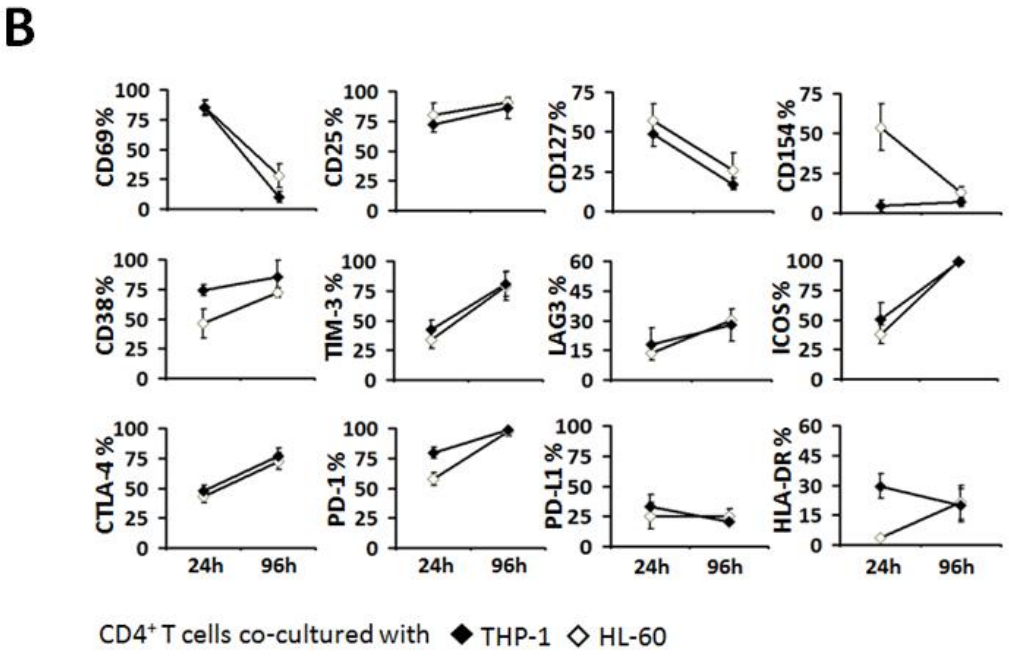

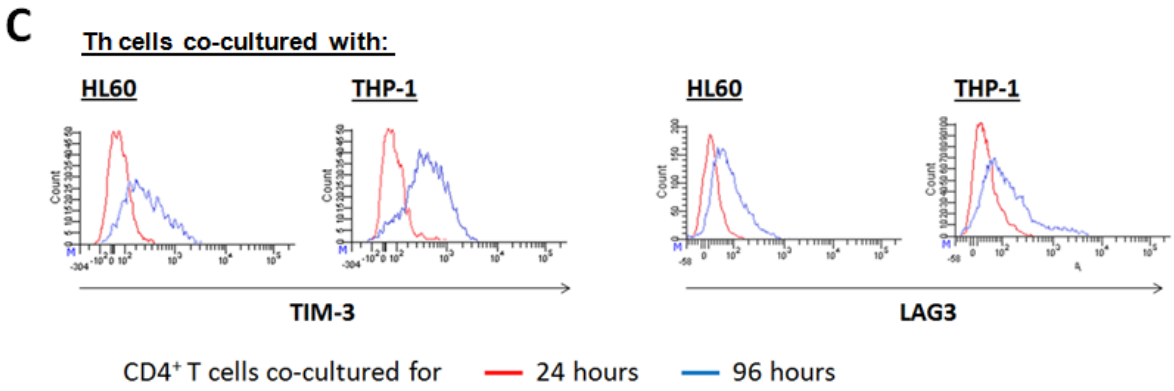

Figure 4.13. Expression kinetics of certain activation/exhaustion-related molecules on Th cells co-cultured with HL-60 or THP-1 cells at 2:1 AML: T cell ratio, in the presence of 25 ng/mL aCD3. Results of the experiments performed (A) for 6, 12, 24 hours (B) for 24 and 96 hours. Zero hour indicates the expression of corresponding markers on naïve T cells. C) Representative histograms for TIM-3 and LAG3 expression on $CD4^+$ T cells co-cultured with HL-60 or THP-1 for 24 and 96 hours (**P*<0.05, ***P*<0.001, n≥3).

4.3.4. AML-induced Th cell exhaustion/activation compared to that of monocytes

Freshly obtained $CD14^+$ monocytes were co-cultured with $CD4^+$ T cells in the presence of 25 ng/mL aCD3 and immunophenotyping was performed at the end of 96 hours of incubation. A comparison between T cells in AML co-cultures and in monocyte co-cultures for each marker is shown in Figure 4.14A.

TIM-3 and LAG3 expression were quite high in AML co-cultures compared to that of in monocyte co-cultures (HL-60, 75.9±31.5%; THP-1, 84.8±9.5%; monocytes, 30.7±19.2% and HL-60, 27.2±8.8%; THP-1, 19.5±5.4%, monocytes, 7.0±5.0%, respectively). CD127 was not downregulated on $CD4^+$ T cells co-cultured with monocytes, but its expression was significantly low in AML co-cultures (HL-60, 25.6±10.1%; THP-1, 17.1±3.5%; monocytes, 45.1±21.3%). PD-1 and CD25 expressing T cells were above 75% in all three co-cultures. CTLA-4 expressing T cell percentage was around 75% in the co-cultures. Almost all T cells in the AML

co-cultures (about 100%) were positive for ICOS, but, even though it is not significant, it was almost 75% in the monocytes co-cultures. Representative results of these distinctive markers are illustrated in Figure 4.13B.

Additionally, the percentages of TIM-3^{+}LAG3^{+} and CD25^{+}CD127^{-} T cell populations in the co-cultures were evaluated (Figure 4.15). The percentage of T cells co-expressing LAG3 and TIM-3were 22.8±8.2%, 12.7±4.0% and 4.9±3.3% in HL-60, THP-1 and monocytes co-cultures, respectively. For CD25^{+}CD127^{-} populations, T cell percentages were 68.8±6.5% in HL-60, 61.3±5.7% in THP-1, 39.2±7.9% in monocytes co-cultures.

CD25^{+}CD127^{-} CD4^{+} T cells can represent regulatory T cells (Treg) which are commonly positive for FoxP3. Thus, in order to check if there is Treg differentiation, FoxP3 expression in the co-cultured T cells was evaluated (Figure 4.15C and Figure 4.15D). The amount of FoxP3^{+} T cells did not differ between the co-cultures and was very low (approximately 5%). Therefore, Treg differentiation was not critically evident in the co-cultures.

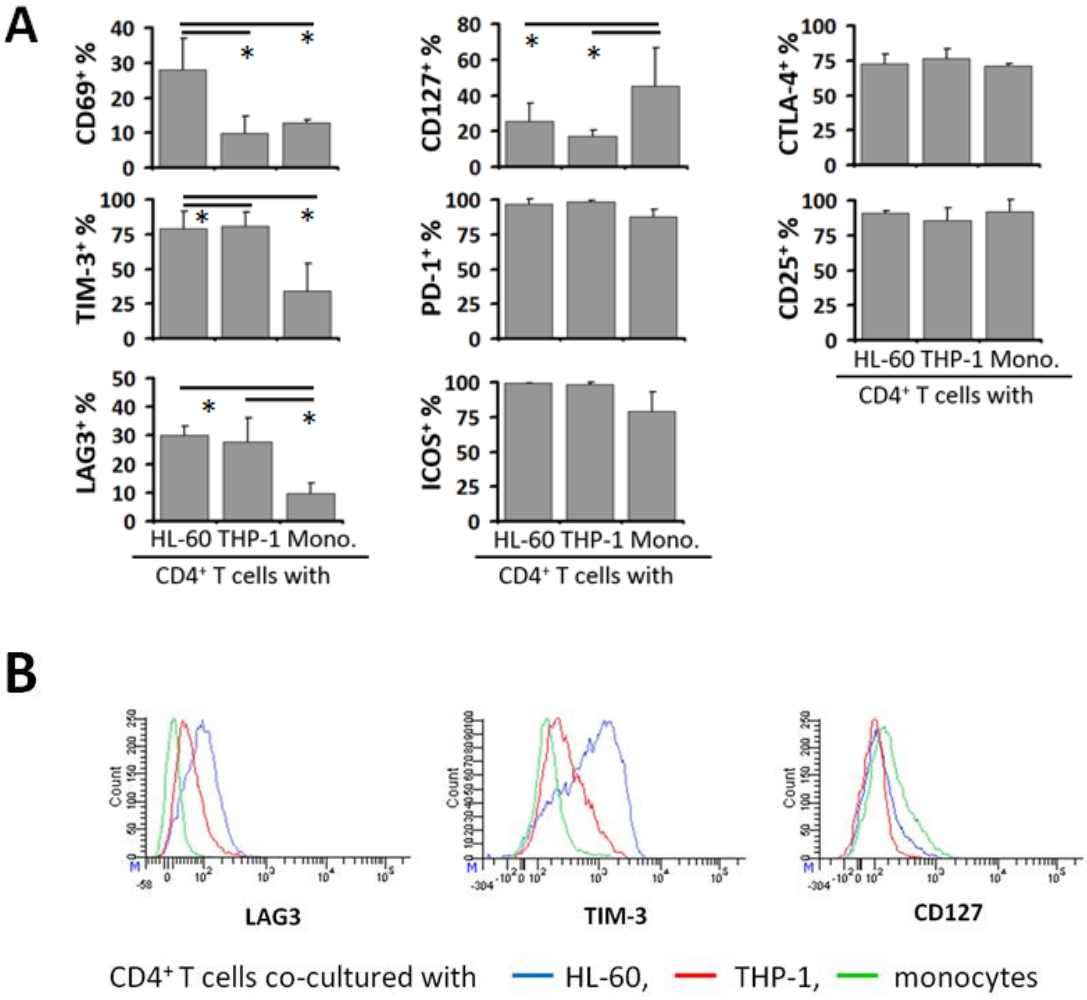

Figure 4.14. AML-induced T cell activation/exhaustion compared to that of induced with monocytes. A) The percentages of $CD4^+$ T cells expressing CD69, CD127, CTLA-4, TIM-3, PD-1, CD25, LAG3, ICOS in the co-cultures with HL-60, THP-1 or monocytes (co-culture ratio 2:1, 25 ng/mL aCD3). B) Representative histograms for LAG3, TIM-3 and CD127 expressions (**P*<0.05, ***P*<0.001, n≥3).

4.3.5. Functional evaluation of T cells in the co-cultures

IL-2, TNF-α, IFN-γ, IL-10, TGF-β and IL-4 cytokine levels in supernatants collected from each co-culture were determined by ELISA (Figure 4.16). IL-4 and TGF-β levels were below the detection limits in all three co-cultures, so their data were not shown. IL-2, TNF-α and IFN-γ levels were significantly low in AML co-cultures, while it was very high in monocyte

co-cultures on the other hand, IL-10 levels were elevated in AML co-cultures compared to that of in monocytes.

In fact, IL-2 level was around 10 pg/mL in HL-60 co-cultures and approximately 30 pg/mL in monocytes co-cultures, meaning among AML co-cultures, HL-60 co-cultures contained more IL-2. IL-2 levels in THP-1 co-cultures were below the detection limits. All in all, IL-2 levels were significantly low in AML co-cultures compared to that of monocytes.

TNF-α secretion was about 100 pg/mL in HL-60, 50 pg/mL in THP-1 and 150 pg/mL in monocytes co-cultures. Apart from the significant difference between the TNF-α levels in T cell and AML or monocyte co-cultures, AML co-cultures also varied among each other; TNF-α levels were significantly higher in HL-60 co-cultures than that of THP-1.

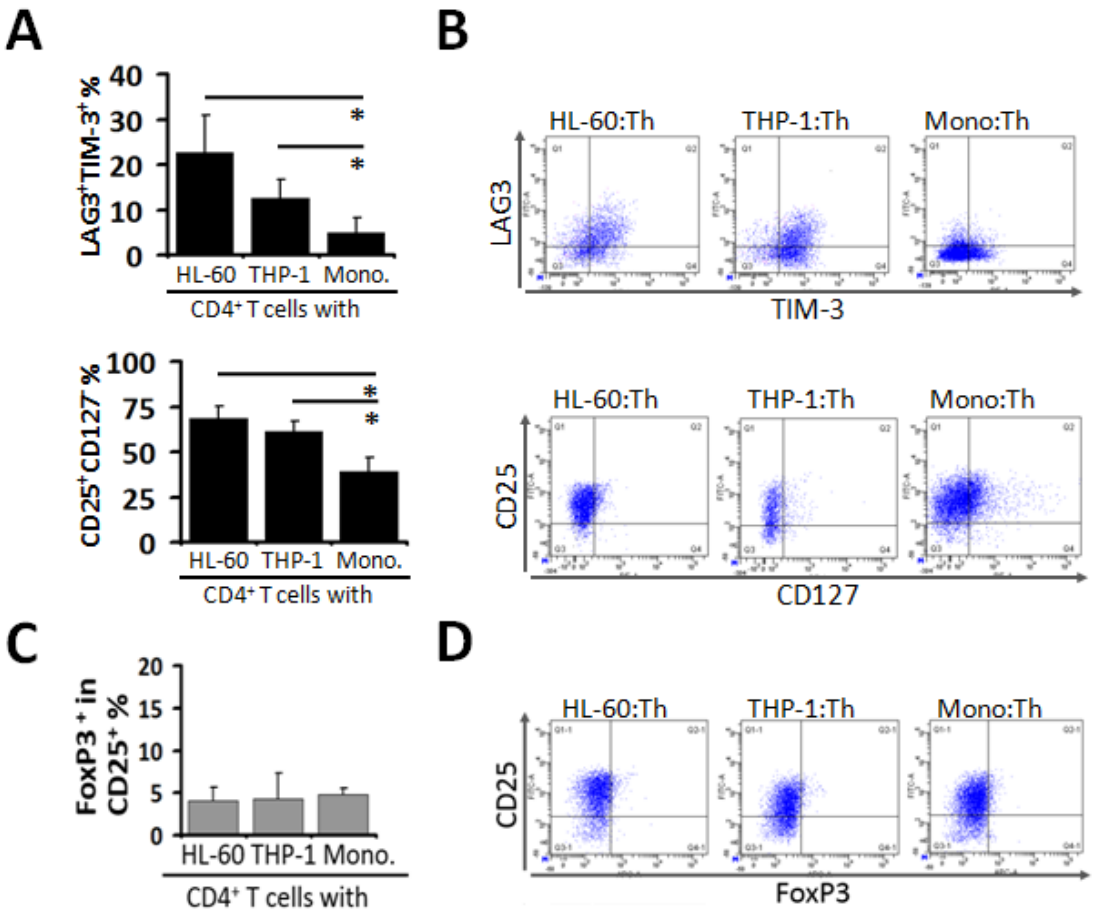

Figure 4.15. A) The percentages of LAG3^{+}TIM-3^{+} and CD25^{+}CD127^{-} CD4^{+} T cells in the co-cultures. B) Representative dot plots for LAG3/TIM-3 and CD25/CD127 expressions in the corresponding co-cultures. C) The percentage of FoxP3 expressing CD25^{+} T cells in the co-cultures with HL-60, THP-1 or monocytes. D) Representative dot plots for CD25 and FoxP3 expression in the co-cultures.

Almost the same trend of AML co-cultures against that of monocytes was evident for IFN-γ levels in all three co-cultures, but quite high levels of IFN-γ levels were detected. It was approximately 3 ng/mL, 1 ng/mL and 4 ng/mL in HL-60, THP-1 and monocytes co-cultures, respectively. Thus, IFN-γ levels were the most abundant cytokine secreted in all three co-cultures.

Suprisingly, IL-10 levels were very high in HL-60 co-cultures (550 pg/mL). It was almost halved in THP-1 co-cultures (300 pg/mL) and even less in monocyte co-cultures (100 pg/mL) with Th cells.

All in all, IL-2, TNF-α and IFN-γ levels were abundantly higher in Th cell co-cultures with monocytes compared to that of established with AML cells. IL-10 was high in AML co-cultures than that of in monocytes co-cultures.

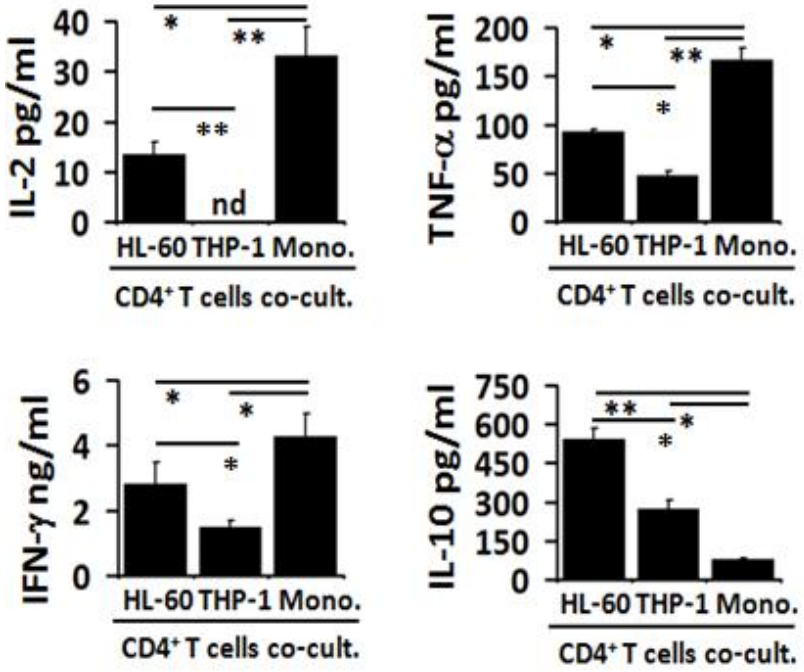

Figure 4.16. IL-2, TNF-α, IFN-γ and IL-10 levels in the HL-60, THP-1 or monocyte co-cultures with Th cells (2:1 cell ratio, 25 ng/mL aCD3) for 96 hours (**P*<0.05, ***P*<0.001, n≥3).

4.3.6. Functional confirmation of T helper cell exhaustion in AML co-cultures

In order to confirm that the Th cells carrying exhaustion markers and secreting diminished amounts of IL-2, TNF-α and IFN-γ are also functionally exhausted, TIM-3 expressing subpopulations were purified by FACS and restimulated with various agents. Accordingly, THP-1 cells were co-cultured with $CD4^+$ T cells at 2:1 AML:T cell ratio in the presence of refreshed 25 ng/mL aCD3 for 96 hours. The cells were harvested and back-sorted based on TIM-3 expression (see Section 3.3.3 and Section 3.3.5 for detailed

description). Two subpopulations enriched in TIM-3$^{-/lo}$ or TIM-3$^{mo/hi}$ cells were restimulated under different conditions and their proliferation capacities were evaluated by flow cytometric CFSE assay (Figure 4.17). The subpopulations without any stimulation were used as controls.

The use of each stimulatory condition addressed to a specific mechanism in CD4^{+} T cells. Upon induction with aCD3, TCR complex was stimulated. aCD28 was used to mimic co-stimulatory signals required for T cell activation. Recombinant IL-2 used to support T cell proliferation whereas co-culture with freshly isolated PBMCs also hosted a physiological milieu capable of providing many mediators that can be required for T cell activation.

Under all conditions, the proliferation activity of TIM-3$^{mo/hi}$ subpopulation was significantly lower than that of TIM-3$^{-/lo}$. CFSE dilution of unstimulated cells was higher in TIM-3$^{-/lo}$ T cells by a factor of 3 compared to that of TIM-3$^{mo/hi}$ T cells. Upon stimulation with plate-bound aCD3 and soluble CD28, it was increased in both groups, making TIM-3$^{mo/hi}$ populations proliferation to reach that of unstimulated TIM-3$^{-/lo}$ cells. When treated with a combination of plate-bound aCD3 and freshly obtained PBMCs, both populations showed a slight increase compared to control groups.

Recombinant IL-2 treatment was quite potent compared to other conditions; proliferation of TIM-3$^{mo/hi}$ population was increased approximately by a factor of 5, while that of TIM-3$^{-/lo}$ was elevated by a factor of 3. The effect of recombinant IL-2 was pronounced when the cells were incubated with plate-bound aCD3 in stimulating the proliferation. TIM-3$^{mo/hi}$ population was increased by a factor of 6 but could only reach to the effect of aCD3 and aCD28 on TIM-3$^{-/lo}$ population. Under this combination stimulus, TIM-3$^{-/lo}$ population’s proliferative activity was maximized. Eventually, the Th cells expressing low levels of TIM-3 were clearly more competent in proliferation compared to TIM-3 high-expressing counterparts. In addition of external IL-2 potentiated the proliferation capacity of TIM-3$^{mo/hi}$ T cells, *in vitro*.

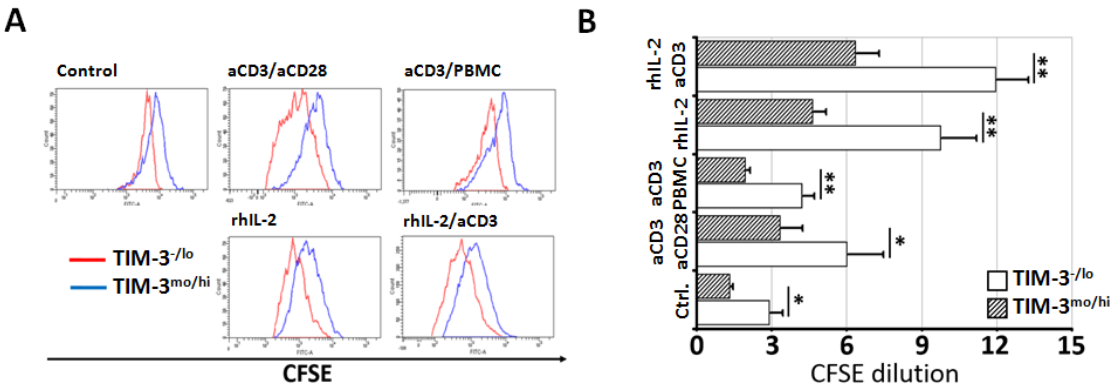

Figure 4.17. Restimulation of TIM-3$^{-/lo}$ and TIM-3$^{mo/hi}$ populations in the presence of plate-bound aCD3, soluble aCD28, recombinant human IL-2 (rhIL-2) and PBMCs. A) Representative histograms of proliferations, B) CFSE dilution of Th cells was calculated in order to reveal proliferation capacities (*P<0.05, **P<0.001, n≥3).

In order to reveal intrinsic production of IL-2, TIM-3$^{-/lo}$ or TIM-3$^{mo/hi}$ subpopulations were stimulated with unspecific activators PMA and ionomycin of T cells. PMA diffuses from the cell membrane which directly activates protein kinase C (PKC) bypassing the need for surface receptor stimulation (199). Ionomycin stimulation, here, was used to mediate calcium release which is required for NFAT signaling (200). Upon stimulation with PMA and ionomycin for 2 or 24 hours, supernatants were harvested. IL-2 levels were measured by ELISA (Figure 4.18).

As expected, IL-2 secretion in 2-hour-induced-cells was either below the detection limit or quite low in quantities. For 24 hours, PMA/ionomycin stimulation becomes potent enough to induce IL-2 secretion in both subpopulations. However, in the supernatants obtained from TIM-3$^{mo/hi}$ Th cells, IL-2 was explicitly lower than that of obtained from TIM-3$^{-/lo}$ subpopulation.

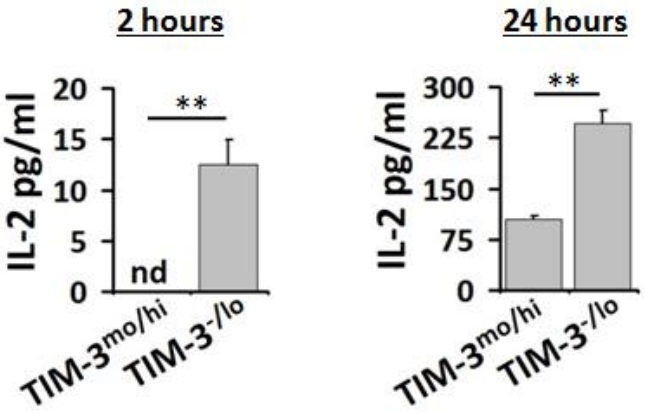

Figure 4.18. IL-2 cytokine levels in TIM-3$^{-/lo}$ and TIM-3$^{mo/hi}$ restimulated with PMA (5 ng/mL)/Ionomycin (0.5 µg/mL) for 2 and 24 hours were evaluated by ELISA (nd, not detected; ***P*<0.001, n≥3).

4.3.7. Confirmation of the AML-Th cell co-culture exhaustion model with additional AML cell lines

Since certain Th cell surface markers (TIM-3, LAG3, PD-1, CTLA-4, ICOS, CD25 and CD127) were significantly associated with the exhaustion state, percentage of Th cells positive for these markers were also evaluated in the co-cultures established with several other AML cell lines, KG-1, Kasumi-1 and U937. The amount of CD25^{+}CD127^{-} and LAG3^{+}TIM-3^{+} cells was also evaluated in the co-cultures. Similar to HL-60 and THP-1, KG-1, Kasumi-1 and U937 AML cells were co-cultured with CD4^{+} T cells at 2:1 ratio in the presence of 25 ng/mL aCD3 stimulation with refreshment for 96 hours.

TIM-3 expression on T cells co-cultured with all five AML cell lines were almost above 80%. LAG3 was expressed less frequently and more diversely. Its expression was ranged between 20-32%, U937 co-cultures showed the least and Kasumi-1 was carrying the maximum percentage of Th cells positive for LAG3 (Table 1). Almost all the co-cultured T cells were positive for PD-1 (>80%) except for Kasumi-1 (60.2±4.9%). Approximately 75% of the co-cultured T cells expressed CTLA-4 and 90% were positive for ICOS. CD25 expressing T cell percentages were above 80%. On the other hand, CD127 expression on these AML co-cultured T cells varied heavily. While only 17% THP-1 co-cultured T cells express CD127, Kasumi-1 co-

cultured T cells remained highly positive for this marker (79.4%) (Table 1).CD127 expression percentages ranged between approximately 17-40% on the co-cultured T cells. The positivity of CD127 on THP-1 co-cultured T cells was the least (17.1±3.5%); whereas, the maximum level of CD127 expression on the co-cultured T cells was inU937 co-cultures (39.7±4.8%).

Table 4.1. TIM-3, LAG3, PD-1, CTLA-4, ICOS, CD25 and CD127 expression on $CD4^+$ T cells co-cultured with KG-1, Kasumi-1, HL-60, THP-1 and U937 cells (Data are shown as mean ± SD).

$CD4^+$ T cells	$TIM\text{-}3^+$ %	$LAG3^+$ %	$PD\text{-}1^+$ %	$CTLA\text{-}4^+$ %	$ICOS^+$ %	$CD25^+$ %	$CD127^+$ %
+ KG-1	79.6±12.9	24.7±13.7	83.6±12.9	74.5±8.3	92.3±4.5	79.0±13.9	26.0±4.6
+ Kasumi-1	91.0 ± 4.7	32.2±4.0	60.2±4.9	83.7±2.2	96.4±1.7	98.8±0.3	22.2±7.9
+ HL-60	79.0±12.2	30.1±3.1	97.0±3.8	72.5±7.2	99.2±0.3	90.7±2.0	25.6±11.2
+ THP-1	80.6±10.1	27.8±8.2	98.5±0.8	76.7±6.5	98.5±1.7	85.8±8.8	17.1±3.5
+ U937	80.7±1.9	20.9±8.0	98.8±0.8	67.0±14.4	96.2±1.8	92.8±5.1	39.7±4.8

Table 4.2. The percentage of $TIM\text{-}3^+$ $LAG3^+$ and $CD25^+CD127^-$ Th cell subpopulations in the co-cultures with KG-1, Kasumi-1, HL-60, THP-1 and U937 cells (Data was shown as mean ± SD).

$CD4^+$ T cells	$TIM\text{-}3^+LAG3^+$ %	$CD25^+CD127^-$ %
+ KG-1	12.3±9.5	37.3±12.9
+ Kasumi-1	19.2±3.1	52.9±5.2
+ HL-60	22.8±8.2	68.8±6.5
+ THP-1	12.7±4.0	56.4±1.1
+ U937	8.4±2.3	52.9±11.3

4.4. The effect of co-stimulatory signals derived from AML cells on Th cells' exhaustion

In order to reveal the effect of co-stimulation on T cell exhaustion, besides the standard co-culture ratio of 2:1 and 25 ng/mL aCD3, we used a low-stimulating condition with AML:Th cell co-culture ratio 0.25:1 and 6.25 ng/mL aCD3. Both of these conditions resulted in significant Th proliferation.

However, the rate of Th cell proliferation was lower when THP-1 ratio was decreased from 2 to 0.25 and the concentration of aCD3 mAb was decreased from 25 ng/mL to 6.25 ng/mL. Expectedly, when both the co-stimulatory signals and TCR stimulation were lowered 8 times in this low-stimulating condition, the percentage of TIM-3^{+} and/or LAG3^{+}Th cells was explicitly downregulated (Figure 4.19).

In order to reveal the role of co-stimulatory pathways, blocking agents of ICOS, CTLA-4 and PD-1 which targets a specific ligand for each receptor were used. ICOS-Fc aims to inhibit ICOS-LG, CTLA-4-Fc targets for both CD80 and CD86, and PD-1-Fc binds to the PD-L1 and PD-L2 ligands. It should be noted that interference with these pathways can hamper T cell activation. Thus, the concentrations of blocking agents were kept at optimum concentrations that do not intervene Th cell proliferation in the co-cultures (Figure 4.20A).

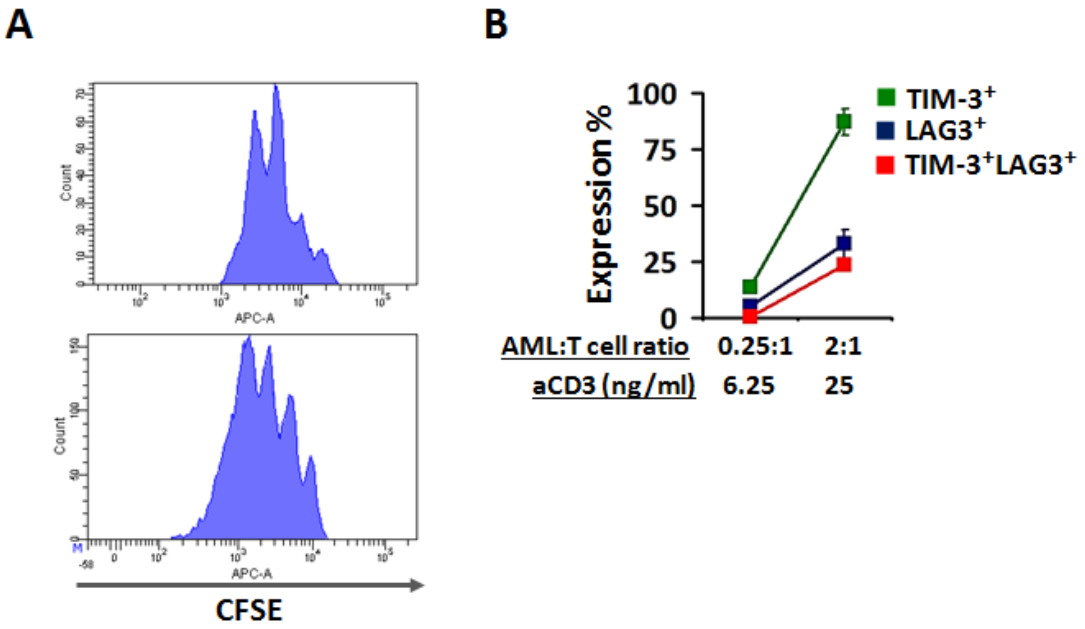

Figure 4.19. A) Representative histograms for proliferation (upper panel: 2:1 ratio, 25 ng/mL aCD3; lower panel: 0.25:1 ratio, 6.25 ng/mL) and B) TIM-3 and/or LAG3 expression on Th cells co-cultured at 2:1 or 0.25:1 AML:Th cell ratio, in the presence of 25 ng/mL or 6.25 ng/mL aCD3 concentrations (n≥3).

THP-1 cells were co-cultured with $CD4^+$ T cells under standard or low-stimulating conditions with appropriate concentrations of blocking agents (considering the binding affinities, 1.5 µg/mL rhICOS-Fc, 0.5 µg/mL rhCTLA-4-Fc, 1.5 µg/mL rhPD-1-Fc) were also included in the cultures. Isotype-matched IgG antibody was used as control. The co-cultures were maintained for 96 hours and refreshed at constant concentration of aCD3 together with corresponding blocking agents. LAG3 and TIM-3 positivity of Th cells were evaluated by flow cytometry (Figure 4.20B).

Blockings with CTLA-4-Fc and ICOS-Fc caused a prominent reduction in LAG3 and TIM-3 expressions and their co-expressions (up to 30-40%). LAG3 expression was hardly any change upon treatment with PD-1-Fc for both LAG3 and TIM-3 expression and their co-expressions (around 10% and 5%).

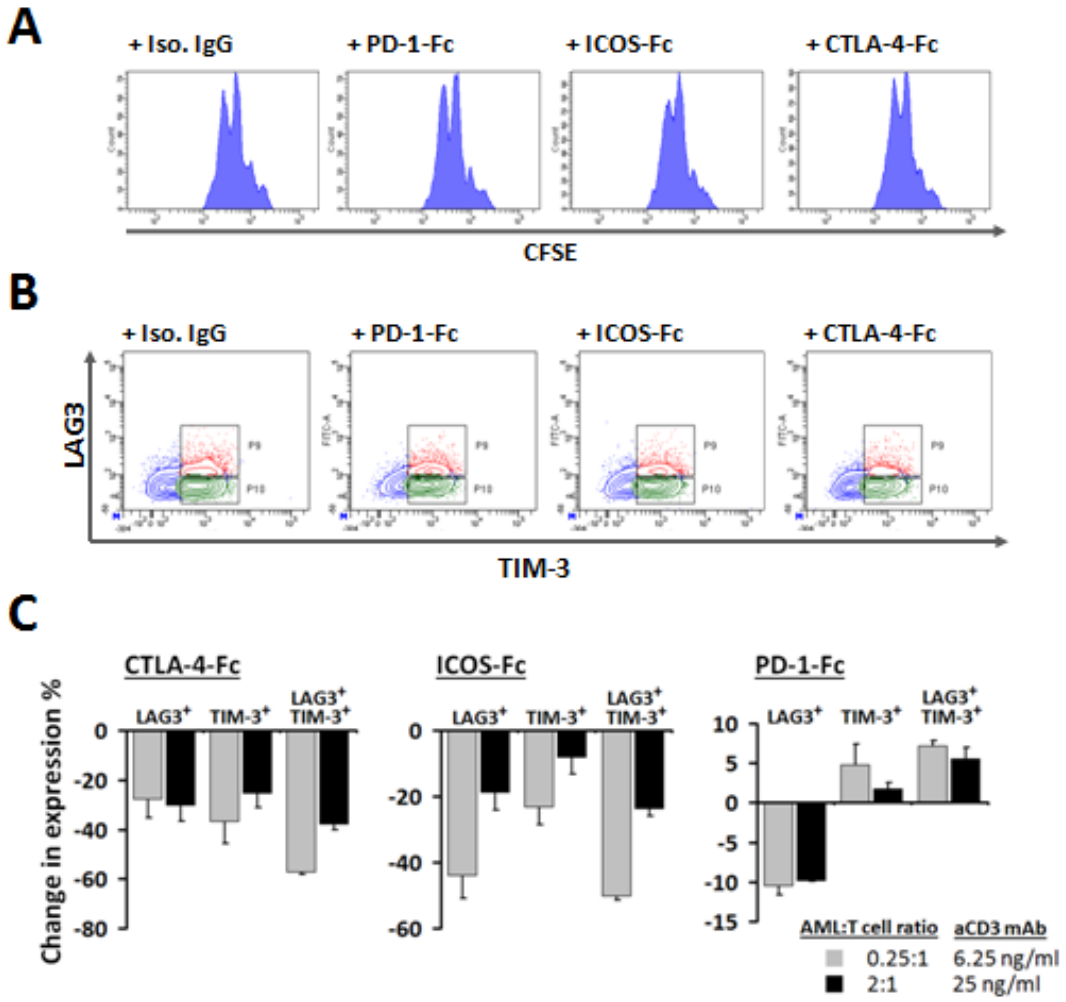

Figure 4.20. A) Representative histograms of Th cells proliferation activity. B) Representative contour plots for LAG3 and TIM-3 expressions on Th cells. P9 shows LAG3^{+}TIM-3^{+} and P10 shows LAG3^{-}TIM-3^{+} populations. C) Change in the percentage of LAG3^{+} and/or TIM-3^{+}Th cells in the co-cultures treated with rhICOS-Fc, rhCTLA-4-Fc or rhPD-1-Fc, (n≥3).

CTLA-4-Fc blocking resulted in reduction (~25%) in LAG3 expression in both low- and high-stimulating conditions. Only TIM-3 expression in low-stimulating condition was more pronounced than that of high-stimulating condition. The co-expression of these two molecules was reduced quite radically (60%) in low-stimulating condition. But, it was still only 40% for high-stimulating condition.

When blocked with ICOS-Fc, LAG3-expressing Th cells were decreased about 40% and 20% under low- and high-stimulating conditions,

respectively. TIM-3 positivity showed only around 12-20% reduction in both of the groups. However, the amount of Th cells co-expressing TIM-3 and LAG3 was drastically decreased similar to that observed in CTLA-4-Fc treatments.

For further evaluation of the effect of these blockings on Th cells' activation state, the level of IL-2, TNF-α and IFN-γ was measured from the 96 h co-culture supernatants by ELISA (Figure 4.21).

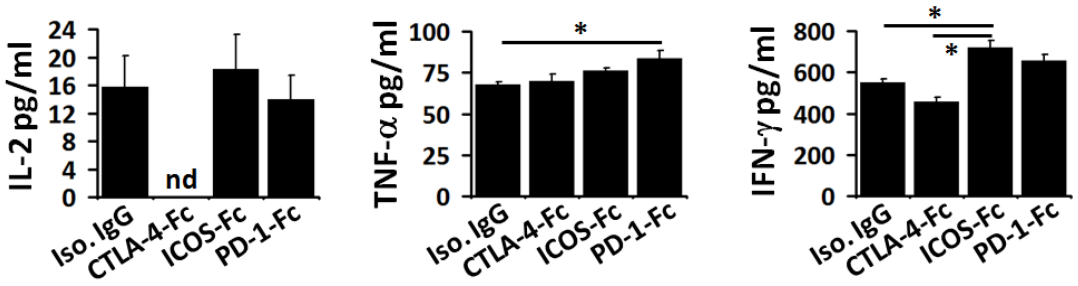

Figure 4.21. IL-2, TNF-α and IFN-γ cytokine levels in THP-1 co-cultures with blocking agents of rhICOS-Fc, rhCTLA-4-Fc or rhPD-1-Fc for 96 h were evaluated by ELISA (nd, not detected; **P*<0.05, n≥3).

IL-2 levels were not changed significantly in ICOS-Fc or PD-1-Fc treatments. It was barely detectable in all four conditions. Intriguingly, IL-2 levels in CTLA-4-treated supernatants, was below detection limits. TNF-α level in the supernatants ranged between 70-80 pg/mL in all treatment conditions. It was only slightly different from Iso.IgG group upon blocking the PD-1 ligands. IFN-γ levels ranged between 450-700 pg/mL in the co-cultures under co-stimulation blocking conditions. Only, ICOS-Fc blocking significantly elevated the IFN-γ levels. IFN-γ level was lower in CTLA-4 blocking than that of in ICOS blocking.

5. DISCUSSION

Being exposed to chronic antigen stimulation in the tumor microenvironment, the T cells that are restricted to tumor antigens can undergo functional exhaustion over time and consequently fail to effectively eradicate the tumor cells. This is manifested by progressive loss of cytokine production, decreased proliferation and resistance to reactivation. This persistence in antigenic stimulation is believed to maintain the state of exhaustion through signals received by TCR (201). However, because T cells require the sum of three signals, derived from antigen recognition, co-stimulation and cytokines, for activation, in fact, the overall magnitude of transduced signals may potentially contribute to the exhaustion (202).

Highly immunogenic cancers and/or malignant cells that already express co-stimulatory molecules or secrete pro-inflammatory cytokines can evoke T cell responses to certain extend. Nevertheless, this stimulation is not sufficient enough to fully eradicate cancer and may eventually contribute to the differentiation of regulatory cells or exhaustion of effector cells. Thus, we hypothesized that co-stimulatory signals, CD86 and ICOS-LG, might contribute to exhaustion in helper T cells.

ICOS-LG, which interacts with ICOS on activated T cells, is expressed by the cells of myeloid origin (106). CD86 expression is widely detected on AML cell lines and on the blasts obtained from patients (10). Moreover, the presence of this co-stimulatory molecule has been associated with poor prognosis and disease severity (8,203). ICOS-LG can also be found on AML cells (8). Correspondingly in our study, both the percentage of ICOS-LG^{+} monocytes and expression level (MFI values) of ICOS-LG were lower than those of AML cell lines. On the other hand, short time exposure to the major anti-tumor cytokine, IFN-γ, significantly upregulated its expression on monocytes and AML cells. Hence, in response to anti-tumor immunity, the amount of co-stimulatory signals provided by the target AML cells can be augmented.

This study aimed to reveal potential contribution of AML cells and their co-stimulatory ligands to helper T cell exhaustion. Here, we designed and

verified an *in vitro* exhaustion model wherein AML cell ratio appeared to be more critical than TCR agonist aCD3 in promoting Th cell activation and exhaustion. Th cell activation supported by AML cells resulted in upregulation of CTLA-4, PD-1 and ICOS receptors. Therefore, these Th cells became prone to co-stimulatory signals. Out of thirteen Th cell activation/exhaustion-related surface markers evaluated, the increase in TIM-3, LAG3, PD-1 and CTLA-4 exhaustion-associated molecules were accompanied by the downregulation of CD69 and CD127. Additionally, the cytokines, IFN-γ, TNF-α and IL-2 that are usually reduced in the state of exhaustion, were also diminished in our model (130). The stability and reliability of exhaustion-related phenotype observed in this *in vitro* co-culture model was further confirmed functionally. Indeed, exhaustion is a loss of function state that aborts T cell effector functions (136). Since exhausted T cells stably and highly expressed TIM-3, we isolated T cells from the co-cultures, wherein exhaustion was modeled, based on TIM-3 positivity. Accordingly, the IL-2 secretion and proliferation capacity of the subpopulation enriched in TIM-$3^{mo/hi}$ cells were highly diminished, in which proliferation could be later rescued by exogenous supplementation of recombinantIL-2.

Collectively, this co-culture model can recapitulate *in vivo* exhaustion or form an *in vitro* platform to examine the impact of AML cells and the co-stimulatory signals thereof on Th cell activation and exhaustion. Accordingly, when co-stimulatory signals of ICOS-LG or CD86 were blocked at a level avoiding hinder to T cells' proliferation, the percentage of Th cells with exhausted immune-phenotype was decreased. Therefore, in a newly established *in vitro* exhaustion model, this study indicates that T cell exhaustion might represent an immune modulatory mechanism imposed by AML cells via constitutive induction of co-stimulatory pathways.

For the sake of activation and survival of T cells, IL-2 and IL-7 are crucial in supporting the co-stimulatory signals. Engagement to IL-7 enhances TCR-mediated signaling, and thus, primes the newly activated T cell for proliferation and IL-2 production (165). IL-2Rα, by itself, is not a signaling receptor, but it is able to form a signaling receptor complex with its

counterparts (IL-2Rβ and IL-2Rγ) for IL-2 (163). CD127 is downregulated on activated T cells, but IL-2 receptor is upregulated so that IL-2 can compensate (163,204). Therefore, activated T cells reduce their capacity to respond IL-7 and IL-2 dependency is elevated. Although at physiological conditions, TCR/CD28 stimuli lead to IL-2-driven expansion in T cells, prolonged stimulation was shown to bypass the need for autocrine IL-2 secretion, culminating IL-2-independent lymphocyte proliferation (205). On the other hand, the exhausted T cells forfeit the ability to secrete IL-2 at the same time they cease to proliferate, but these cells possess capacity to respond to IL-2. Therefore, decreased capacity of T cells to proliferate under exhaustion is not simply associated with the lack of IL-2 production. Accordingly, obtained from AML co-cultures, Th cells with an exhaustion-related immune-phenotype, TIM-3$^{mo/hi}$, showed defects both in autocrine IL-2 secretion and in proliferation.

It should be noted that these TIM-3$^{mo/hi}$ cells were also positive for CD25, PD-1, ICOS and CTLA-4 which were unequivocally expressed by all Th cells after co-culturing 96 h with AML cells. Moreover, a portion of these cells were also potentially carrying LAG3 and had downregulated CD127 and CD69 levels. Following the receipt of activation signals, T cells gain certain surface molecules that indicate their activation and/or differentiation status. Most of these activation markers display transient expression dynamics. T cell activation can roughly divided into early and late stages. In addition to the very early activation marker CD69, the presence of CD154 also indicates T cells in early activation (162,163). CD25, CD38, ICOS, CTLA-4 and PD-1 are also upregulated during early activation but their expression can be prolonged since these molecules are responsible for modulation and/or termination of T cell responses (206). Alternatively, HLA-DR, PD-L1, TIM-3 and LAG3 are indicators of later activation periods (207). Nevertheless, none of these markers can strictly discriminate between early and late activation, since each one of them is expressed with distinct kinetics and regulated differentially under specific inflammatory conditions. As observed in AML-Th cell exhaustion co-cultures, exhaustion-related molecules (TIM-3, LAG3,

CTLA-4) were hardly induced on a minority of Th cells as early as 24 h. However, at the end of 96 h, these markers were almost found on all of the T cells, whereas, the modulation of CD25, CD69 and PD-1 was an early event.

Several studies on exhaustion previously denoted that T cell activation may be followed by an exhaustion state which progresses under the influence of a number of signals (124,201,208,209). Although there is evidence that T cells are marked by expression of exhaustion-associated molecules such as TIM-3, LAG3, PD-1, activation and exhaustion marker expressions may overlap over the time. Thus, exhaustion immune-phenotype should be determined by the combination of the all aforementioned markers.

The current results obtained from the co-cultures modeled with two prototypical AML cell lines, HL-60 or THP-1, showed differential induction of HLA-DR and CD154; in addition CD38 and CCR7 expression was either high at basal levels or not modulated significantly. Therefore, to avoid cell-to-cell variation due to the heterogeneity in AML cell lines, CD25, CD127, TIM-3, LAG3, ICOS, PD-1 and CTLA-4 was selected as appropriate and coherent markers to follow T cell exhaustion. This was further confirmed by the employment of several other AML cell lines in the co-cultures and consistent results were obtained. Of all, TIM-3 was the most highly and restrictedly expressed surface molecule found on exhausted Th cells.

Although the role of TIM-3 is not well-defined, it is known as an activation-induced inhibitory molecule involved in tolerance and exhaustion in many cancer types (148,150,184,210). As part of the TIM family, its expression is naturally modulated post-activation and it is able to function as co-activatory and co-inhibitory depending on the circumstances (211). In a study, it was shown that in the absence of any exogenous ligands, TIM-3 can positively contribute to T cell signaling pathway following the stimulation through TCR/CD3 and CD28 receptors (208). This enhancement of activation may accelerate the shift to an exhausted phenotype, while TIM-3 facilitates co-inhibitory functions upon binding to its ligand, galectin-9 (208). Thus, in our study, the upregulation of TIM-3 on a small portion of Th cells after 12 hours was not surprising in the early phases of activation. Nevertheless, TIM-

3 expression is rather correlated with dysfunctional $CD4^+$ and $CD8^+$ T cells at the settings of various chronic inflammatory diseases including several cancer types (148,152,153,155,156,184,185,201,209,210,212). TIM-3 can be co-expressed with PD-1 on exhausted T cells wherein this non-functional state can be reversed with dual blockade of these molecules (156,213). Alternatively, some studies state that these T cells may only be at a phase of late activation (150). Our study also confirms that TIM-3 is expressed and stabilized on activated T cells. On the other hand, a functional dysregulation was manifested by TIM-$3^{mo/hi}$ T cells. It is important to note that, exhaustion progresses in T cells that are activated, but these cells fail to maintain their effector functions. At this point, there are two views available; TIM-3 can be just a late activation/exhaustion marker and/or this co-inhibitory molecule with late expression can directly contribute to the exhaustion process.

The ligand for TIM-3, Galectin-9 (Gal-9), can be expressed by the cells of myeloid origin. Gal-9 found on AML cells contribute to the suppression of anti-tumor immunity (214). Even though we did not check if the cell lines used are positive for Gal-9, the effect of this ligand on TIM-3^+Th cells cannot be underscored in the co-cultures.

Similar to TIM-3, LAG3 inhibits T cell expansion by blocking the entry of activated T cells into the growth phase of the cell cycle, so they halt and accumulate at the S-phase. It is also capable of limiting the expansion of activated T cells and controlling the size of memory T cells (215). The ligand for LAG3, HLA-DR is upregulated on AML cells (including HL-60) in response to inflammatory stimuli. In addition, AML cells at certain differentiation stages (including THP-1) carry HLA-DR molecule. Thus, LAG3-expressing Th cells may be potentially under the influence of this cognate interaction in the co-cultures.

In addition to the ligands of TIM-3 and LAG3, it has been acknowledged that PD-1 ligands, PD-L1 and PD-L2, are also upregulated on AML cells in response to Th1-mediated immunity, especially IFN-γ (9,216). Thus, in the co-cultures established, Th cells were proliferated under copious amount of both positive and negative signals. Critically, at the initial periods

of co-culturing, the activating signals dominated and as clearly understood by the proliferation rate and activation status of T cells, the co-inhibitory signals were overwhelmed. Hence, not underscoring the impact of co-inhibition, in the current *in vitro* model, exhaustion can be directly attributed to the potency of activatory signals. Correspondingly, only when both TCR induction (aCD3 stimulation) and AML cell ratio (co-stimulation) were decreased, the generation of $LAG3^+$ or $TIM\text{-}3^+$Th cells was reduced.

Simply, if exhaustion is a direct consequence of chronic activation, the role of inhibitory receptors might be in the maintenance of this state. Indeed, if the activated T cells are prematurely inhibited by co-inhibitory receptors, such as PD-1 and CTLA-4 which have early expression kinetics, T cell responses would not have proceed to late activation and/or exhaustion. For example, PD-1 and CTLA-4 signals cause a prompt retention in T cell activity and restrict cellular mechanisms such as reduction in proliferation and IL-2 secretion (206). Alternatively, if inhibitory signals are omitted the T cells can regain activation but eventually they would become prone to exhaustion due to increased amount of positive signals present in the same microenvironment. It should be mentioned that both co-inhibition and exhaustion are regarded as a part of immunological program to avoid hypersensitivity and immunopathology during chronic reactions. In chronic viral infection and cancer models, it has been clearly shown that if so-called ‘non-functional’ T cells with exhausted phenotype are depleted, the disease progresses. Thus, exhaustion is not a complete loss-of-function state for T cells, it is rather a deliberate/physiological weakening of T cell activity, but these cells can still be in charge of controlling the spread of infections and malignancies.

Treg cells can also carry the surface molecules CD25, PD-1, CTLA-4, ICOS, LAG3 and TIM-3. Moreover, CD127 is also downregulated on $CD25^+$ regulatory cells. However, in the co-cultures, there was a scant amount of FoxP3 positivity. Therefore, the decrease of TNF-α, IFN-γ and IL-2 levels in the AML co-cultures might not be due to inhibitory functions of Tregs. In addition, the high amount of IL-10 in the co-cultures with AML cells when

compared to that of in the monocytes co-cultures might not be derived from Treg cells. Since AML cells, HL-60 and THP-1, are not able to secrete Th1 related cytokines, the source of TNF-α, IL-2, IFN-γ and IL-10 can only be co-cultured T cells (87,217-219). The decrease in the Th1 cytokines can be due to a skewing towards Th2 subtype (220,221). IL-4 (Th2-related cytokine) and TGF-β (Treg-associated cytokine) are not detected in the co-cultures. However, IL-10 is also associated with Th2. Since Tregs was not present in these co-cultures, IL-10 might be originating from the Th2 cells. Thus, in the presence of low levels of Th1-associated-cytokines in AML co-cultures, IL-10 levels seem to be putatively increased in comparison to the co-cultures with monocytes.

Unless TCR signaling is supported by the co-stimulatory signals, T cells' activation fails. Thus, TCR signal is obligated to be followed by co-stimulatory signals (especially co-activatory signals mediated by CD28 and ICOS) that lead to activation and proliferation of T cells (135). This was also evident in our co-culture model. T cell activation supported by AML cells demonstrated a remarkable proliferation rate even in the presence of very low TCR stimulation. Additionally, the co-stimulation signals provided by AML cells were so efficient that differential aCD3 concentrations did not significantly change the level of marker expressions at a single 2:1 AML:Th cell ratio. However, when the ratio of AML cells was increased (i.e. the level of co-stimulation was increased), the exhaustion-associated markers were also gradually increased. Therefore, the exhaustion state of T cells relied more heavily on the co-culture ratio than that of aCD3 (TCR) stimulation.

In order to mimic TCR signaling, anti-CD3 monoclonal antibody, clone HIT3a, was chosen among others (OKT3, UCHT1 and TRX4) frequently used in the literature (222). Ideally, in order to maintain a strong TCR signaling, plate-bound aCD3 of OKT3 is usually recommended, especially for T cells isolated from PBMCs (223). In our co-culture setting HIT3a mAb was used in soluble form which would lead to a weaker TCR signal than that could have been generated through plate-bound form. However, soluble aCD3 was still sufficient enough for T cells stimulation. Additionally, we took

the advantage of using soluble aCD3 and maintained the co-cultures with aCD3 and refreshed regularly to mimic persistent TCR stimulation to recapitulate exhaustion-inducing conditions. In the literature, the recommended concentration for soluble aCD3 (HIT3a) ranges between 8 ng/mL – 1 µg/mL (222). In our model, a suboptimal concentration of 25 ng/mL was used as a standard, moreover in certain assays it was lowered to down to 6.25 ng/mL. When aCD3 concentrations were increased up to 0.1 µg/mL with a 16-fold difference between the maximum and the minimum concentrations, the expression of exhaustion-associated markers were not modulated potentially due to co-stimulatory signals provided by AML cells.

Accordingly, CD86 on AML blasts binds to CD28 on Th cells to yield potent co-stimulatory signals (87). Therefore, upon a stringent of blocking CD86 signaling in AML:Th cell co-cultures, T cell activation and proliferation still observed even though at lower levels (87). The remaining activity is probably maintained by the soluble factors (e.g., cytokines) and/or other co-stimulatory pathways such as ICOS/ICOS-LG. Several studies provided that AML cells express CD86 molecule; whereas, very low or no CD80 (10,87). Correspondingly in this study, it was shown that ICOS-LG was promiscuously found on AML cell lines under steady state conditions. ICOS-LG is also expressed on monocytes at moderate levels, so monocytes are also capable of inducing co-stimulatory signals to a certain extend. Thus, AML cells were presumed to be more talented in providing co-stimulatory signals than that of monocytes. Accordingly, in the co-cultures with AML cells providing higher co-stimulatory signals, LAG3 and TIM-3 expression were elevated, while, CD127 levels were low compared to that of in monocyte co-cultures.

Exhaustion state is determined by the combination of several cellular characteristics; diminished cytokine production, immune-phenotype and lastly, impaired proliferation capacity. TIM-3 is a widely used exhaustion-associated molecule that is stably expressed on T cells infiltrating various cancer types (185,209,212). TIM-3 was also prominently expressed on T cells in our co-culture model. Therefore, we used this reliable exhaustion marker’s expression to isolate two subpopulations which were enriched and

restimulated. Firstly, plate-bound aCD3 stimulation was preferred over soluble stimulation to increase TCR stimulation potency. Together with plate-bound aCD3, CD28-stimulating antibody was used in a soluble form and/or PBMCs were added. The proliferation observed in unstimulated TIM-3$^{-/lo}$ or TIM-3$^{mo/hi}$ can be due to the fact that these cells were already exposed to aCD3 and AML cells prior to purification from the co-cultures, so the effect of previous co-culture conditions was ongoing at the baseline level, but TIM-3$^{mo/hi}$ cells had a lower proliferation rate. Upon stimulation with the combination of aCD3/aCD28, proliferation rates of the two subpopulations were elevated, but there was still a significant difference between the two. When aCD28 was replaced with PBMCs, their proliferation was also elevated but PBMCs were not as effective as aCD28 stimulation. It may be because artificial aCD28 stimulation was extremely potent compared to freshly isolated, naïve PBMCs. In addition to this, during the maintenance of T cell exhaustion state, T cells were shown to exhibit high levels of Erk1/2, p38, and STAT5, which possibly reflects constant engagement of TCR and CD28 (148). Thus, additional induction (restimulation) with aCD3 and aCD28 may not be effective enough to further enhance the signaling pathways that are already under constitutive activation. Since these cells were previously stimulated in the co-stimulation-rich AML co-cultures in the presence of aCD3, they were already exposed to aCD3 and aCD28 stimulations. aCD3/aCD28 stimulation was reported to upregulate complexes of CD28-responsive element present in the promoter of human IL-2 gene (224). However, TIM-3$^{mo/hi}$ cells were deprived of IL-2 production. Therefore, addition of rhIL-2 complemented the missing element in these restimulations.

In our *in vitro* co-culture model, AML cell lines of HL-60 and THP-1 was used. The more mature THP-1 cell line, indeed, more potently induced T cells in the co-cultures. Therefore, in most of the experiments, THP-1 was used. In addition, alternative AML cell lines of different maturation stages were also used to confirm our model. These AML cells were also capable of inducing proliferation on T cell and mediate exhaustion state by the upregulation of exhaustion-associated markers. All AML cell lines efficiently

induced proliferation and exhaustion states, since all these AML cells expressed high levels of CD86 and ICOS-LG co-stimulatory molecules independent from their maturation stages (e.g., FAB classes)(8,10,203).

In order to confirm if the co-stimulatory signals derived from AML cells maintain the exhaustion state of cells, blocking agents against ligands of ICOS, CTLA-4 and PD-1 were applied. By the usage of these agents, ICOS-LG, CD80/CD86 and PD-L1/PD-L2 were blocked, respectively. In order to not to hamper T cell activation that is accompanied by proliferation, which is the main inducer of exhaustion, the concentrations of blocking agents used were adjusted. Since AML cells were highly positive for CD86, CTLA-Fc blocking was the most effective agent amongst. This blockade can result in dampening of CD28 signaling. Expectedly, moderation of CD86/CD28-derived signals lead to the most significant reduction in the level of exhausted T cells. Prevention of ICOS-LG from interacting with ICOS expressed on T cells via ICOS-Fc was also rescued certain amount of T cells from exhaustion. Collectively, these main co-activatory pathways can also work as contributors to Th cells' exhaustion.

The strategy of PD-1/PD-L1 blocking is extensively used with the intension of reversing the exhaustion states of T cells (90,137,225,226). Because PD-L1 is heavily upregulated on activated T cells, this blocking strategy seems to reverse the exhaustion phenotype to a certain level. Here, it is important to emphasize that co-stimulatory signals establish the exhaustion state of T cells; so, quiescence of inhibitory signals can eventually result in elevated activation signals and will again inevitably induce exhaustion state. There is a delicate balance between the co-stimulation and the activation. Thus, in case of PD-L1 inhibition, activatory signals were overwhelmed and it caused only a small trend towards the exhaustion-associated marker positivity. This phenomenon has been previously evidenced in other studies with PD-1/PD-L1 blockings (213,227).

All in all, in this *in vitro* co-culture model of exhaustion, T cells were functionally exhausted and AML-derived co-stimulatory signals were determined as critical contributors to this exhausted state.

6. RESULTS AND RECOMMENDATION

- ICOS-LG was expressed promiscuously on AML cell lines (HL-60, THP-1, U937, Kasumi-1 and KG-1) at different maturation stages and was at moderate levels on $CD14^+$ monocytes under steady state conditions.

- *In vitro* stimulation with IFN-γ was able to induce maturation and simultaneously modulate ICOS-LG expression on AML cells. This modulation was distinctive in each AML cell in close correlation with their monocytic differentiation stages. $CD14^+$ monocytes were also treated with IFN-γ or LPS and upregulated CD14 and ICOS-LG percentages in response.

- ICOS-LG mRNA levels greatly varied in AML cell lines, either slightly changed (HL-60) or temporarily increased for 16 hours of IFN-γ treatment. ICOS-LG gene expression was downregulated at longer exposure to IFN-γ.

- The myeloid cell:Th cell co-culture conditions supported the T cell proliferation rates and the viability of the cells across the changing concentrations of aCD3 and different AML (THP-1 or HL-60) cell ratio.

- AML cell ratio appeared to be more critical than TCR agonist aCD3 concentration in promoting Th cell activation and exhaustion in the AML-derived *in vitro* co-culture system.

- TIM-3, LAG3, PD-1, CTLA-4 and ICOS levels were heavily and consistently altered in the different AML cell ratios.

- The increase in exhaustion-associated molecules, TIM-3, LAG3, PD-1 and CTLA-4, were accompanied by the downregulation of CD69 and CD127 in Th cell activation/exhaustion-related surface markers.

- The early-onset modulation of CD69, CD127 and CD154 by 12 hours showed that most of the co-cultured T cells were activated as early as 12 hours. CD25, CD38, TIM-3, LAG3, ICOS, CTLA-4, PD-1, PD-L1 and HLA-DR expressions were prominently detected at 24 hours.
- There was high positivity for TIM-3 and LAG3, and the absence of CD69 and CD127 in the AML co-cultures compared to that of monocytes.

- The percentages of TIM-3^{+}LAG3^{+} and CD25^{+}CD127^{-} T cell populations demonstrated a significant difference between the AML co-cultured and that of monocytes.

- FoxP3 positivity, i.e. Treg cells, in all co-cultures was very low.

- IFN-γ, TNF-α, and IL-2 cytokine levels were diminished in the AML co-cultures compared to that of in monocyte co-cultures. However, IL-10 levels were higher in AML co-cultures than in monocyte co-cultures. IL-4 and TGF-β was below detection limits.

- The cells were recovered from the co-cultures and enriched in TIM-$3^{mo/hi}$ and TIM-$3^{-/lo}$ subpopulations and re-stimulated. Under various activating conditions, TIM-$3^{mo/hi}$ T cells showed lower proliferation than TIM-$3^{-/lo}$. Exhaustion was reversed by exogenous IL-2.

- The immune-phenotypic findings were confirmed in the co-cultures established with additional AML cell lines (U937, Kasumi-1 and KG-1).

- ICOS-LG and CD80/CD86 blockade showed robust reduction in LAG3 and TIM-3 and co-expression profiles; whereas, for PD-1 ligands' blockade was not very effective.

- IL-2, TNF-α, and IFN-γ cytokine levels were not generally altered upon treatment with blocking agents.

- In a study to be planned, distinct marker expression patterns associated with exhaustion can be evaluated on T cells obtained from AML patients.

- The co-stimulatory signals deriving both from CD86 and from ICOS-LG can be simultaneously modulated with combination of blockade in order to reveal overall impact of AML-derived co-stimulation on T cell exhaustion.
- The expression and impact of inhibitory ligands such as Gal-9 and HLA-DR on AML cells can be determined and experiments can be performed with TIM-3 and/or LAG3 blocking agents.

- In order to increase the co-stimulatory capacity of AML cells, CD86 or ICOS-LG expression DNA cassettes can be introduced and additional experiments may be performed with these genetically-modified cells.

- The impact of soluble factors secreted by the AML cells on T cells exhaustion can be determined.

- Similar experiments can also be performed with $CD8^+$ T cells in order to reveal if AML cells can also induce exhaustion in cytotoxic T cells.

REFERENCES

1. Burnet, M. (1957) Cancer; a biological approach. I. The processes of control. *Br Med J*, 1 (5022), 779-786.

2. Thomas, L. (1982) On immunosurveillance in human cancer. *Yale J Biol Med*, 55 (3-4), 329-333.

3. Dunn, G.P., Bruce, A.T., Ikeda, H., Old, L.J.,Schreiber, R.D. (2002) Cancer immunoediting: from immunosurveillance to tumor escape. *Nat Immunol*, 3 (11), 991-998.

4. Romero, P., Dunbar, P.R., Valmori, D., Pittet, M., Ogg, G.S., Rimoldi, D.et al. (1998) Ex vivo staining of metastatic lymph nodes by class I major histocompatibility complex tetramers reveals high numbers of antigen-experienced tumor-specific cytolytic T lymphocytes. *J Exp Med*, 188 (9), 1641-1650.

5. Pardoll, D.M. (2012) The blockade of immune checkpoints in cancer immunotherapy. *Nat Rev Cancer*, 12 (4), 252-264.

6. Crespo, J., Sun, H., Welling, T.H., Tian, Z.,Zou, W. (2013) T cell anergy, exhaustion, senescence, and stemness in the tumor microenvironment. *Curr Opin Immunol*, 25 (2), 214-221.

7. Wherry, E.J., Ha, S.J., Kaech, S.M., Haining, W.N., Sarkar, S., Kalia, V.et al. (2007) Molecular signature of CD8+ T cell exhaustion during chronic viral infection. *Immunity*, 27 (4), 670-684.

8. Tamura, H., Dan, K., Tamada, K., Nakamura, K., Shioi, Y., Hyodo, H.et al. (2005) Expression of functional B7-H2 and B7.2 costimulatory molecules and their prognostic implications in de novo acute myeloid leukemia. *Clin Cancer Res*, 11 (16), 5708-5717.

9. Creery, W.D., Diaz-Mitoma, F., Filion, L.,Kumar, A. (1996) Differential modulation of B7-1 and B7-2 isoform expression on human monocytes by cytokines which influence the development of T helper cell phenotype. *Eur J Immunol*, 26 (6), 1273-1277.

10. Maeda, A., Yamamoto, K., Yamashita, K., Asagoe, K., Nohgawa, M., Kita, K.et al. (1998) The expression of co-stimulatory molecules and their relationship to the prognosis of human acute myeloid leukaemia: poor prognosis of B7-2-positive leukaemia. *Br J Haematol*, 102 (5), 1257-1262.

11. Sadrzadeh, H., Abtahi, S.M.,Fathi, A.T. (2012) Infectious pathogens and hematologic malignancy. *Discov Med*, 14 (79), 421-433.

12. Ayala, F., Dewar, R., Kieran, M.,Kalluri, R. (2009) Contribution of bone microenvironment to leukemogenesis and leukemia progression. *Leukemia*, 23 (12), 2233-2241.

13. Mufti, G.J.,Galton, D.A. (1986) Myelodysplastic syndromes: natural history and features of prognostic importance. *Clin Haematol*, 15 (4), 953-971.

14. Heaney, M.L.,Golde, D.W. (1999) Myelodysplasia. *N Engl J Med*, 340 (21), 1649-1660.

15. Kouides, P.A.,Bennett, J.M. (1997) Understanding the Myelodysplastic Syndromes. *Oncologist*, 2 (6), 389-401.

16. Estey, E., Thall, P., Beran, M., Kantarjian, H., Pierce, S.,Keating, M. (1997) Effect of diagnosis (refractory anemia with excess blasts, refractory anemia with excess blasts in transformation, or acute myeloid leukemia [AML]) on outcome of AML-type chemotherapy. *Blood*, 90 (8), 2969-2977.

17. Guinn, B.A., Mohamedali, A., Thomas, N.S.,Mills, K.I. (2007) Immunotherapy of myeloid leukaemia. *Cancer Immunol Immunother*, 56 (7), 943-957.

18. Estey, E.,Dohner, H. (2006) Acute myeloid leukaemia. *Lancet*, 368 (9550), 1894-1907.

19. Mengis, C., Aebi, S., Tobler, A., Dahler, W.,Fey, M.F. (2003) Assessment of differences in patient populations selected for excluded from participation in clinical phase III acute myelogenous leukemia trials. *J Clin Oncol*, 21 (21), 3933-3939.

20. Kottaridis, P.D., Gale, R.E., Langabeer, S.E., Frew, M.E., Bowen, D.T.,Linch, D.C. (2002) Studies of FLT3 mutations in paired presentation and relapse samples from patients with acute myeloid leukemia: implications for the role of FLT3 mutations in leukemogenesis, minimal residual disease detection, and possible therapy with FLT3 inhibitors. *Blood*, 100 (7), 2393-2398.

21. Poppe, B., Vandesompele, J., Schoch, C., Lindvall, C., Mrozek, K., Bloomfield, C.D.et al. (2004) Expression analyses identify MLL as a prominent target of 11q23 amplification and support an etiologic role for MLL gain of function in myeloid malignancies. *Blood*, 103 (1), 229-235.

22. Stone, R.M., O'Donnell, M.R.,Sekeres, M.A. (2004) Acute myeloid leukemia. *Hematology Am Soc Hematol Educ Program*, 98-117.

23. Estey, E.H. (2014) Acute myeloid leukemia: 2014 update on risk-stratification and management. *Am J Hematol*, 89 (11), 1063-1081.

24. Bullinger, L.,Valk, P.J. (2005) Gene expression profiling in acute myeloid leukemia. *J Clin Oncol*, 23 (26), 6296-6305.

25. Yanada, M., Suzuki, M., Kawashima, K., Kiyoi, H., Kinoshita, T., Emi, N.et al. (2005) Long-term outcomes for unselected patients with acute myeloid leukemia categorized according to the World Health Organization classification: a single-center experience. *Eur J Haematol*, 74 (5), 418-423.

26. Rothe, G.,Schmitz, G. (1996) Consensus protocol for the flow cytometric immunophenotyping of hematopoietic malignancies. Working Group on Flow Cytometry and Image Analysis. *Leukemia*, 10 (5), 877-895.

27. Foucar, K. (2009) Myelodysplastic/myeloproliferative neoplasms. *Am J Clin Pathol*, 132 (2), 281-289.

28. Foucar, K.,Anastasi, J. (2015) Acute Myeloid Leukemia With Recurrent Cytogenetic Abnormalities. *Am J Clin Pathol*, 144 (1), 6-18.

29. Salem, D.A.,Abd El-Aziz, S.M. (2012) Flowcytometric immunophenotypic profile of acute leukemia: mansoura experience. *Indian J Hematol Blood Transfus*, 28 (2), 89-96.

30. Penn, I. (1986) Cancer is a complication of severe immunosuppression. *Surg Gynecol Obstet*, 162 (6), 603-610.

31. Engels, E.A., Pfeiffer, R.M., Fraumeni, J.F., Jr., Kasiske, B.L., Israni, A.K., Snyder, J.J.et al. (2011) Spectrum of cancer risk among US solid organ transplant recipients. *JAMA*, 306 (17), 1891-1901.

32. van Leeuwen, M.T., Webster, A.C., McCredie, M.R., Stewart, J.H., McDonald, S.P., Amin, J.et al. (2010) Effect of reduced immunosuppression after kidney transplant failure on risk of cancer: population based retrospective cohort study. *BMJ*, 340, c570.

33. Dunn, G.P., Old, L.J.,Schreiber, R.D. (2004) The immunobiology of cancer immunosurveillance and immunoediting. *Immunity*, 21 (2), 137-148.

34. Dunn, G.P., Old, L.J.,Schreiber, R.D. (2004) The three Es of cancer immunoediting. *Annu Rev Immunol*, 22, 329-360.

35. Schreiber, R.D., Old, L.J.,Smyth, M.J. (2011) Cancer immunoediting: integrating immunity's roles in cancer suppression and promotion. *Science*, 331 (6024), 1565-1570.

36. Vesely, M.D., Kershaw, M.H., Schreiber, R.D.,Smyth, M.J. (2011) Natural innate and adaptive immunity to cancer. *Annu Rev Immunol*, 29, 235-271.

37. Diamond, M.S., Kinder, M., Matsushita, H., Mashayekhi, M., Dunn, G.P., Archambault, J.M.et al. (2011) Type I interferon is selectively required by dendritic cells for immune rejection of tumors. *J Exp Med*, 208 (10), 1989-2003.

38. Fuertes, M.B., Kacha, A.K., Kline, J., Woo, S.R., Kranz, D.M., Murphy, K.M.et al. (2011) Host type I IFN signals are required for antitumor CD8+ T cell responses through CD8{alpha}+ dendritic cells. *J Exp Med*, 208 (10), 2005-2016.

39. Guicciardi, M.E.,Gores, G.J. (2009) Life and death by death receptors. *FASEB J*, 23 (6), 1625-1637.

40. Dunn, G.P., Koebel, C.M.,Schreiber, R.D. (2006) Interferons, immunity and cancer immunoediting. *Nat Rev Immunol*, 6 (11), 836-848.

41. Restifo, N.P., Marincola, F.M., Kawakami, Y., Taubenberger, J., Yannelli, J.R.,Rosenberg, S.A. (1996) Loss of functional beta 2-microglobulin in metastatic melanomas from five patients receiving immunotherapy. *J Natl Cancer Inst*, 88 (2), 100-108.

42. Khong, H.T., Wang, Q.J.,Rosenberg, S.A. (2004) Identification of multiple antigens recognized by tumor-infiltrating lymphocytes from a single patient: tumor escape by antigen loss and loss of MHC expression. *J Immunother*, 27 (3), 184-190.

43. Jager, E., Ringhoffer, M., Karbach, J., Arand, M., Oesch, F.,Knuth, A. (1996) Inverse relationship of melanocyte differentiation antigen expression in melanoma tissues and CD8+ cytotoxic-T-cell responses: evidence for immunoselection of antigen-loss variants in vivo. *Int J Cancer*, 66 (4), 470-476.

44. Dunn, G.P., Sheehan, K.C., Old, L.J.,Schreiber, R.D. (2005) IFN unresponsiveness in LNCaP cells due to the lack of JAK1 gene expression. *Cancer Res*, 65 (8), 3447-3453.

45. Stern-Ginossar, N., Gur, C., Biton, M., Horwitz, E., Elboim, M., Stanietsky, N.et al. (2008) Human microRNAs regulate stress-induced immune responses mediated by the receptor NKG2D. *Nat Immunol*, 9 (9), 1065-1073.

46. Wang, T., Niu, G., Kortylewski, M., Burdelya, L., Shain, K., Zhang, S.et al. (2004) Regulation of the innate and adaptive immune responses by Stat-3 signaling in tumor cells. *Nat Med*, 10 (1), 48-54.

47. Kataoka, T., Schroter, M., Hahne, M., Schneider, P., Irmler, M., Thome, M.et al. (1998) FLIP prevents apoptosis induced by death receptors but not by perforin/granzyme B, chemotherapeutic drugs, and gamma irradiation. *J Immunol*, 161 (8), 3936-3942.

48. Hinz, S., Trauzold, A., Boenicke, L., Sandberg, C., Beckmann, S., Bayer, E.et al. (2000) Bcl-XL protects pancreatic adenocarcinoma cells against CD95- and TRAIL-receptor-mediated apoptosis. *Oncogene*, 19 (48), 5477-5486.

49. Shin, M.S., Kim, H.S., Lee, S.H., Park, W.S., Kim, S.Y., Park, J.Y.et al. (2001) Mutations of tumor necrosis factor-related apoptosis-inducing ligand receptor 1 (TRAIL-R1) and receptor 2 (TRAIL-R2) genes in metastatic breast cancers. *Cancer Res*, 61 (13), 4942-4946.

50. Takahashi, H., Feuerhake, F., Kutok, J.L., Monti, S., Dal Cin, P., Neuberg, D.et al. (2006) FAS death domain deletions and cellular FADD-like interleukin 1beta converting enzyme inhibitory protein (long) overexpression: alternative mechanisms for deregulating the extrinsic apoptotic pathway in diffuse large B-cell lymphoma subtypes. *Clin Cancer Res*, 12 (11 Pt 1), 3265-3271.

51. Wrzesinski, S.H., Wan, Y.Y.,Flavell, R.A. (2007) Transforming growth factor-beta and the immune response: implications for anticancer therapy. *Clin Cancer Res*, 13 (18 Pt 1), 5262-5270.

52. Aruga, A., Aruga, E., Tanigawa, K., Bishop, D.K., Sondak, V.K.,Chang, A.E. (1997) Type 1 versus type 2 cytokine release by Vbeta T cell subpopulations determines in vivo antitumor reactivity: IL-10 mediates a suppressive role. *J Immunol*, 159 (2), 664-673.

53. Fujii, S., Shimizu, K., Shimizu, T.,Lotze, M.T. (2001) Interleukin-10 promotes the maintenance of antitumor CD8(+) T-cell effector function in situ. *Blood*, 98 (7), 2143-2151.

54. Dong, H., Strome, S.E., Salomao, D.R., Tamura, H., Hirano, F., Flies, D.B.et al. (2002) Tumor-associated B7-H1 promotes T-cell apoptosis: a potential mechanism of immune evasion. *Nat Med*, 8 (8), 793-800.

55. Tripathi, P.,Agrawal, S. (2006) Non-classical HLA-G antigen and its role in the cancer progression. *Cancer Invest*, 24 (2), 178-186.

56. Derre, L., Corvaisier, M., Charreau, B., Moreau, A., Godefroy, E., Moreau-Aubry, A.et al. (2006) Expression and release of HLA-E by melanoma cells and melanocytes: potential impact on the response of cytotoxic effector cells. *J Immunol*, 177 (5), 3100-3107.

57. Terabe, M.,Berzofsky, J.A. (2004) Immunoregulatory T cells in tumor immunity. *Curr Opin Immunol*, 16 (2), 157-162.

58. Sakaguchi, S., Wing, K., Onishi, Y., Prieto-Martin, P.,Yamaguchi, T. (2009) Regulatory T cells: how do they suppress immune responses? *Int Immunol*, 21 (10), 1105-1111.

59. Gabrilovich, D.I.,Nagaraj, S. (2009) Myeloid-derived suppressor cells as regulators of the immune system. *Nat Rev Immunol*, 9 (3), 162-174.

60. Srivastava, M.K., Sinha, P., Clements, V.K., Rodriguez, P.,Ostrand-Rosenberg, S. (2010) Myeloid-derived suppressor cells inhibit T-cell activation by depleting cystine and cysteine. *Cancer Res*, 70 (1), 68-77.

61. Nagaraj, S., Gupta, K., Pisarev, V., Kinarsky, L., Sherman, S., Kang, L.et al. (2007) Altered recognition of antigen is a mechanism of CD8+ T cell tolerance in cancer. *Nat Med*, 13 (7), 828-835.

62. Huang, B., Pan, P.Y., Li, Q., Sato, A.I., Levy, D.E., Bromberg, J.et al. (2006) Gr-1+CD115+ immature myeloid suppressor cells mediate the development of tumor-induced T regulatory cells and T-cell anergy in tumor-bearing host. *Cancer Res*, 66 (2), 1123-1131.

63. Wei, S., Kryczek, I., Zou, L., Daniel, B., Cheng, P., Mottram, P.et al. (2005) Plasmacytoid dendritic cells induce CD8+ regulatory T cells in human ovarian carcinoma. *Cancer Res*, 65 (12), 5020-5026.

64. Sica, A., Larghi, P., Mancino, A., Rubino, L., Porta, C., Totaro, M.G.et al. (2008) Macrophage polarization in tumour progression. *Semin Cancer Biol*, 18 (5), 349-355.

65. Degli-Esposti, M.A.,Smyth, M.J. (2005) Close encounters of different kinds: dendritic cells and NK cells take centre stage. *Nat Rev Immunol*, 5 (2), 112-124.

66. Isidori, A., Salvestrini, V., Ciciarello, M., Loscocco, F., Visani, G., Parisi, S.et al. (2014) The role of the immunosuppressive microenvironment in acute myeloid leukemia development and treatment. *Expert Rev Hematol*, 7 (6), 807-818.

67. Aversa, F., Tabilio, A., Velardi, A., Cunningham, I., Terenzi, A., Falzetti, F.et al. (1998) Treatment of high-risk acute leukemia with T-cell-depleted stem cells from related donors with one fully mismatched HLA haplotype. *N Engl J Med*, 339 (17), 1186-1193.

68. Ruggeri, L., Capanni, M., Urbani, E., Perruccio, K., Shlomchik, W.D., Tosti, A.et al. (2002) Effectiveness of donor natural killer cell alloreactivity in mismatched hematopoietic transplants. *Science*, 295 (5562), 2097-2100.

69. Costello, R.T., Sivori, S., Marcenaro, E., Lafage-Pochitaloff, M., Mozziconacci, M.J., Reviron, D.et al. (2002) Defective expression and function of natural killer cell-triggering receptors in patients with acute myeloid leukemia. *Blood*, 99 (10), 3661-3667.

70. Fauriat, C., Just-Landi, S., Mallet, F., Arnoulet, C., Sainty, D., Olive, D.et al. (2007) Deficient expression of NCR in NK cells from acute

myeloid leukemia: Evolution during leukemia treatment and impact of leukemia cells in NCRdull phenotype induction. *Blood*, 109 (1), 323-330.

71. Szczepanski, M.J., Szajnik, M., Welsh, A., Foon, K.A., Whiteside, T.L.,Boyiadzis, M. (2010) Interleukin-15 enhances natural killer cell cytotoxicity in patients with acute myeloid leukemia by upregulating the activating NK cell receptors. *Cancer Immunol Immunother*, 59 (1), 73-79.

72. Verheyden, S., Bernier, M.,Demanet, C. (2004) Identification of natural killer cell receptor phenotypes associated with leukemia. *Leukemia*, 18 (12), 2002-2007.

73. Nowbakht, P., Ionescu, M.C., Rohner, A., Kalberer, C.P., Rossy, E., Mori, L.et al. (2005) Ligands for natural killer cell-activating receptors are expressed upon the maturation of normal myelomonocytic cells but at low levels in acute myeloid leukemias. *Blood*, 105 (9), 3615-3622.

74. Coles, S.J., Wang, E.C., Man, S., Hills, R.K., Burnett, A.K., Tonks, A.et al. (2011) CD200 expression suppresses natural killer cell function and directly inhibits patient anti-tumor response in acute myeloid leukemia. *Leukemia*, 25 (5), 792-799.

75. Riccioni, R., Pasquini, L., Mariani, G., Saulle, E., Rossini, A., Diverio, D.et al. (2005) TRAIL decoy receptors mediate resistance of acute myeloid leukemia cells to TRAIL. *Haematologica*, 90 (5), 612-624.

76. Chamuleau, M.E., Ossenkoppele, G.J., van Rhenen, A., van Dreunen, L., Jirka, S.M., Zevenbergen, A.et al. (2011) High TRAIL-R3 expression on leukemic blasts is associated with poor outcome and induces apoptosis-resistance which can be overcome by targeting TRAIL-R2. *Leuk Res*, 35 (6), 741-749.

77. Tourneur, L., Delluc, S., Levy, V., Valensi, F., Radford-Weiss, I., Legrand, O.et al. (2004) Absence or low expression of fas-associated protein with death domain in acute myeloid leukemia cells predicts resistance to chemotherapy and poor outcome. *Cancer Res*, 64 (21), 8101-8108.

78. Fauriat, C., Moretta, A., Olive, D.,Costello, R.T. (2005) Defective killing of dendritic cells by autologous natural killer cells from acute myeloid leukemia patients. *Blood*, 106 (6), 2186-2188.

79. Zamai, L., Ponti, C., Mirandola, P., Gobbi, G., Papa, S., Galeotti, L.et al. (2007) NK cells and cancer. *J Immunol*, 178 (7), 4011-4016.

80. Brossart, P., Schneider, A., Dill, P., Schammann, T., Grunebach, F., Wirths, S.et al. (2001) The epithelial tumor antigen MUC1 is expressed

in hematological malignancies and is recognized by MUC1-specific cytotoxic T-lymphocytes. *Cancer Res*, 61 (18), 6846-6850.

81. Dengler, R., Munstermann, U., al-Batran, S., Hausner, I., Faderl, S., Nerl, C.et al. (1995) Immunocytochemical and flow cytometric detection of proteinase 3 (myeloblastin) in normal and leukaemic myeloid cells. *Br J Haematol*, 89 (2), 250-257.

82. Frumento, G., Rotondo, R., Tonetti, M., Damonte, G., Benatti, U.,Ferrara, G.B. (2002) Tryptophan-derived catabolites are responsible for inhibition of T and natural killer cell proliferation induced by indoleamine 2,3-dioxygenase. *J Exp Med*, 196 (4), 459-468.

83. Curti, A., Pandolfi, S., Valzasina, B., Aluigi, M., Isidori, A., Ferri, E.et al. (2007) Modulation of tryptophan catabolism by human leukemic cells results in the conversion of CD25- into CD25+ T regulatory cells. *Blood*, 109 (7), 2871-2877.

84. Gabrilovich, D.I., Ostrand-Rosenberg, S.,Bronte, V. (2012) Coordinated regulation of myeloid cells by tumours. *Nat Rev Immunol*, 12 (4), 253-268.

85. Mussai, F., De Santo, C., Abu-Dayyeh, I., Booth, S., Quek, L., McEwen-Smith, R.M.et al. (2013) Acute myeloid leukemia creates an arginase-dependent immunosuppressive microenvironment. *Blood*, 122 (5), 749-758.

86. Whiteway, A., Corbett, T., Anderson, R., Macdonald, I.,Prentice, H.G. (2003) Expression of co-stimulatory molecules on acute myeloid leukaemia blasts may effect duration of first remission. *Br J Haematol*, 120 (3), 442-451.

87. Dolen, Y.,Esendagli, G. (2013) Myeloid leukemia cells with a B7-2(+) subpopulation provoke Th-cell responses and become immuno-suppressive through the modulation of B7 ligands. *Eur J Immunol*, 43 (3), 747-757.

88. Nurieva, R.I., Liu, X.,Dong, C. (2009) Yin-Yang of costimulation: crucial controls of immune tolerance and function. *Immunol Rev*, 229 (1), 88-100.

89. Yang, H., Bueso-Ramos, C., DiNardo, C., Estecio, M.R., Davanlou, M., Geng, Q.R.et al. (2014) Expression of PD-L1, PD-L2, PD-1 and CTLA4 in myelodysplastic syndromes is enhanced by treatment with hypomethylating agents. *Leukemia*, 28 (6), 1280-1288.

90. John, L.B., Devaud, C., Duong, C.P., Yong, C.S., Beavis, P.A., Haynes, N.M.et al. (2013) Anti-PD-1 antibody therapy potently enhances the

eradication of established tumors by gene-modified T cells. *Clin Cancer Res*, 19 (20), 5636-5646.

91. Pilon-Thomas, S., Mackay, A., Vohra, N.,Mule, J.J. (2010) Blockade of programmed death ligand 1 enhances the therapeutic efficacy of combination immunotherapy against melanoma. *J Immunol*, 184 (7), 3442-3449.

92. Zhou, Q., Xiao, H., Liu, Y., Peng, Y., Hong, Y., Yagita, H.et al. (2010) Blockade of programmed death-1 pathway rescues the effector function of tumor-infiltrating T cells and enhances the antitumor efficacy of lentivector immunization. *J Immunol*, 185 (9), 5082-5092.

93. Perez-Garcia, A., Brunet, S., Berlanga, J.J., Tormo, M., Nomdedeu, J., Guardia, R.et al. (2009) CTLA-4 genotype and relapse incidence in patients with acute myeloid leukemia in first complete remission after induction chemotherapy. *Leukemia*, 23 (3), 486-491.

94. Kapsenberg, M.L. (2003) Dendritic-cell control of pathogen-driven T-cell polarization. *Nat Rev Immunol*, 3 (12), 984-993.

95. Driessens, G., Kline, J.,Gajewski, T.F. (2009) Costimulatory and coinhibitory receptors in anti-tumor immunity. *Immunol Rev*, 229 (1), 126-144.

96. Mueller, D.L., Jenkins, M.K.,Schwartz, R.H. (1989) Clonal expansion versus functional clonal inactivation: a costimulatory signalling pathway determines the outcome of T cell antigen receptor occupancy. *Annu Rev Immunol*, 7, 445-480.

97. Liechtenstein, T., Dufait, I., Lanna, A., Breckpot, K.,Escors, D. (2012) Modulating Co-Stimulation during Antigen Presentation to Enhance Cancer Immunotherapy. *Immunol Endocr Metab Agents Med Chem*, 12 (3), 224-235.

98. Gonzalez, L.C., Loyet, K.M., Calemine-Fenaux, J., Chauhan, V., Wranik, B., Ouyang, W.et al. (2005) A coreceptor interaction between the CD28 and TNF receptor family members B and T lymphocyte attenuator and herpesvirus entry mediator. *Proc Natl Acad Sci U S A*, 102 (4), 1116-1121.

99. Collins, M., Ling, V.,Carreno, B.M. (2005) The B7 family of immune-regulatory ligands. *Genome Biol*, 6 (6), 223.

100. Rudd, C.E., Taylor, A.,Schneider, H. (2009) CD28 and CTLA-4 coreceptor expression and signal transduction. *Immunol Rev*, 229 (1), 12-26.

101. Boomer, J.S.,Green, J.M. (2010) An enigmatic tail of CD28 signaling. *Cold Spring Harb Perspect Biol*, 2 (8), a002436.

102. Janardhan, S.V., Praveen, K., Marks, R.,Gajewski, T.F. (2011) Evidence implicating the Ras pathway in multiple CD28 costimulatory functions in CD4+ T cells. *PLoS One*, 6 (9), e24931.

103. Simpson, T.R., Quezada, S.A.,Allison, J.P. (2010) Regulation of CD4 T cell activation and effector function by inducible costimulator (ICOS). *Curr Opin Immunol*, 22 (3), 326-332.

104. Rudd, C.E.,Schneider, H. (2003) Unifying concepts in CD28, ICOS and CTLA4 co-receptor signalling. *Nat Rev Immunol*, 3 (7), 544-556.

105. Sheppard, K.A., Fitz, L.J., Lee, J.M., Benander, C., George, J.A., Wooters, J.et al. (2004) PD-1 inhibits T-cell receptor induced phosphorylation of the ZAP70/CD3zeta signalosome and downstream signaling to PKCtheta. *FEBS Lett*, 574 (1-3), 37-41.

106. Yao, S., Zhu, Y., Zhu, G., Augustine, M., Zheng, L., Goode, D.J.et al. (2011) B7-h2 is a costimulatory ligand for CD28 in human. *Immunity*, 34 (5), 729-740.

107. McAdam, A.J., Chang, T.T., Lumelsky, A.E., Greenfield, E.A., Boussiotis, V.A., Duke-Cohan, J.S.et al. (2000) Mouse inducible costimulatory molecule (ICOS) expression is enhanced by CD28 costimulation and regulates differentiation of CD4+ T cells. *J Immunol*, 165 (9), 5035-5040.

108. Linsley, P.S., Greene, J.L., Brady, W., Bajorath, J., Ledbetter, J.A.,Peach, R. (1994) Human B7-1 (CD80) and B7-2 (CD86) bind with similar avidities but distinct kinetics to CD28 and CTLA-4 receptors. *Immunity*, 1 (9), 793-801.

109. Lin, D.Y., Tanaka, Y., Iwasaki, M., Gittis, A.G., Su, H.P., Mikami, B.et al. (2008) The PD-1/PD-L1 complex resembles the antigen-binding Fv domains of antibodies and T cell receptors. *Proc Natl Acad Sci U S A*, 105 (8), 3011-3016.

110. Blank, C., Brown, I., Peterson, A.C., Spiotto, M., Iwai, Y., Honjo, T.et al. (2004) PD-L1/B7H-1 inhibits the effector phase of tumor rejection by T cell receptor (TCR) transgenic CD8+ T cells. *Cancer Res*, 64 (3), 1140-1145.

111. Fourcade, J., Kudela, P., Sun, Z., Shen, H., Land, S.R., Lenzner, D.et al. (2009) PD-1 is a regulator of NY-ESO-1-specific CD8+ T cell expansion in melanoma patients. *J Immunol*, 182 (9), 5240-5249.

112. Goldberg, M.V., Maris, C.H., Hipkiss, E.L., Flies, A.S., Zhen, L., Tuder, R.M.et al. (2007) Role of PD-1 and its ligand, B7-H1, in early fate decisions of CD8 T cells. *Blood*, 110 (1), 186-192.

113. Greenwald, R.J., Freeman, G.J.,Sharpe, A.H. (2005) The B7 family revisited. *Annu Rev Immunol*, 23, 515-548.

114. Yokosuka, T., Takamatsu, M., Kobayashi-Imanishi, W., Hashimoto-Tane, A., Azuma, M.,Saito, T. (2012) Programmed cell death 1 forms negative costimulatory microclusters that directly inhibit T cell receptor signaling by recruiting phosphatase SHP2. *J Exp Med*, 209 (6), 1201-1217.

115. Riley, J.L. (2009) PD-1 signaling in primary T cells. *Immunol Rev*, 229 (1), 114-125.

116. Woo, S.R., Turnis, M.E., Goldberg, M.V., Bankoti, J., Selby, M., Nirschl, C.J.et al. (2012) Immune inhibitory molecules LAG-3 and PD-1 synergistically regulate T-cell function to promote tumoral immune escape. *Cancer Res*, 72 (4), 917-927.

117. Zhou, Q., Munger, M.E., Highfill, S.L., Tolar, J., Weigel, B.J., Riddle, M.et al. (2010) Program death-1 signaling and regulatory T cells collaborate to resist the function of adoptively transferred cytotoxic T lymphocytes in advanced acute myeloid leukemia. *Blood*, 116 (14), 2484-2493.

118. Kaech, S.M., Wherry, E.J.,Ahmed, R. (2002) Effector and memory T-cell differentiation: implications for vaccine development. *Nat Rev Immunol*, 2 (4), 251-262.

119. Wherry, E.J.,Ahmed, R. (2004) Memory CD8 T-cell differentiation during viral infection. *J Virol*, 78 (11), 5535-5545.

120. Schluns, K.S.,Lefrancois, L. (2003) Cytokine control of memory T-cell development and survival. *Nat Rev Immunol*, 3 (4), 269-279.

121. Surh, C.D., Boyman, O., Purton, J.F.,Sprent, J. (2006) Homeostasis of memory T cells. *Immunol Rev*, 211, 154-163.

122. Shin, H.,Wherry, E.J. (2007) CD8 T cell dysfunction during chronic viral infection. *Curr Opin Immunol*, 19 (4), 408-415.

123. Zajac, A.J., Blattman, J.N., Murali-Krishna, K., Sourdive, D.J., Suresh, M., Altman, J.D.et al. (1998) Viral immune evasion due to persistence of activated T cells without effector function. *J Exp Med*, 188 (12), 2205-2213.

124. Gallimore, A., Glithero, A., Godkin, A., Tissot, A.C., Pluckthun, A., Elliott, T.et al. (1998) Induction and exhaustion of lymphocytic choriomeningitis virus-specific cytotoxic T lymphocytes visualized using soluble tetrameric major histocompatibility complex class I-peptide complexes. *J Exp Med*, 187 (9), 1383-1393.

125. Wherry, E.J., Blattman, J.N., Murali-Krishna, K., van der Most, R.,Ahmed, R. (2003) Viral persistence alters CD8 T-cell immunodominance and tissue distribution and results in distinct stages of functional impairment. *J Virol*, 77 (8), 4911-4927.

126. Fuller, M.J.,Zajac, A.J. (2003) Ablation of CD8 and CD4 T cell responses by high viral loads. *J Immunol*, 170 (1), 477-486.

127. Fuller, M.J., Khanolkar, A., Tebo, A.E.,Zajac, A.J. (2004) Maintenance, loss, and resurgence of T cell responses during acute, protracted, and chronic viral infections. *J Immunol*, 172 (7), 4204-4214.

128. Matloubian, M., Concepcion, R.J.,Ahmed, R. (1994) CD4+ T cells are required to sustain CD8+ cytotoxic T-cell responses during chronic viral infection. *J Virol*, 68 (12), 8056-8063.

129. Ou, R., Zhou, S., Huang, L.,Moskophidis, D. (2001) Critical role for alpha/beta and gamma interferons in persistence of lymphocytic choriomeningitis virus by clonal exhaustion of cytotoxic T cells. *J Virol*, 75 (18), 8407-8423.

130. Yi, J.S., Cox, M.A.,Zajac, A.J. (2010) T-cell exhaustion: characteristics, causes and conversion. *Immunology*, 129 (4), 474-481.

131. Crawford, A., Angelosanto, J.M., Kao, C., Doering, T.A., Odorizzi, P.M., Barnett, B.E.et al. (2014) Molecular and transcriptional basis of CD4(+) T cell dysfunction during chronic infection. *Immunity*, 40 (2), 289-302.

132. Freeman, G.J., Wherry, E.J., Ahmed, R.,Sharpe, A.H. (2006) Reinvigorating exhausted HIV-specific T cells via PD-1-PD-1 ligand blockade. *J Exp Med*, 203 (10), 2223-2227.

133. Virgin, H.W., Wherry, E.J.,Ahmed, R. (2009) Redefining chronic viral infection. *Cell*, 138 (1), 30-50.

134. Legat, A., Speiser, D.E., Pircher, H., Zehn, D.,Fuertes Marraco, S.A. (2013) Inhibitory Receptor Expression Depends More Dominantly on Differentiation and Activation than "Exhaustion" of Human CD8 T Cells. *Front Immunol*, 4, 455.

135. Chen, L.,Flies, D.B. (2013) Molecular mechanisms of T cell co-stimulation and co-inhibition. *Nat Rev Immunol*, 13 (4), 227-242.

136. Wherry, E.J. (2011) T cell exhaustion. *Nat Immunol*, 12 (6), 492-499.

137. Barber, D.L., Wherry, E.J., Masopust, D., Zhu, B., Allison, J.P., Sharpe, A.H.et al. (2006) Restoring function in exhausted CD8 T cells during chronic viral infection. *Nature*, 439 (7077), 682-687.

138. Day, C.L., Kaufmann, D.E., Kiepiela, P., Brown, J.A., Moodley, E.S., Reddy, S.et al. (2006) PD-1 expression on HIV-specific T cells is associated with T-cell exhaustion and disease progression. *Nature*, 443 (7109), 350-354.

139. Petrovas, C., Casazza, J.P., Brenchley, J.M., Price, D.A., Gostick, E., Adams, W.C.et al. (2006) PD-1 is a regulator of virus-specific CD8+ T cell survival in HIV infection. *J Exp Med*, 203 (10), 2281-2292.

140. Trautmann, L., Janbazian, L., Chomont, N., Said, E.A., Gimmig, S., Bessette, B.et al. (2006) Upregulation of PD-1 expression on HIV-specific CD8+ T cells leads to reversible immune dysfunction. *Nat Med*, 12 (10), 1198-1202.

141. Boettler, T., Panther, E., Bengsch, B., Nazarova, N., Spangenberg, H.C., Blum, H.E.et al. (2006) Expression of the interleukin-7 receptor alpha chain (CD127) on virus-specific CD8+ T cells identifies functionally and phenotypically defined memory T cells during acute resolving hepatitis B virus infection. *J Virol*, 80 (7), 3532-3540.

142. Urbani, S., Amadei, B., Tola, D., Massari, M., Schivazappa, S., Missale, G.et al. (2006) PD-1 expression in acute hepatitis C virus (HCV) infection is associated with HCV-specific CD8 exhaustion. *J Virol*, 80 (22), 11398-11403.

143. Velu, V., Titanji, K., Zhu, B., Husain, S., Pladevega, A., Lai, L.et al. (2009) Enhancing SIV-specific immunity in vivo by PD-1 blockade. *Nature*, 458 (7235), 206-210.

144. Kaufmann, D.E., Kavanagh, D.G., Pereyra, F., Zaunders, J.J., Mackey, E.W., Miura, T.et al. (2007) Upregulation of CTLA-4 by HIV-specific CD4+ T cells correlates with disease progression and defines a reversible immune dysfunction. *Nat Immunol*, 8 (11), 1246-1254.

145. Nakamoto, N., Cho, H., Shaked, A., Olthoff, K., Valiga, M.E., Kaminski, M.et al. (2009) Synergistic reversal of intrahepatic HCV-specific CD8 T cell exhaustion by combined PD-1/CTLA-4 blockade. *PLoS Pathog*, 5 (2), e1000313.

146. Wang, F., He, W., Zhou, H., Yuan, J., Wu, K., Xu, L.et al. (2007) The Tim-3 ligand galectin-9 negatively regulates CD8+ alloreactive T cell and prolongs survival of skin graft. *Cell Immunol*, 250 (1-2), 68-74.

147. Anderson, A.C., Anderson, D.E., Bregoli, L., Hastings, W.D., Kassam, N., Lei, C.et al. (2007) Promotion of tissue inflammation by the immune receptor Tim-3 expressed on innate immune cells. *Science*, 318 (5853), 1141-1143.

148. Jones, R.B., Ndhlovu, L.C., Barbour, J.D., Sheth, P.M., Jha, A.R., Long, B.R.et al. (2008) Tim-3 expression defines a novel population of dysfunctional T cells with highly elevated frequencies in progressive HIV-1 infection. *J Exp Med*, 205 (12), 2763-2779.

149. Rabinovich, G.A., Rubinstein, N.,Toscano, M.A. (2002) Role of galectins in inflammatory and immunomodulatory processes. *Biochim Biophys Acta*, 1572 (2-3), 274-284.

150. Sabatos, C.A., Chakravarti, S., Cha, E., Schubart, A., Sanchez-Fueyo, A., Zheng, X.X.et al. (2003) Interaction of Tim-3 and Tim-3 ligand regulates T helper type 1 responses and induction of peripheral tolerance. *Nat Immunol*, 4 (11), 1102-1110.

151. Nagahara, K., Arikawa, T., Oomizu, S., Kontani, K., Nobumoto, A., Tateno, H.et al. (2008) Galectin-9 increases Tim-3+ dendritic cells and CD8+ T cells and enhances antitumor immunity via galectin-9-Tim-3 interactions. *J Immunol*, 181 (11), 7660-7669.

152. Jin, H.T., Anderson, A.C., Tan, W.G., West, E.E., Ha, S.J., Araki, K.et al. (2010) Cooperation of Tim-3 and PD-1 in CD8 T-cell exhaustion during chronic viral infection. *Proc Natl Acad Sci U S A*, 107 (33), 14733-14738.

153. Golden-Mason, L., Palmer, B.E., Kassam, N., Townshend-Bulson, L., Livingston, S., McMahon, B.J.et al. (2009) Negative immune regulator Tim-3 is overexpressed on T cells in hepatitis C virus infection and its blockade rescues dysfunctional CD4+ and CD8+ T cells. *J Virol*, 83 (18), 9122-9130.

154. Richter, K., Agnellini, P.,Oxenius, A. (2010) On the role of the inhibitory receptor LAG-3 in acute and chronic LCMV infection. *Int Immunol*, 22 (1), 13-23.

155. Li, H., Wu, K., Tao, K., Chen, L., Zheng, Q., Lu, X.et al. (2012) Tim-3/galectin-9 signaling pathway mediates T-cell dysfunction and predicts poor prognosis in patients with hepatitis B virus-associated hepatocellular carcinoma. *Hepatology*, 56 (4), 1342-1351.

156. Dietze, K.K., Zelinskyy, G., Liu, J., Kretzmer, F., Schimmer, S.,Dittmer, U. (2013) Combining regulatory T cell depletion and inhibitory receptor blockade improves reactivation of exhausted virus-specific CD8+ T cells and efficiently reduces chronic retroviral loads. *PLoS Pathog*, 9 (12), e1003798.

157. Blackburn, S.D., Shin, H., Haining, W.N., Zou, T., Workman, C.J., Polley, A.et al. (2009) Coregulation of CD8+ T cell exhaustion by multiple inhibitory receptors during chronic viral infection. *Nat Immunol*, 10 (1), 29-37.

158. Cai, G., Anumanthan, A., Brown, J.A., Greenfield, E.A., Zhu, B.,Freeman, G.J. (2008) CD160 inhibits activation of human CD4+ T cells through interaction with herpesvirus entry mediator. *Nat Immunol*, 9 (2), 176-185.

159. Durham, N.M., Nirschl, C.J., Jackson, C.M., Elias, J., Kochel, C.M., Anders, R.A.et al. (2014) Lymphocyte Activation Gene 3 (LAG-3) modulates the ability of CD4 T-cells to be suppressed in vivo. *PLoS One*, 9 (11), e109080.

160. Simms, P.E.,Ellis, T.M. (1996) Utility of flow cytometric detection of CD69 expression as a rapid method for determining poly- and oligoclonal lymphocyte activation. *Clin Diagn Lab Immunol*, 3 (3), 301-304.

161. Posselt, A.M., Vincenti, F., Bedolli, M., Lantz, M., Roberts, J.P.,Hirose, R. (2003) CD69 expression on peripheral CD8 T cells correlates with acute rejection in renal transplant recipients. *Transplantation*, 76 (1), 190-195.

162. Maino, V.C., Suni, M.A.,Ruitenberg, J.J. (1995) Rapid flow cytometric method for measuring lymphocyte subset activation. *Cytometry*, 20 (2), 127-133.

163. Taniguchi, T.,Minami, Y. (1993) The IL-2/IL-2 receptor system: a current overview. *Cell*, 73 (1), 5-8.

164. Liu, W., Putnam, A.L., Xu-Yu, Z., Szot, G.L., Lee, M.R., Zhu, S.et al. (2006) CD127 expression inversely correlates with FoxP3 and suppressive function of human CD4+ T reg cells. *J Exp Med*, 203 (7), 1701-1711.

165. Fry, T.J.,Mackall, C.L. (2001) Interleukin-7: master regulator of peripheral T-cell homeostasis? *Trends Immunol*, 22 (10), 564-571.

166. Fontenot, J.D., Gavin, M.A.,Rudensky, A.Y. (2003) Foxp3 programs the development and function of CD4+CD25+ regulatory T cells. *Nat Immunol*, 4 (4), 330-336.

167. Hori, S., Nomura, T.,Sakaguchi, S. (2003) Control of regulatory T cell development by the transcription factor Foxp3. *Science*, 299 (5609), 1057-1061.

168. Seddiki, N., Santner-Nanan, B., Martinson, J., Zaunders, J., Sasson, S., Landay, A.et al. (2006) Expression of interleukin (IL)-2 and IL-7 receptors discriminates between human regulatory and activated T cells. *J Exp Med*, 203 (7), 1693-1700.

169. Glasova, M., Konikova, E., Stasakova, J.,Babusikova, O. (1998) The relationship of HLA-DR, CD38 and CD71 markers to activation,

proliferation and differentiation of some human leukemia and lymphoma cells. *Neoplasma*, 45 (2), 88-95.

170. Harvey, K., Higgins, N., Akard, L., Chang, Q., Jansen, J., Thompson, J.et al. (1997) Lineage commitment of HLA-DR/CD38-defined progenitor cell subpopulations in bone marrow and mobilized peripheral blood assessed by four-color immunofluorescence. *J Hematother*, 6 (3), 243-252.

171. Kestens, L., Vanham, G., Vereecken, C., Vandenbruaene, M., Vercauteren, G., Colebunders, R.L.et al. (1994) Selective increase of activation antigens HLA-DR and CD38 on CD4+ CD45RO+ T lymphocytes during HIV-1 infection. *Clin Exp Immunol*, 95 (3), 436-441.

172. Kim, P.S.,Ahmed, R. (2010) Features of responding T cells in cancer and chronic infection. *Curr Opin Immunol*, 22 (2), 223-230.

173. Klebanoff, C.A., Gattinoni, L., Torabi-Parizi, P., Kerstann, K., Cardones, A.R., Finkelstein, S.E.et al. (2005) Central memory self/tumor-reactive CD8+ T cells confer superior antitumor immunity compared with effector memory T cells. *Proc Natl Acad Sci U S A*, 102 (27), 9571-9576.

174. Mueller, K., Schweier, O.,Pircher, H. (2008) Efficacy of IL-2- versus IL-15-stimulated CD8 T cells in adoptive immunotherapy. *Eur J Immunol*, 38 (10), 2874-2885.

175. Xie, Y., Akpinarli, A., Maris, C., Hipkiss, E.L., Lane, M., Kwon, E.K.et al. (2010) Naive tumor-specific CD4(+) T cells differentiated in vivo eradicate established melanoma. *J Exp Med*, 207 (3), 651-667.

176. Quezada, S.A., Simpson, T.R., Peggs, K.S., Merghoub, T., Vider, J., Fan, X.et al. (2010) Tumor-reactive CD4(+) T cells develop cytotoxic activity and eradicate large established melanoma after transfer into lymphopenic hosts. *J Exp Med*, 207 (3), 637-650.

177. Kamphorst, A.O.,Ahmed, R. (2013) CD4 T-cell immunotherapy for chronic viral infections and cancer. *Immunotherapy*, 5 (9), 975-987.

178. Landsberg, J., Kohlmeyer, J., Renn, M., Bald, T., Rogava, M., Cron, M.et al. (2012) Melanomas resist T-cell therapy through inflammation-induced reversible dedifferentiation. *Nature*, 490 (7420), 412-416.

179. Jensen, S.M., Twitty, C.G., Maston, L.D., Antony, P.A., Lim, M., Hu, H.M.et al. (2012) Increased frequency of suppressive regulatory T cells and T cell-mediated antigen loss results in murine melanoma recurrence. *J Immunol*, 189 (2), 767-776.

180. Mumprecht, S., Schurch, C., Schwaller, J., Solenthaler, M.,Ochsenbein, A.F. (2009) Programmed death 1 signaling on chronic myeloid

leukemia-specific T cells results in T-cell exhaustion and disease progression. *Blood*, 114 (8), 1528-1536.

181. Ahmadzadeh, M., Johnson, L.A., Heemskerk, B., Wunderlich, J.R., Dudley, M.E., White, D.E.et al. (2009) Tumor antigen-specific CD8 T cells infiltrating the tumor express high levels of PD-1 and are functionally impaired. *Blood*, 114 (8), 1537-1544.

182. Grosso, J.F., Kelleher, C.C., Harris, T.J., Maris, C.H., Hipkiss, E.L., De Marzo, A.et al. (2007) LAG-3 regulates CD8+ T cell accumulation and effector function in murine self- and tumor-tolerance systems. *J Clin Invest*, 117 (11), 3383-3392.

183. Gandhi, M.K., Lambley, E., Duraiswamy, J., Dua, U., Smith, C., Elliott, S.et al. (2006) Expression of LAG-3 by tumor-infiltrating lymphocytes is coincident with the suppression of latent membrane antigen-specific CD8+ T-cell function in Hodgkin lymphoma patients. *Blood*, 108 (7), 2280-2289.

184. Sakuishi, K., Apetoh, L., Sullivan, J.M., Blazar, B.R., Kuchroo, V.K.,Anderson, A.C. (2010) Targeting Tim-3 and PD-1 pathways to reverse T cell exhaustion and restore anti-tumor immunity. *J Exp Med*, 207 (10), 2187-2194.

185. Zhou, Q., Munger, M.E., Veenstra, R.G., Weigel, B.J., Hirashima, M., Munn, D.H.et al. (2011) Coexpression of Tim-3 and PD-1 identifies a CD8+ T-cell exhaustion phenotype in mice with disseminated acute myelogenous leukemia. *Blood*, 117 (17), 4501-4510.

186. Riches, J.C., Davies, J.K., McClanahan, F., Fatah, R., Iqbal, S., Agrawal, S.et al. (2013) T cells from CLL patients exhibit features of T-cell exhaustion but retain capacity for cytokine production. *Blood*, 121 (9), 1612-1621.

187. Zenz, T. (2013) Exhausting T cells in CLL. *Blood*, 121 (9), 1485-1486.

188. Koeffler, H.P., Billing, R., Lusis, A.J., Sparkes, R.,Golde, D.W. (1980) An undifferentiated variant derived from the human acute myelogenous leukemia cell line (KG-1). *Blood*, 56 (2), 265-273.

189. Dijk, M., Murphy, E., Morrell, R., Knapper, S., O'Dwyer, M., Samali, A.et al. (2011) The Proteasome Inhibitor Bortezomib Sensitizes AML with Myelomonocytic Differentiation to TRAIL Mediated Apoptosis. *Cancers (Basel)*, 3 (1), 1329-1350.

190. Asou, H., Tashiro, S., Hamamoto, K., Otsuji, A., Kita, K.,Kamada, N. (1991) Establishment of a human acute myeloid leukemia cell line (Kasumi-1) with 8;21 chromosome translocation. *Blood*, 77 (9), 2031-2036.

191. Gallagher, R., Collins, S., Trujillo, J., McCredie, K., Ahearn, M., Tsai, S.et al. (1979) Characterization of the continuous, differentiating myeloid cell line (HL-60) from a patient with acute promyelocytic leukemia. *Blood*, 54 (3), 713-733.

192. Sundstrom, C.,Nilsson, K. (1976) Establishment and characterization of a human histiocytic lymphoma cell line (U-937). *Int J Cancer*, 17 (5), 565-577.

193. Nestal de Moraes, G., Castro, C.P., Salustiano, E.J., Dumas, M.L., Costas, F., Lam, E.W.et al. (2014) The pterocarpanquinone LQB-118 induces apoptosis in acute myeloid leukemia cells of distinct molecular subtypes and targets FoxO3a and FoxM1 transcription factors. *Int J Oncol*, 45 (5), 1949-1958.

194. Wang, X., Gocek, E., Novik, V., Harrison, J.S., Danilenko, M.,Studzinski, G.P. (2010) Inhibition of Cot1/Tlp2 oncogene in AML cells reduces ERK5 activation and up-regulates p27Kip1 concomitant with enhancement of differentiation and cell cycle arrest induced by silibinin and 1,25-dihydroxyvitamin D(3). *Cell Cycle*, 9 (22), 4542-4551.

195. Tsuchiya, S., Yamabe, M., Yamaguchi, Y., Kobayashi, Y., Konno, T.,Tada, K. (1980) Establishment and characterization of a human acute monocytic leukemia cell line (THP-1). *Int J Cancer*, 26 (2), 171-176.

196. Tsujimura, H., Nagamura-Inoue, T., Tamura, T.,Ozato, K. (2002) IFN consensus sequence binding protein/IFN regulatory factor-8 guides bone marrow progenitor cells toward the macrophage lineage. *J Immunol*, 169 (3), 1261-1269.

197. Kirchheimer, J.C., Nong, Y.H.,Remold, H.G. (1988) IFN-gamma, tumor necrosis factor-alpha, and urokinase regulate the expression of urokinase receptors on human monocytes. *J Immunol*, 141 (12), 4229-4234.

198. Costello, R.T., Mallet, F., Sainty, D., Maraninchi, D., Gastaut, J.A.,Olive, D. (1998) Regulation of CD80/B7-1 and CD86/B7-2 molecule expression in human primary acute myeloid leukemia and their role in allogenic immune recognition. *Eur J Immunol*, 28 (1), 90-103.

199. Park, J.W., Jang, M.A., Lee, Y.H., Passaniti, A.,Kwon, T.K. (2001) p53-independent elevation of p21 expression by PMA results from PKC-mediated mRNA stabilization. *Biochem Biophys Res Commun*, 280 (1), 244-248.

200. Chatila, T., Silverman, L., Miller, R.,Geha, R. (1989) Mechanisms of T cell activation by the calcium ionophore ionomycin. *J Immunol*, 143 (4), 1283-1289.

201. Ferris, R.L., Lu, B.,Kane, L.P. (2014) Too much of a good thing? Tim-3 and TCR signaling in T cell exhaustion. *J Immunol*, 193 (4), 1525-1530.

202. Pen, J.J., Keersmaecker, B.D., Heirman, C., Corthals, J., Liechtenstein, T., Escors, D.et al. (2014) Interference with PD-L1/PD-1 co-stimulation during antigen presentation enhances the multifunctionality of antigen-specific T cells. *Gene Ther*, 21 (3), 262-271.

203. Hirano, N., Takahashi, T., Takahashi, T., Ohtake, S., Hirashima, K., Emi, N.et al. (1996) Expression of costimulatory molecules in human leukemias. *Leukemia*, 10 (7), 1168-1176.

204. Ma, A., Koka, R.,Burkett, P. (2006) Diverse functions of IL-2, IL-15, and IL-7 in lymphoid homeostasis. *Annu Rev Immunol*, 24, 657-679.

205. Colombetti, S., Basso, V., Mueller, D.L.,Mondino, A. (2006) Prolonged TCR/CD28 engagement drives IL-2-independent T cell clonal expansion through signaling mediated by the mammalian target of rapamycin. *J Immunol*, 176 (5), 2730-2738.

206. Parry, R.V., Chemnitz, J.M., Frauwirth, K.A., Lanfranco, A.R., Braunstein, I., Kobayashi, S.V.et al. (2005) CTLA-4 and PD-1 receptors inhibit T-cell activation by distinct mechanisms. *Mol Cell Biol*, 25 (21), 9543-9553.

207. Loertscher, R., Forbes, R.D., Halabi, G., Lavery, P.,Quinn, T. (1994) Expression of early and late activation markers on peripheral blood T lymphocytes does not reliably reflect immune events in transplanted hearts. *Clin Transplant*, 8 (3 Pt 1), 230-238.

208. Lee, J., Su, E.W., Zhu, C., Hainline, S., Phuah, J., Moroco, J.A.et al. (2011) Phosphotyrosine-dependent coupling of Tim-3 to T-cell receptor signaling pathways. *Mol Cell Biol*, 31 (19), 3963-3974.

209. Zhang, Z.N., Zhu, M.L., Chen, Y.H., Fu, Y.J., Zhang, T.W., Jiang, Y.J.et al. (2015) Elevation of Tim-3 and PD-1 expression on T cells appears early in HIV infection, and differential Tim-3 and PD-1 expression patterns can be induced by common gamma -chain cytokines. *Biomed Res Int*, 2015, 916936.

210. Monney, L., Sabatos, C.A., Gaglia, J.L., Ryu, A., Waldner, H., Chernova, T.et al. (2002) Th1-specific cell surface protein Tim-3 regulates macrophage activation and severity of an autoimmune disease. *Nature*, 415 (6871), 536-541.

211. Huang, Y.H., Zhu, C., Kondo, Y., Anderson, A.C., Gandhi, A., Russell, A.et al. (2015) CEACAM1 regulates TIM-3-mediated tolerance and exhaustion. *Nature*, 517 (7534), 386-390.

212. Morou, A., Palmer, B.E.,Kaufmann, D.E. (2014) Distinctive features of CD4+ T cell dysfunction in chronic viral infections. *Curr Opin HIV AIDS*, 9 (5), 446-451.

213. Jing, W., Gershan, J.A., Weber, J., Tlomak, D., McOlash, L., Sabatos-Peyton, C.et al. (2015) Combined immune checkpoint protein blockade and low dose whole body irradiation as immunotherapy for myeloma. *J Immunother Cancer*, 3 (1), 2.

214. Folgiero, V., Cifaldi, L., Li Pira, G., Goffredo, B.M., Vinti, L.,Locatelli, F. (2015) TIM-3/Gal-9 interaction induces IFNgamma-dependent IDO1 expression in acute myeloid leukemia blast cells. *J Hematol Oncol*, 8, 36.

215. Workman, C.J., Cauley, L.S., Kim, I.J., Blackman, M.A., Woodland, D.L.,Vignali, D.A. (2004) Lymphocyte activation gene-3 (CD223) regulates the size of the expanding T cell population following antigen activation in vivo. *J Immunol*, 172 (9), 5450-5455.

216. Braumuller, H., Wieder, T., Brenner, E., Assmann, S., Hahn, M., Alkhaled, M.et al. (2013) T-helper-1-cell cytokines drive cancer into senescence. *Nature*, 494 (7437), 361-365.

217. Kupsa, T., Vasatova, M., Karesova, I., Zak, P.,Horacek, J.M. (2014) Baseline serum levels of multiple cytokines and adhesion molecules in patients with acute myeloid leukemia: results of a pivotal trial. *Exp Oncol*, 36 (4), 252-257.

218. Sun, Y.X., Kong, H.L., Liu, C.F., Yu, S., Tian, T., Ma, D.X.et al. (2014) The imbalanced profile and clinical significance of T helper associated cytokines in bone marrow microenvironment of the patients with acute myeloid leukemia. *Hum Immunol*, 75 (2), 113-118.

219. Tian, T., Yu, S., Wang, M., Yuan, C., Zhang, H., Ji, C.et al. (2013) Aberrant T helper 17 cells and related cytokines in bone marrow microenvironment of patients with acute myeloid leukemia. *Clin Dev Immunol*, 2013, 915873.

220. Bashyam, H. (2007) Th1/Th2 cross-regulation and the discovery of IL-10. *J Exp Med*, 204 (2), 237.

221. Fishman, M.A.,Perelson, A.S. (1999) Th1/Th2 differentiation and cross-regulation. *Bull Math Biol*, 61 (3), 403-436.

222. Li, L., Nishio, J., van Maurik, A., Mathis, D.,Benoist, C. (2013) Differential response of regulatory and conventional CD4(+) lymphocytes to CD3 engagement: clues to a possible mechanism of anti-CD3 action? *J Immunol*, 191 (7), 3694-3704.

223. Smeltz, R.B. (2007) Profound enhancement of the IL-12/IL-18 pathway of IFN-gamma secretion in human CD8+ memory T cell subsets via IL-15. *J Immunol*, 178 (8), 4786-4792.

224. Ghosh, P., Tan, T.H., Rice, N.R., Sica, A.,Young, H.A. (1993) The interleukin 2 CD28-responsive complex contains at least three members of the NF kappa B family: c-Rel, p50, and p65. *Proc Natl Acad Sci U S A*, 90 (5), 1696-1700.

225. McClanahan, F., Hanna, B., Miller, S., Clear, A.J., Lichter, P., Gribben, J.G.et al. (2015) PD-L1 Checkpoint Blockade Prevents Immune Dysfunction and Leukemia Development in a Mouse Model of Chronic Lymphocytic Leukemia. *Blood*.

226. Wang, W., Lau, R., Yu, D., Zhu, W., Korman, A.,Weber, J. (2009) PD1 blockade reverses the suppression of melanoma antigen-specific CTL by CD4+ CD25(Hi) regulatory T cells. *Int Immunol*, 21 (9), 1065-1077.

227. Bachireddy, P., Hainz, U., Rooney, M., Pozdnyakova, O., Aldridge, J., Zhang, W.et al. (2014) Reversal of in situ T-cell exhaustion during effective human antileukemia responses to donor lymphocyte infusion. *Blood*, 123 (9), 1412-1421.

APPENDICES

APPENDIX 1: Ethics Committee Approval

T.C.
HACETTEPE ÜNİVERSİTESİ
Girişimsel Olmayan Klinik Araştırmalar Etik Kurulu

Sayı : 16969557-12.00

01 Ara 2014

ARAŞTIRMA PROJESİ DEĞERLENDİRME RAPORU

Toplantı Tarihi	: 26.11.2014 ÇARŞAMBA
Toplantı No	: 2014/17
Proje No	: GO 14/606 (Değerlendirme Tarihi: 26.11.2014)
Karar No	: GO 14/606 – 31

Üniversitemiz Kanser Estitüsü Temel Onkoloji Anabilim Dalı öğretim üyelerinden Doç.Dr. Güneş ESENDAĞLI'nın sorumlu araştırmacısı olduğu, Bio. Didem ÖZKAZANÇ'ın tezi olan GO 14/606 kayıt numaralı ve ***"Uyarılabilen Ko-Stmülatör Ligand (ICOS-LG) Eksprese Eden Akut Miyeloid Lösemi Hücrelerinin T Lenfosit Aktivasyonuna ve Yorulmasına Etkisi"*** başlıklı proje önerisi araştırmanın gerekçe, amaç, yaklaşım ve yöntemleri dikkate alınarak incelenmiş olup, tıbbi etik açıdan uygun bulunmuştur.

1.Prof. Dr. Nurten Akarsu	(Başkan)	8 Prof. Dr. Rahime Nohutçu	(Üye)
İZİNLİ			
2. Prof. Dr. Nüket Örnek Buken	(Üye)	9. Prof. Dr. R. Köksal Özgül	(Üye)
3. Prof. Dr. M. Yıldırım Sara	(Üye)	10. Prof. Dr. Ayşe Lale Doğan	(Üye)
4. Prof. Dr. Sevda F. Müftüoğlu	(Üye)	11. Doç. Dr. S. Kutay Demirkan	(Üye)
5. Prof. Dr. Cenk Sökmensüer	(Üye)	12 Prof. Dr Leyla Dinç	(Üye)
6. Prof. Dr. Volga Bayrakçı Tunay	(Üye)	13. Yrd. Doç. Dr. H. Hüsrev Turnagöl	(Üye)
İZİNLİ			
7. Prof. Dr. Ali Düzova	(Üye)	14. Av. Meltem Onurlu	(Üye)

Hacettepe Üniversitesi Girişimsel Olmayan Klinik Araştırmalar Etik Kurulu
06100 Sıhhiye-Ankara
Telefon: 0 (312) 305 1082 • Faks: 0 (312) 310 0580 • E-posta: goetik@hacettepe.edu.tr

Ayrıntılı Bilgi için: